THERMAL INSULATION SYSTEM FOR LARGE FLAME BUCKETS

E. Eugene Callens, Jr.
Tonya Pleshette Gamblin

Department of Mechanical and Industrial Engineering
Louisiana Tech University
P.O. Box 10348
Ruston, LA 71272-0046

October 1996

Technical Report

Contract No. 31-4136-59060
and NASA (1995)-Stennis-06
and NAS13-580

Prepared for:
National Aeronautics and Space Administration
John C. Stennis Space Center
Stennis Space Center, MS 39529-6000

ABSTRACT

The objective of this study is to investigate the use of thermal protection coatings, single tiles, and layered insulation systems to protect the walls of the flame buckets used in the testing of the Space Shuttle Main Engine, while reducing the cost and maintenance of the system. The physical behavior of the system is modeled by a plane wall boundary value problem with a convective frontface condition and a backface condition designed to provide higher heat rates through the material.

The research includes a study of various ceramics and metals that may be suitable for use in a thermal protection system depending on their theoretical performance under simulated plume conditions. The equations developed here were used to calculate important thermal parameters including temperature distributions through the material, maximum times the materials can withstand plume conditions before failure, steady state surface temperatures in single layer designs, steady state surface and interface temperatures in composite layer designs, and expected heat loads that the system must be able to handle. The designs with the best thermal performance involved partial replacement of the flame bucket material with either tantalum, hafnium, or niobium carbide as the insulation material and aluminum as the support material.

TABLE OF CONTENTS

LIST OF FIGURES

Page

Page

LIST OF TABLES

CHAPTER 1

INTRODUCTION

Background

NASA's John C. Stennis Space Center has over 30 years of experience in propulsion testing. Four test facilities are currently available for large liquid propellant rocket engine testing, two of which are capable of simulating altitude conditions up to 54,000 ft (16,460 m) for the Space Shuttle Main Engine. The "A" Test Complex consists of two single-position, vertical-firing test stands designated A-1 and A-2. Both test stands are capable of static firing test articles up to 33 ft (10 m) in diameter and can generate up to 1.1 million pounds (4.9 million Newtons) of thrust. The "B" Test Complex consists of a dual-position, vertical-firing test stand designated the B-1/B-2 test stand. Each B test position is also capable of testing articles up to 33 ft (10 m) in diameter and can generate up to 11 million pounds (49 million Newtons) of thrust [1]. The testing of the Space Shuttle Main Engine (SSME) produces approximately 450,000 to 500,000 pounds (2,000,000 to 2,200,000 Newtons) of thrust that utilizes very large flame buckets and diffusers to control, deflect, cool, condition, and reduce the sound level of the plume before reaching the atmosphere. The exhaust produced by the engine during static-test firing is at extremely high temperatures, approximately 6538°R (3632 K); therefore, the walls of the flame bucket and the diffuser must be able to withstand the pressure load and

the high temperatures of the plume [2]. Since the walls are made of steel, a significant amount of cooling is required to reduce the temperature of the wall and the plume to reasonable values. This is accomplished through a process called transpiration cooling, in which 300,000 gallons per minute (19 m^3/s) of water are forced into the hot stream through holes on the surface of the flame buckets and cooling of the plume occurs through vaporization of the water [3]. While transpiration cooling has been effective, the cost of pumping such large amounts of water makes this process very expensive.

One alternative is the use of cryogenic lines and vessels which are used to maintain fluids at extremely cold, high pressure conditions. The utilization of cryogenics typically involves the design of liquefication, purification, refrigeration, storage, and transportation systems for the cryogenic fluids. These systems require expensive vacuum jackets, expansion joints, and devices; therefore, the implementation of a cryogenic system is not cost-effective. Other alternatives may exist in the research and development of thermal protection coating, tiles, and insulation systems.

Objective

The objective of this project is to investigate the feasibility of utilizing a thermal protection system to protect the walls of the flame buckets and diffusers used in the testing of liquid rocket systems, while at the same time providing operational cost savings with reduced maintenance. The study includes the potential use of coatings, and single and composite layer tiles as possible candidates for a protection system.

Coatings

The use of coatings is one alternative for utilization in a thermal protection system. Coatings are generally categorized as those applicable for metal surfaces such as gas turbines, rocket engines, furnace inner covers, radiant tubes, and electric elements, and those designed for refractory materials such as ceramic fibers, graphite, insulating brick, hard dense brick, and castables used for furnace linings. Some of the technological basis for the development of coatings includes surface protection, thermal shock resistance, chemical resistance, and reduced heat loss which lead to energy savings. Ceramic coatings are categorized into two areas, refractory coatings and metal coatings. Refractory coatings are generally formulated to prevent oxidation and fluxing of refractories at temperatures up to 4960°R (2756 K), while metal coatings are designed to prevent oxidation at temperatures up to 2660°R (1478 K). Ceramic coatings are being used effectively in various elevated temperature applications. Considering that high temperature corrosion takes place 500 to 5,000 times the rate of normal ambient air temperature corrosion, the use of coatings will extend the service life of components exposed to high temperatures, reduce the cost associated with replacing components, and increase production [4].

While coatings have several advantages, they also have many disadvantages. First, the occurrence of defects in coating systems causes the service life to fall short of the service life theoretically achievable with a flawless coating. In silicide and aluminide coatings, cracks are either introduced during application of the coating or are formed during exposure. These cracks are enlarged by thermal cycling until they penetrate

through the coating to the substrate material causing localized failure in a fraction of the time required for the coating as a whole to fail. Compositional defects are thus important considerations in selecting or tailoring a coating system, but even in the absence of cracking, a protective coating would ultimately fail at high temperatures because of the unavoidable progress of oxidation, diffusion, and evaporation reactions.

Second, lack of thickness control is one of the major reasons for premature coating failures. It is evident that protective life is to some degree a function of coating thickness; therefore, it should accurately be controlled for reproducible coating life from batch to batch or for uniform protection over a finished part. Applying an excessive coating usually is not practical because the weight increase may be unacceptable and excessively thick coatings can cause other problems such as edge growth or thermal stress cracking.

Third, inadequate reliability and a relatively short effective life are also major shortcomings. Premature coating failure, which occurs most frequently at the edges, is the factor that causes poor reliability. This can be due either to thinly coated areas or to the formation of edge fractures.

Fourth, coatings contribute to the high cost of coated refractory and metal components. The total coating cost is attributed more to the requirement for edge preparations, cleaning, inspection, and handling and joining restrictions than to the actual coating application process.

Last, the lack of very high temperature resistance is a major disadvantage. As stated before, coatings are only effective up to 4960°R (2756 K) for refractories and up to 2660°R (1478 K) for metals [5]. In some cases, these maximum operating temperatures

may be adequate, but in this study the stagnation temperature of 6538°R (3632 K) in the plume is well above these temperatures. While coating systems offers several advantages, the disadvantages associated with their use makes them unable to withstand the conditions of the plume; therefore, another alternative such as tiles must be investigated.

Metals and Metal Alloys

Metals and metal alloys can be considered as a first option for a thermal tile protection system. Metals can be described as elements that are defined by their properties such as hardness, toughness, malleability, electrical conductivity, and thermal expansion. They are well known for their high strength, toughness, and electrical and thermal conductance, as well as their resistance to moderate temperatures and prolonged stress. Although three-fourths of the elements used by mankind consist of metals, for several reasons few are used in their pure form. Pure metals may be too hard or too soft for use or they may be too expensive because of their scarcity. Above all, the most significant reason is that most desired properties sought in engineering are obtained by blending metals and other elements to form alloys [6].

The main disadvantage in the use of metals as a thermal tile protection system is their characteristically low service temperatures. Thus, metals with exposed surfaces can only be used in the flame bucket if they are cooled by transpiration cooling. However, their high strength and high thermal conductivity make them good candidates for support structures in the composite layer design discussed in Chapter 6. The following is a listing of the metals that are reasonable for the current application.

- Aluminum and aluminum alloys -- Aluminum is the most abundant of all metals found in the earth's crust, comprising about 8% of the crust and is produced in quantities second only to iron. Bauxite, which is the principal ore for aluminum, is composed of hydrous aluminum oxide and various other oxides. The bauxite ore is crushed into powder and treated with hot caustic soda to remove impurities. From this solution, alumina (aluminum oxide) is extracted and dissolved in a molten sodium-fluoride bath at 2185 - 2260°R (1214 - 1256 K) and then subjected to direct-current electrolysis. Aluminum metal forms at the cathode, while oxygen is released at the anode.

  Aluminum and its alloys are favored because of their high strength-to-weight ratio, resistance to corrosion by various chemicals, high electrical and thermal conductivity, nontoxicity, reflectivity, and ease of formability and machinability [7]. As with most metals, aluminum has a relatively low service temperature, approximately 1260°R (700 K), which makes it an undesirable material for use as a tile insulation material, but its high thermal conductivity, 133 Btu/hr•ft•°R (230 W/m•K), makes it an attractive material for use as a support material in composite layer tiles [8].

- Carbon steels -- Various elements are added to steels to impart properties of hardenability, strength, hardness, toughness, wear resistance, workability, weldability, and machinability. The higher the percentages of these elements in steel, the higher are the particular properties that they impart. For carbon steels, a higher carbon content improves the strength, hardness, and wear resistance, and

reduces the ductility, weldability, and toughness of the steel. Low-carbon steel, sometimes referred to as mild steel, has less than 0.30% carbon. It is used in common products that do not require high strength. Medium-carbon steel has 0.30% to 0.60% carbon and is generally used in applications requiring higher strength than low-carbon steels. High-carbon steel has more than 0.60% carbon and is generally used for parts requiring strength, hardness, and wear resistance. On the average, carbon steels have relatively low thermal conductivities, approximately 17 Btu/hr•ft•°R (29 W/m•K), and have service temperatures around 2400°R (1333 K).

- Copper and copper alloys -- Copper is found in several types of ores with the most common being sulfide ores. The ores are usually obtained from open-pit mines and are generally considered low grade, even though some contain up to 15% copper. The ore is crushed and formed into a slurry (a watery mixture with insoluble solid particles) and then ground into fine particles in ball mills. Chemicals and oil are then added, and the mixture is agitated until the mineral particles form a froth, which is scraped and dried. The dry copper concentrate, containing as much as one-third copper, is typically smelted and refined. The copper is further refined electrolytically to a purity of at least 99.95 % for applications such as electrical conductors.

Copper and its alloys have properties somewhat similar to those of aluminum alloys. They are also considered some of the best conductors of electricity and heat, and have good corrosion resistance. Because of their

properties, copper and its alloys are among the most important metals. Copper alloys are desired for applications where a combination of electrical, mechanical, corrosion resistant, nonmagnetic, thermal conductive, and wear resistant properties are needed [7]. One disadvantage of copper in its use as a tile insulation material is its relatively low service temperature, approximately 1830°R (1017 K), but its high thermal conductivity, 231 Btu/hr•ft•°R (400 W/m•K), makes it a desirable material for use as a support material in composite layer tiles [8].

- Titanium and titanium alloys -- Ores containing titanium are reduced to titanium carbide in an arc furnace and are then converted to titanium chloride in a chlorine atmosphere. The compound is reduced further by distillation and leaching (dissolving) which forms sponge titanium. It is then pressed into billets, melted, and poured into ingots to be processed later into various shapes. The complexity of the operations adds to the high cost of titanium. Titanium alloys have been developed for service temperatures up to 1460°R (811 K) for extended periods of time and up to 1860°R (1033 K) for shorter periods. Although expensive, it is attractive for applications where high strength-to-weight ratio and corrosion resistance are important such as aircraft, jet engine, racing-car, chemical, petrochemical, and marine components; submarine hulls; and biomaterials. Pure titanium has excellent corrosion resistance for applications where strength is considered secondary [7].

Refractory Metals and Alloys

The use of refractory metals and alloys is a second option for a thermal tile protection system. Molybdenum, niobium (columbium), tungsten, and tantalum are classified as refractory metals because of their high melting points. Refractory metals and alloys maintain their strength at elevated temperatures more than the majority of other metals and alloys. Because of this advantage, they are most useful in electronics, nuclear power, rocket engines, gas turbines, and various other aerospace applications. The temperature range for some of these applications is between 2460°R (1367 K) and 4460°R (2478 K) where strength and oxidation are a major concern [7].

The refractory metals form a volatile oxide at high temperatures; therefore, they must be processed in a vacuum or protective atmospheres with the use of special melting and casting techniques [9]. While oxidation resistance can be improved by suitable alloying, this process compromises high temperature strength, and the improvement in oxidation resistance is insufficient for most high temperature purposes. It is generally accepted that the use of these refractory metals depends on suitable protective coverings [10]. The following is a listing of the refractory metals.

- Molybdenum -- The main source for molybdenum is the mineral molybdenite (molybdenum disulfide). The ore is processed, concentrated, and reduced by reactions with oxygen and then hydrogen. The molybdenum is further processed into various shapes with the use of powder metallurgy techniques. Several properties of molybdenum are high melting point, high modulus of elasticity, good resistance to thermal shock, and good electrical and thermal conductivity.

Molybdenum is used in larger amounts than any other refractory metal. It is an important alloying element in casting and wrought alloys and imparts strength, toughness, and corrosion resistance. The low resistance of molybdenum to oxidation is a major disadvantage. It tends to oxidize at temperatures above 1410°R (783 K); therefore, the use of protective coatings is necessary. Molybdenum is typically used in the production of solid propellant rockets, jet engines, honeycomb structures, electronic components, heating elements, and dies for die casting.

- Niobium (Columbium) -- Niobium is processed from ores by reduction and refinement, and from powder by melting and shaping into ingots. It is also used as an alloying element in various alloys and superalloys. Niobium possesses good ductility and formability and has higher oxidation resistance than other refractory metals. Combined with other alloying elements, niobium alloys can be produced with moderate strength and good fabrication characteristics. The principal uses of niobium alloys are in rocket, missile, nuclear, chemical, and superconductor applications.

- Tantalum -- Tantalum possesses a high melting point of 5885°R (3269 K), good ductility, and resistance to corrosion, but its high density and poor resistance to chemical oxidation at temperatures above 760°R (422 K) are major disadvantages. Typical applications for tantalum are in electrolytic capacitors; various components in the electrical, electronic, and chemical industries; and thermal applications such

as furnaces and acid-resistant heat exchangers. Tantalum-based alloys are available in forms for use in missiles and aircraft.

- Tungsten -- Tungsten, which is the most plentiful of all refractory metals, is processed from ore concentrates by chemical decomposition. It is further processed in a hydrogen atmosphere by powder metallurgy techniques. Tungsten has the highest melting point of any metal (6630°R, 3683 K) and is known for its high strength at elevated temperatures, but it has high density, brittleness at low temperatures, and poor resistance to oxidation. Tungsten and its alloys are used in applications involving temperatures above 3460°R (1922 K), such as nozzle throat liners in missiles, jet and rocket engine components, circuit breakers, welding electrodes, and spark-plug electrodes. Tungsten is also an important element in tool and die steels, imparting strength and hardness at elevated temperatures [7].

Ceramics

The third choice for a thermal protection system involves the use of advanced ceramics. Ceramics, one of the three main families of materials, are defined as crystalline compounds of metallic and nonmetallic elements. As a class, there are four principal distinguishing traits of ceramics. First, they are crystalline structures, like metals, and have little or no electrical conductivity at room temperature because of the presence of fewer free electrons. Second, they have higher melting points on average, high stability, and greater chemical resistance than metals and organic materials. Third, they are typically the hardest of engineering materials. Last, they are extremely stiff and rigid, and

under mechanical stress they demonstrate little or no yield and exhibit brittle fracture. The following is a list of the main eight classes of ceramic type materials that are of primary interest to industry.

1. Various types of glass, which are based on silica (SiO_2), with additives to reduce the melting point or give other distinctive properties.
2. Traditional vitreous ceramics or clay products used to make pottery, plates, cups, sanitary ware, tiles, and bricks.
3. Advanced high-performance ceramics which have applications in cutting tools, dies, engine parts, and wear-resistant parts.
4. Cement and concrete, two of the three primary bulk materials of civil engineering.
5. Rocks and minerals.
6. Ceramic composites, including fibers, particulates, and whiskers.
7. Refractory ceramics, including oxides, carbides, borides, and nitrides.
8. Other miscellaneous ceramics such as beryllides, aluminides, silicides, and lanxides which are classified as metals, but are often thought of as ceramics because their physical characteristics are similar to those materials in the ceramic family [11].

The discerning difference between advanced ceramics and traditional ceramics is attributed to the specialized properties that advanced ceramics possess and the sophisticated processing they require. Traditional ceramic materials are based primarily on natural raw materials of clay and silica, processed by forming and sintering to produce pottery and brick, while advanced ceramics include artificial raw materials such as alumina (AlO_3), silicon carbide (SiC), silicon nitride (Si_3N_4), and zirconium oxide (ZrO_2), as well as hydroxides, carbonates, and others. Applications for advanced ceramics include rockets, turbine blades, nuclear reactors, automobile engine parts, mechanical parts, and artificial

bones for the human body. All ceramics have attractively low densities, high moduli, and high melting points which lead to a low creep rate. In addition to these properties, advanced ceramics have distinctive properties such as high resistance to heat, wear, and corrosion, as well as specialized electrical and optical properties, which allow them to perform well in various high value applications. The three principal barriers that affect their widespread use include the unreliability of many products of advanced ceramics, which results from the tendency of these ceramics to fail at an unacceptably high rate because of their inherent brittleness, the expensiveness of the sophisticated processing required to produce many advanced ceramic parts, and the difficulty of producing parts with consistent properties [12]. While advanced ceramics have a number of desirable properties, they also have various negative properties that stand in the way of their widespread application in industry. The properties of these advanced ceramics are dependent upon the molecular bonding of the ceramic material and the ceramic processing during fabrication.

Bonding of ceramics. Atoms in a ceramic material are primarily held together by covalent or ionic bonding, or a combination of the two. Covalent bonding involves the sharing of electrons by two adjacent atoms resulting in a directional bond. Ceramics formed by covalent bonding have distinctive characteristics which include high hardness, superior chemical inertness, no ductility, low thermal expansion, and low electrical conductivity. These bonds can generate strong, rigid three-dimensional structures such as diamond, silicon carbide (SiC), or silicon nitride (Si_3N_4) fibrous chain structures such as

asbestos, and laminar structures such as graphite, mica, and clays. Ionic bonding involves the transfer of one or more electrons between adjacent atoms resulting in oppositely charged atoms bonded by a coulombic attraction. Ceramics formed by ionic bonding have characteristics such as low ductility, high thermal expansion, and low electrical conductivity. Ionic ceramics tend to form close-packed structures such as sodium chloride calcium, fluoride, and magnesium oxide. There are some oxides such as Al_2O_3, SiO_2, and ZrO_2 that exhibit both ionic and covalent characteristics.

Ceramic processing. The multistage fabrication process for ceramics includes powder production, powder conditioning, shaping, and densification. Ceramic materials are very sensitive to small flaws introduced during processing, and these flaws, either chemical (impurities leading to second phases, particularly liquids) or physical (foreign inclusions or porosity), can occur in each of the stages and cannot be corrected in the subsequent processing stages. Inadequate fabrication techniques and the high sensitivity of ceramics to thermal and mechanical shock, a result of inherent brittleness, are two specific problem areas receiving the most attention. These two problems are the major focus of intense worldwide research by scientists, engineers, chemists, designers, and material specialists. In time, the issue involving inadequate fabrication techniques will be solved as technology matures, but the problem of inherent brittleness cannot be alleviated so methods must be found to combat this obstacle. The properties of ceramics, which will be discussed in the following sections, result from a combination of the effects of atomic bonding and microstructure.

Brittleness and low strain tolerance. Brittleness is the primary limitation to the wider use of ceramics. Ceramics fail in brittle mode because of the presence of fabrication and structural flaws that result in stress concentration and fracture at a load well below the theoretical strength. These flaws arise either during the preparation of the ceramics for use, such as in the course of machining and handling when chipping at the corners and edges occurs, or during service when unexpected particle impact may lead to chipping. The brittleness of ceramics can sometimes be associated with their limited strain to failure or low strain tolerance. Since they are sensitive to flaws, catastrophic failure precedes plastic deformation for polycrystalline ceramics. Ceramics usually have high moduli which result in failure strains that are on an order of magnitude or more lower than those for metals [11].

Mechanical strength. The risk of structural failure is another big stumbling block to many potential uses of ceramics at the present time and is the cause of the understandable wariness of engineers offered a brittle material in substitution for a metal. Ceramics such as silicon carbide possess only a tensile strength around 15,000 psi (103 MPa) at room temperature compared to a tensile strength of 100,000 psi (690 MPa) for certain metal alloys, but ceramics often have superior compressive strength [6]. Some ceramics have tensile strengths around 29,000 psi (200 MPa), about half that of steel, while others such as pottery, brick, and stone have tensile strength much lower, around 2900 psi (20 MPa) [13].

Modulus of elasticity (Young's modulus). As a class, ceramics are the most rigid of all materials. A majority of them are stiffer than most metals, with a modulus of elasticity in tension of 4.93 to 6.41×10^6 psi (34,000 to 44,200 MPa), compared with 2.86×10^6 psi (19,700 MPa) for steel [11]. The larger ceramic moduli reflects the greater stiffness of the ionic bond in simple oxides and of the covalent bond in silicates [13].

Toughness. Most ceramic materials are not tough. Cracks in ceramic materials propagate rapidly and result in fracture of the part. There have been two approaches to the problem of low toughness, from both a design and a materials aspect. The principal design approach has been to prestress the ceramic in compression by shrink-fit or lamination, but this approach only increases the resistance to crack initiation and does not increase the toughness. The broader material approach concentrates on increasing the toughness of ceramic materials with the use of ductile additives such as cobalt and nickel [11].

Hardness. Ceramics are the hardest of all solid materials. They are intrinsically hard because of the presence of ionic or covalent bonds which introduce enormous lattice resistance to the motion of a dislocation. Ceramics such as corundum (Al_2O_3), silicon carbide (SiC), and diamond © are so hard that they are used as abrasives. They will cut, grind, or polish almost anything including glass [13].

Density. Since ceramics are largely composed of light atoms such as oxygen, carbon, silicon, and aluminum, and their structures usually contain large open spaces, their densities tend to be low.

Joint stresses. In practical applications, ceramics have to be attached to another ceramic or metal. Several common ways in which this is accomplished are by diffusion, welding, cosintering, or suitable interlayers. Certain ceramics such as silicon nitrides and silicon carbides have obstacles that arise during the bonding process such as their chemical inertness to several of the braze filler materials or metals. Localized high stresses at the joint interfaces, resulting in either debonding or fracture within the ceramic, can be a repercussion of excessive mismatches in Young's modulus, the thermal expansion coefficient, and Poisson's ratio.

Thermal shock resistance. Fracture caused by sudden changes in temperature is a problem with ceramics. Mechanical strength, elastic modulus, thermal conductivity, and the coefficient of thermal expansion are the significant properties that govern thermal shock. The severity of thermal shock is a strong function of the operating conditions and the geometry of the component. The effect of thermal stresses on various materials depends on the stress level, the stress distribution in the body, and the stress duration; therefore, it is impossible to define a single thermal stress resistance factor that satisfies all situations [11]. While some ceramics, like ordinary glass, will take only a temperature "shock" of 636°R (353 K) before they break, others, like silicon nitride, will stand a

sudden change of 1392°R (773 K) which makes them prime candidates for environments as violent as internal combustion engines [13].

Melting temperature. The melting temperature of a material is a function of the strength of its atomic bond. Multivalent ionic ceramics such as beryllia (BeO), alumina (Al_2O_3), and zirconia (ZrO_2) have much higher melting temperatures, and covalent ceramics such as titanium carbide (TiC) and hafnium carbide (HfC) have the highest melting temperatures of all ceramics.

Thermal conductivity. Thermal conductivity is controlled by the amount of heat energy present, the nature of the heat carrier in the material, and the amount of heat dissipation. Lattice vibrations and radiation are the primary ways to carry heat in ceramics.

Thermal expansion. The rate of thermal expansion of ceramics is determined by the bond strength and the atomic structure. Covalent bonding is directional and produces ceramic structures having large open spaces. When a covalent bond is heated, some of the expansion can be absorbed by the open space within the structure or by bond angle shifts, resulting in low expansion. Ionic ceramics have close-packed atomic structures; therefore, they have relatively high coefficients of thermal expansion [11].

Creep of ceramics. Creep becomes a problem when the temperature of a ceramic is greater than one-third of its melting temperature. Since the melting temperature of engineering ceramics is over 4092°R (2273 K), the design problem dealing with creep

effects occurs only during very high temperature applications [13]. Typically, the creep strain of high performance ceramics at elevated temperatures is several orders of magnitude less than that for metals at a given temperature and stress level [11].

Because of their heat-resistant qualities, ceramics have become an important class of materials for advanced material applications. Most of the desirable properties needed for application as a thermal tile protection system are found in ceramics. These properties include high melting temperatures, high strength and hardness at elevated temperatures, high modulus of elasticity, low density, low thermal expansion, low thermal conductivity, and high temperature corrosion resistance. However, ceramics are inherently brittle and possess tensile strengths that are approximately one order of magnitude lower than their compressive strengths [7]. The brittleness of ceramics combined with their low tensile strength are the major reasons why a single layer ceramic tile protection system would not be a practical design.

CHAPTER 2

CLASSES OF CERAMICS

Introduction

As the applications for ceramic materials increase, it has become necessary for material engineers to have reliable ceramic property data on which to base their material selection and design limitations. Regardless of the amount of published ceramic property data, the type and quality of data required for design are scarce. This is due to the lack of extensive testing of a given ceramic and the sensitivity of the properties of ceramics to fabrication and testing techniques, which makes comparisons of data from various sources difficult. As a result, during initial material selection it is necessary to conduct property evaluations on specimens of the selected materials [14]. The following information serves as a basic introduction to the general characteristics of various ceramic materials.

Aluminides

Aluminides are intermetallic compounds of aluminum and another metal (Me_xAl_y). Although these compounds are classified as metals, they are included in the ceramic family because of their physical characteristics which are similar to those of ceramic materials. Interest in aluminides exists because of their strength and oxidation resistance. Of the aluminides, nickel aluminide (NiAl) has been investigated more extensively than any other aluminide.

Physical properties. None of the aluminides have melting temperatures greater than 4460°R (2478 K). Only a few of the aluminides have melting temperatures above 3460°R (1922 K).

Thermal properties. Linear thermal expansions of NiAl, CrAl, and UAl_2 are less than 1.3% at 1960°R (1089 K).

Mechanical properties. Bend strengths of the aluminides of titanium and nickel range from 90 to 150×10^3 psi (620 to 1034 MPa) at temperatures between 530 and 1960°R (294 to 1089 K). Metallic additions of titanium, zirconium, or nickel improve the strength values of the aluminides. For composites such as NiAl-Zr and NiAl-Ti, impact strengths of 90 and 54 in•lb (1.04 and 0.62 m•kg) have been reported at room temperature. Below 1560°R (867 K), NiAl has brittle characteristics of ceramic materials, and above 1560°R (867 K) it has ductile characteristics similar to those of metals. The modulus of elasticity for NiAl decreases from 25 to 18×10^6 psi (17 to 12×10^4) at temperatures ranging from 530 to 1960°R (294 to 1089 K). Typically, the microhardnesses of aluminides of cobalt, titanium, tantalum, nickel, and thorium are below 7.1×10^5 lbm/in^2 (5.0×10^8 kg/m^2).

Oxidation resistance. One of the most desirable properties of aluminides is their oxidation resistance. Aluminides have good oxidation resistance up to 2460°R (1367 K) [14].

Common aluminides. Two notable types of aluminides include nickel aluminide and titanium aluminide (TiAl and Ti_3Al). The characteristics of these two aluminides are quite similar and are listed below.

- Nickel aluminide (Ni_3Al) -- Nickel aluminide has been forseen as the next generation of superalloys or high temperature structural alloys. It has high strength and oxidation resistance at elevated temperatures and lower density than traditional superalloys and titanium alloys. The compounds are extremely brittle at room temperature, but ductility can be improved by alloying and controlled thermomechanical processing.
- Titanium aluminide (TiAl and Ti_3Al) -- Titanium aluminide is another intermetallic that is considered as the next generation of superalloys or high temperature structural alloys. The status of titanium aluminide is mainly due to its high strength and temperature at elevated temperatures and lower density than traditional superalloys and titanium alloys. The compounds of titanium aluminide are very brittle at room temperature, but the ductility can be improved by alloying and controlling the thermomechanical processing [15].

Beryllides

Beryllides are intermetallic compounds of beryllium and another metal (Me_xBe_y). Although these compounds are classified as metals, they are included in the ceramic family because of their physical characteristics which are similar to those of ceramic materials. Beryllides are a class of refractory materials and are mainly of interest because of their

high strength, strength retention at elevated temperatures, thermal shock resistance, and oxidation resistance. The limiting use temperature of beryllides appears to be about 3460°R (1922 K). Beryllides of tantalum, niobium, and zirconium are the only materials in this class that have potential for structural applications at elevated temperatures.

Physical properties. Of the beryllides, tungsten beryllide (WBe_2) has the highest density, approximately 636.8 lbm/ft^3 (10,200 kg/m^3), while titanium beryllide ($TiBe_{12}$) with a density of 143.6 lbm/ft^3 (2300 kg/m^3) is the least dense. Most beryllides have densities that range from 187.3 to 312.1 lbm/ft^3 (3000 to 5000 kg/m^3).

Thermal properties. Tantalum and hafnium beryllides have low specific heats, approximately 0.25 Btu/lbm•°R (1047 J/kg•K) in a temperature range of 1460 to 2960°R (811 to 1644 K), while molybdenum, zirconium, and niobium beryllides have higher specific heat values of about 0.4 Btu/lbm•°R (1675 J/kg•K) in the same temperature range. The linear thermal expansions of uranium, zirconium, hafnium, niobium, and tantalum beryllides are approximately 2% at 2960°R (1644 K). Beryllides of zirconium, niobium, tantalum, molybdenum, and uranium are reported to have thermal conductivities which range from 50 to 20 Btu/hr•ft•°R (87 to 35 W/m•K) between 1160 and 3160°R (644 and 1756 K).

Mechanical properties. For beryllides at 530°R (294 K), the moduli of elasticity are below 50×10^6 psi (34×10^4 MPa). Microhardnesses for beryllides range between 7.1×10^5 and 1.85×10^6 lbm/in^2 (5.0×10^8 and 1.3×10^9 kg/m^2) at 530°R (294 K). The bend

strengths of the beryllides of tantalum and niobium are about 30×10^3 psi (207 MPa) between 530 and 1460°R (294 and 811 K), with maximum strengths of about 35×10^3 psi (241 MPa) occurring at 2710°R (1506 K).

Oxidation resistance. Beryllides of tantalum, niobium, zirconium, and titanium have good oxidation resistance. An oxide layer less than 1/1000 of an inch in (2.54×10^{-5} m) depth develops up to 2960°R (1644 K). The oxidation rate increases moderately between 2960 to 3460°R (1644 to 1922 K) after 100 hours in moderately flowing air, dry and moist, but above 3460°R (1922 K) the oxidation becomes severe [14].

Borides

Borides are compounds of metals with boron (Me_xB_y). The commercial applications of boride ceramics are limited, and they are not produced significantly. Of the boride ceramics, refractory diborides (MeB_2) are the subject of extensive research for potential applications as structural materials in the aerospace industry. Their use is based on their high oxidation resistance and strength retention at elevated temperatures. Most of the data available is limited to diborides of the transition metals.

Physical properties. Metal-boron compounds range from Me_3B to MeB_{12}. The diborides are characterized by their hexagonal structure, and they are considered the most temperature-stable of all the boride compounds. Of the borides, hafnium diboride has the highest melting temperature, approximately 6360°R (3533 K). The densities of the

refractory borides range from 156.1 to 1042.5 lbm/ft^3 (2500 to 17,000 kg/m^3), with tungsten boride (W_2B) having the highest density.

Thermal properties. Typically, the specific heats of borides up to 4460°R (2478 K) are less than 0.35 Btu/lbm•R (1465 J/kg•K). For borides in the range of 530 to 4460°R (294 to 2478 K) , linear thermal expansion coefficients vary 2% or less. The thermal conductivity data available for borides are limited, and the values obtained from different sources disagree significantly. In general, borides have moderate conductivities with average values of approximately of 80 and 15 Btu/hr•ft•°R (139 and 26 W/m•K) at 530 and 3460°R (294 and 1922 K), respectively.

Mechanical properties. At room temperature, the elastic moduli for diborides is in the range from 30 to 60×10^6 psi (21 to 41×10^4 MPa). Values for microhardness range between 1.85 to 4.69×10^6 lbm/in^2 (1.3 to 3.3×10^9 kg/m^2). The data on the strength of borides at elevated temperatures are limited and poorly defined; therefore, no general statements can be made about strength properties.

Oxidation resistance. The main interest in the boride family revolves around their resistance to oxidation, with HfB_2, ZrB_2, and CrB being the most significant materials in this respect. At temperatures where liquid B_2O_3 would normally be present (above 1530°R, 850 K), water vapor increases the rate of oxidation of borides, but at temperatures at which B_2O_3 vaporizes as rapidly as it forms (above 3190°R, 1772 K) the effects of water vapor are not significant [14].

Common borides. Two typical borides include chromium boride and zirconium boride. Some properties and general characteristics of these materials are listed below.

- Chromium boride (CrB, Cr_2B, Cr_3B_2) -- Chromium boride occurs as very hard crystalline powder in several phases, with the CrB orthorhombic crystal melting at 3192°R (1773 K), the hexagonal crystal Cr_2B melting at 3822°R (2123 K), and the tetragonal crystal Cr_3B_2 melting at 4020°R (2233 K). Chromium boride has good resistance to oxidation at high temperatures, is stable to strong acids, and has high heat-shock resistance up to 2860°R (1589 K). The transverse rupture strength is from 80,000 to 135,000 psi (552 to 9308 MPa).
- Zirconium boride (ZrB_2) -- Zirconium boride has a melting point of 5856°R (3253 K) and a tensile strength of 35,000 to 40,000 psi (241 to 276 MPa). It is resistant to nitric and hydrochloric acids, molten aluminum and silicon, and oxidation. Zirconium boride is mainly used for crucibles and rocket nozzles [15].

Carbides

Carbides are compounds of elements with carbon (Me_xC_y). The materials included in this group are considered the most important engineering materials because they have the highest melting temperatures and are extremely hard. The general limitation of most carbides is the lack of oxidation resistance in a moist atmosphere. Silicon carbide is the only exception to this drawback, and because of this, its products are used commercially in high-temperature oxidizing environments.

Physical properties. Metal-carbon refractory compounds range from Me_2C to MeC_2. In general, the crystal structures of carbides vary extensively, but in carbides of the transition metals the cubic crystal structure predominates. Of the carbides, the monocarbides of hafnium and tantalum have the highest melting temperature, approximately 7560°R (4200 K). The densities of the more stable refractory carbides range from 156.1 to 1,061.3 lbm/ft^3 (2500 to 17,000 kg/m^3), with the tungsten carbides, WC and W_2C, having the highest density and the beryllium and boron carbides having the lowest density.

Thermal properties. At room temperatures the specific heats of carbides range between 0.05 and 0.3 Btu/lbm•°R (209 to 1256 J/kg•K), with beryllium carbide (Be_2C) and boron carbide (B_4C) having the highest specific heats at elevated temperatures. For carbides between 530 to 4460°R (294 to 2478K), linear thermal expansion coefficients range from 3 to 6×10^{-6}/°R (1.7 to 3.3×10^{-6}/K) , with uranium carbide (UC) and plutonium carbide (PuC) having the highest coefficients and B_4C, SiC, and WC having the lowest coefficients. Carbides tend to exhibit an increase in thermal conductivity with an increase in temperature. At temperatures in the range of 1460 to 3460°R (811 to 1922 K), carbides have thermal conductivities between 10 and 30 Btu/hr•ft•°R (17 and 52 W/m•K), respectively.

Mechanical properties. At room temperature, most carbides possess an elastic modulus of approximately 50×10^6 psi (34×10^4 MPa), with the tungsten carbides having the higher moduli. Microhardness values for carbides range from 1.14 to 4.55×10^6 lbm/in^2

(8.02×10^8 to 3.2×10^9 kg/m^2), with B_4C, SiC, and TiC having the higher hardnesses. The data on the strength of carbides vary widely and are limited and poorly defined; therefore, no general statements can be made about their strength properties.

Oxidation resistance. With the exception of silicon carbide, carbides generally have poor oxidation resistance. Silicon carbide is the most resistant of all the carbides up to 3460°R (1922 K) [14].

Common carbides. Two common types of carbides include boron carbide and silicon carbide. General characteristics of these carbides are listed below.

- Boron Carbide (B_4C) -- Boron carbide is one of the hardest ceramic materials. Its use is limited to low temperatures and to applications in which high hardness and wear resistance are required and high component cost is justified.
- Silicon Carbide (SiC) -- This ceramic seems to be the best bet for high temperature structural use. The creep resistance is outstanding up to 2832°R (1573K), and the low thermal expansion and high thermal conductivity give silicon carbides an excellent thermal shock resistance in spite of its low toughness [12].

Mixed Oxides

Mixed oxides are a group of ceramic materials that consists of mixtures of two or more oxides that may form glasses, compounds, or solid solutions. The first ceramic products were made of mixed oxides, and from them a wide range of compositions has evolved for commercial application. The melting point in all mixed oxide compounds is

always lower than that of the refractory component in the compound. Zirconates, best known for their electrical properties, have relatively high melting points, approximately 2260°R (1256 K), in comparison to other mixed oxides. Due to their lower melting temperatures, mixed oxides are less desirable for high temperature applications than pure oxides. Among the mixed oxides, the silicates of aluminum, magnesium, and zirconium and the aluminate of magnesium hold the most interest for structural applications up to 3460°R (1922 K), but silicates, in general, have poor resistance to high temperature stress because of glass formation. One of the strongest materials in the mixed oxide group is magnesium aluminate.

Nitrides

Nitrides are compounds of elements with nitrogen (Me_xN_y). Of this class, the most readily available and useful materials are boron nitride (BN) and silicon nitride (Si_3N_4). Aside from silicon and boron nitrides, there is minimal commercial production of other nitride ceramics.

Physical properties. Typically, the crystal structures of nitrides are either cubic or hexagonal structures. The problem that exists with the use of nitrides is their characteristically poor stability at elevated temperatures. The mononitrides of titanium, zirconium, hafnium, and tantalum are the most refractory and thermally stable of all the nitrides and have melting temperatures of approximately 5960±100°R (3311±56 K). With densities slightly under 998.8 lbm/ft^3 (16,000 kg/m^3), nitrides composed of tantalum and tungsten have the highest theoretical densities, while nitrides of the alkaline-earth metals

such as boron, aluminum, and silicon nitrides have the lowest theoretical densities ranging from 156.1 to 218.5 lbm/ft^3 (2500 to 3500 kg/m^3).

Thermal properties. Above 1460°R (811 K), compounds such as boron nitride (BN), and beryllium nitride (Be_3N_2) have specific heats around 0.4 Btu/lbm•°R (1675 J/kg•K) which are unequaled by any other nitrides. Some nitrides such as Mg_3N_2, AlN, and Si_3N_4 have specific heats around 0.3 Btu/lbm•°R (1256 J/kg•K), while others have values less than 0.2 Btu/lbm•°R (837 J/kg•K). The linear thermal expansion of nitrides is moderate to low. For most nitrides up to 2960°R (1644 K), the thermal expansion is below 1.5%, but the thermal expansion for silicon nitride is exceptionally low around 0.4%. The thermal conductivities of the nitrides that have been measured are less than 20 Btu/hr•ft•°R (35 W/m•K) between 530 and 3460°R (294 to 1922 K). It has been noted that the conductivities of nitrides of the transition metals tend to increase with increasing temperatures.

Mechanical properties. The data on strength and elastic modulus are limited to only a few nitrides. Nitrides such as AlN, TiN, TaN, and ZrN exhibit moderate strength and high elastic moduli, while other nitrides such as BN and Si_3N_4 have low strengths and low moduli of elasticity. In general, the highest and lowest property values are exhibited by AlN and BN, respectively. Strength values for Si_3N_4 vary considerably depending on the composition and manufacturing methods. Most nitrides have values for microhardness that range between 1.42 to 2.84×10^6 lbm/in^2 (9.98×10^8 to 2.0×10^9 kg/m^2). The only exception is BN, which has a hardness of approximately 2.84×10^5 lbm/in^2 (2.0×10^8 kg/m^2)

in its hexagonal form, and a hardness similar to that of diamond in its synthesized cubic form. Both BN and Si_3N_4 have high thermal shock resistance, with BN being the better of the two.

Oxidation resistance. Most nitrides are poor in oxidation resistance, with the notable exceptions up to 2460°R again being BN and Si_3N_4. The nitrides of titanium, zirconium, hafnium, and tantalum have moderate oxidation resistance, while nitrides of vanadium and niobium have relatively poor oxidation resistance. Nitrides of beryllium, aluminum, and the rare earth metals are easily attacked by water vapor [14].

Common nitrides. Two notable types of nitrides are boron nitride and silicon nitride. Some typical characteristics and properties of these materials are listed below.

- Boron Nitride (BN) -- Boron nitride has a very low coefficient of friction, is a nonconductor of electricity, and is attacked by nitric acid. It reacts with carbon at 4092°R (2273 K) to form boron carbide and sublimes at 5892°R (3273 K). When boron nitride is compressed at very high pressure and high heat, the hexagonal crystal structure is converted into a cubic structure forming a pressed material that has great hardness and strength, and is stable up to 3960°R (2200 K) [15].
- Silicon Nitride (Si_3N_4) -- Silicon nitride has an excellent thermal shock resistance because of its high thermal conductivity and low thermal expansion. These qualities combined with a high hot strength make it the prime candidate for ceramic engine components, such as turbine disks and rocket nozzles [12].

Silicides

Silicides are metalloid compounds of silicon and another metal (Me_xSi_y). There are a few desirable properties found in this class, and they include good oxidation resistance and retention of strength up to 2960°R (1644 K). Of the refractory silicides, the disilicides of molybdenum, tungsten, and tantalum have the greatest potential for high temperature applications.

Physical properties. Among the silicides, the highest melting temperatures range from 4460 to 4960°R (2478 to 2756 K). Uranium silicide (U_3Si) has the highest density, approximately 973.9 lbm/ft^3 (15,600 kg/m^3), while the silicides of boron have the lowest density, approximately 149.8 lbm/ft^3 (2400 kg/m^3). The majority of the silicides have densities between 312 and 624 lbm/ft^3 (5000 and 10,000 kg/m^3).

Thermal properties. The silicides of titanium exhibit relatively high specific heats with values of approximately 0.1 to 0.2 Btu/lbm•°R (419 to 837 J/kg•K) between 530 and 2260°R (294 to 1256 K). Silicides with low specific heat values include tantalum, tungsten, and uranium with values varying from about 0.04 to 0.08 Btu/lbm•°R (167 to 335 J/kg•K) between 530 to 2960°R (294 to 1644 K). The silicides of uranium and manganese possess high coefficients of thermal expansion, approximately 9×10^{-6}/°R (16×10^{-6}/K) , while silicides of molybdenum, tantalum, tungsten, and lanthanum have low coefficients of thermal expansion, varying from 3 to 5×10^{-6}/°R (5.4 to 9×10^{-6}/K). Other silicides such as those of chromium, titanium, vanadium, niobium, and cobalt have intermediate values that range from 5 to 7×10^{-6}/°R (9 to 12.6×10^{-6}/K). The highest

reported thermal conductivity for the class of silicides is found in molybdenum disilicide $MoSi_2$, which has a thermal conductivity that decreases from 35 to 12 Btu/hr•ft•°R (61 to 21 W/m•K) between 530 and 2660°R (294 and 1478 K). Lower values of thermal conductivity are exhibited by the silicides of boron, manganese, and uranium, which have values that range from 2 to 10 Btu/hr•ft•°R (3.5 to 17 W/m•K) between 560 and 960°R (311 to 533 K).

Mechanical properties. The silicides of tungsten, molybdenum, and chromium are reported to have relatively high bend strengths, above 40×10^3 psi (276 MPa), and increase with temperature to values twice as high at about 2260°R (1256 K). Moduli of elasticity of approximately 40 to 50×10^6 psi (28 to 34×10^4 MPa) have been recorded for silicides of molybdenum, tungsten, and tantalum up to 2460°R (1367 K). Microhardnesses for silicides range from 7.1×10^5 to 3.56×10^6 lbm/in^2 (5×10^8 to 2.5×10^9 kg/m^2) with high hardness values of approximately 2.84×10^6 lbm/in^2 (2.0×10^9 kg/m^2) reported for boron silicides and low hardness values below 1.42×10^6 lbm/in^2 (9.98×10^8 kg/m^2) for the silicides of titanium, niobium, and uranium. Intermediate hardness values of 1.42 to 2.13×10^6 lbm/in^2 (9.98×10^8 to 1.5×10^9 kg/m^2) are reported for silicides of zirconium, vanadium, tantalum, chromium, molybdenum, thorium, and tungsten.

Oxidation resistance. For silicides, the resistance of oxidation results from the formation of a coating of silica or silicate on the surface upon exposure. At temperatures below 2460°R (1367 K), the surface is poorly protected, but preoxidation alleviates this problem. Good oxidation resistance is reported for silicides of molybdenum, tungsten,

tantalum, titanium, and boron, with compounds having the highest silicon contents being the superior material [14].

Common silicides. Two typical silicides include molybdenum disilicide and tungsten disilicide. Various properties and characteristics of these silicides are listed below.

- Molybdenum disilicide ($MoSi_2$) -- Molybdenum disilicide is a brittle material that can be bent into shape at temperatures above 2460°R (1367 K). It can be produced by sintering molybdenum and silicon powders or by growing single crystals from an arc melt. The tensile strength of sintered parts is 40,000 psi (276 MPa) and the compressive strength is 333,000 psi (2296 MPa). Molybdenum disilicide is used in rod form for heating elements in furnaces.
- Tungsten disilicide (WSi_2) -- Tungsten disilicide is not as hard and resistant to oxidation at high temperatures as typical silicides, but it has a higher melting temperature, approximately 4182°R (2323 K) [15].

Single Oxides

Single oxides are among the most important group of the heat resistant ceramics currently in use. The most desirable characteristic is their greater resistance to oxidation at elevated temperatures than any other class of refractory materials. Single oxide ceramics are widely used for applications as diverse as refractories for industrial furnaces and fuels for nuclear reactors. Special applications for single oxides and customized single oxides, those modified by additives or unique processing, are found in almost all technical

fields. Since oxides occur naturally, they were utilized and developed before most of the other types of refractory materials; therefore, more data have been accumulated for the oxides than for any other class of refractory ceramics.

Physical properties. Single oxides, in general, have crystal structures that are either cubic or hexagonal. The melting temperatures of the single oxides typically range from 4160 to 5660°R (2311 to 3144 K), with the two exceptions being thorium oxide (ThO_2) which has the highest melting point, 6290°R (3494 K), and titanium oxide (TiO_2) which has the lowest melting point, 3800°R (2111 K). Densities of the single oxides range from 187.3 to 717.9 lbm/ft^3 (3000 to 11,500 kg/m^3).

Thermal properties. The specific heats of single oxides are less than 0.3 Btu/lbm•°R (1256 J/kg•K) up to 2460°R (1367 K). Some single oxides such as barium oxide (BaO), thorium oxide (ThO_2), and uranium oxide (UO_2) have values for specific heat as low as 0.06 Btu/lbm•°R (251.2 J/kg•K). Linear thermal expansions ranging from 0.2 to 0.3% at 1060°R (589 K) and 0.8 to 1.5% at 2460°R (1367 K) are indicative of single oxides. At 1060°R (589 K), single oxides such as strontium oxide and calcium oxide have linear thermal expansions, approximately 0.4%, that exceed the typical range, while chromium oxide has a linear thermal expansion, approximately 0.1%, that is below the typical range of values. The thermal conductivities of single oxides range from 1 to 10 Btu/hr•ft•°R (1.7 to 17 W/m•K) at room temperature and 1 to 4 Btu/hr•ft•°R (1.7 to 6.9 W/m•K) at 2460°R (1367 K). The general exceptions are beryllium oxide (BeO),

aluminum oxide (Al_2O_3), and magnesium oxide (MgO) which have thermal conductivities of 14, 20, and 30 Btu/hr•ft•°R (24, 36, and 52 W/m•K), respectively.

Mechanical properties. The moduli of elasticity for single oxides range from 30 to 60×10^6 psi (21 to 41×10^4 MPa) at room temperature. Microhardness values range from 8.53×10^5 to 1.42×10^6 lbm/in^2 (6 to 10×10^8 kg/m^2) for the single oxides, with aluminum oxide (Al_2O_3) being the exception with a microhardness of 4.27×10^6 lbm/in^2 (3×10^9 kg/m^2) Reported bend strengths range from 20 to 40×10^3 psi (138 to 276 MPa) and decrease with temperature to values half as much as 2460°R (1367 K) [14].

Common single oxides. The two most notable oxides in this group are alumina and zirconia. Some characteristics of these materials are listed below.

- Alumina (Al_2O_3) -- Alumina is a strong, hard, and wear-resistant material when in its fine-grained form. One drawback is its combination of a high thermal expansion coefficient and poor thermal conductivity and toughness which gives alumina poor thermal shock resistance [12].
- Zirconia (ZrO_2) -- Zirconia seems to offer the best combination of properties for many heat engine applications. It has a high thermal expansion, near that of steel, low thermal conductivity, high strength and toughness, and good wear resistance [6].

Sulfides

Refractory sulfides have been subject to limited investigation and have not found technical applications in any industry. Physical and chemical instabilities are common problems among the sulfides that account for their status. However, interest in direct energy conversion and in the use of nuclear fuels has stimulated property evaluation of the sulfides of thorium, uranium, plutonium, and the rare earth metals. Limited information exists on selected properties of sulfides that are important to structural applications.

The ceramic type classes listed here were chosen specifically because they are considered as the engineering ceramics of the ceramic family. Thus, any ceramic materials chosen for application as a thermal tile protection system would be expected to emerge from one or more of these groups. Based on the information obtained on ceramics, it is evident that the risk of structural failure is the biggest stumbling block to many potential uses of ceramics at the present time, and is the cause of the understandable wariness of engineers offered a brittle material in substitution for a metal. In general, ceramics have many desirable thermal properties that would be beneficial in their use as a thermal protection system, but their mechanical properties are still a cause for concern.

CHAPTER 3

ANALYTICAL SOLUTION FOR A SINGLE LAYER TILE THERMAL PROTECTION SYSTEM

Plume Impingement

Static-test firing of the SSME requires a minimum run time of 10 minutes [3]; therefore, any design for the flame bucket must be able to withstand the conditions of the plume for that amount of time. The conditions of the plume are important in determining how the impingement of the flow will affect the walls of the flame bucket. Estimation of the environmental conditions in the plume was based on predicted gas flow conditions obtained with the use of the Thermo-Chemical Equilibrium Program [2]. These results showed severe conditions which include a chamber pressure of approximately 3285 psia (23MPa), a stagnation temperature of 6538°R (3632 K), and a sonic velocity of 5324 ft/s (1623 m/s). The equivalent heat loads for these conditions are on the order of 700 $Btu/ft^2 \cdot s$ (7950 kW/m^2).

The design under consideration involves replacement of the steel walls of the flame bucket with a low cost material that may be able to endure the plume conditions with a reduction in the amount of water currently being used in the transpiration cooling process. A schematic of the side view of the A-1 test stand is shown in Figure 1.

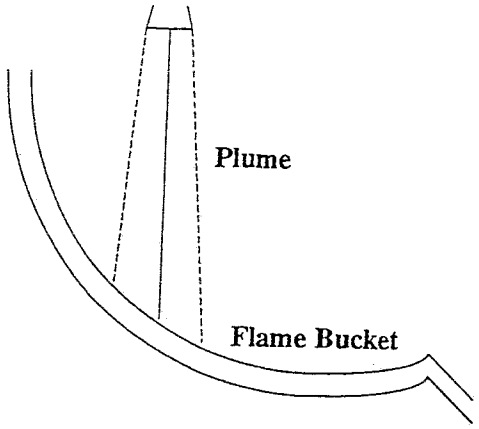

Fig. 1. Side View of the A-1 Test Stand

An actual photograph of the B test stand is shown in Figure 2. On the surface of the material, heat is transferred by convection in which Newton's law of cooling expresses the heat transfer rate.

$$q=hA(T_s-T_\infty) \tag{1}$$

The temperature of the surface is T_s, the temperature of the plume is T_∞, and the heat transfer area is A. The quantity, h, is the heat-transfer coefficient and its value is obtained from such information as fluid properties and fluid velocity. In this case, the heat transfer coefficient was taken to be 1800 Btu/hr•ft²•°R (10,221 W/m²•K) corresponding to the stagnation conditions at the nozzle exit plane [18]. Since the velocity of the fluid layer at the wall will be zero, the heat must be transferred by conduction at this point.

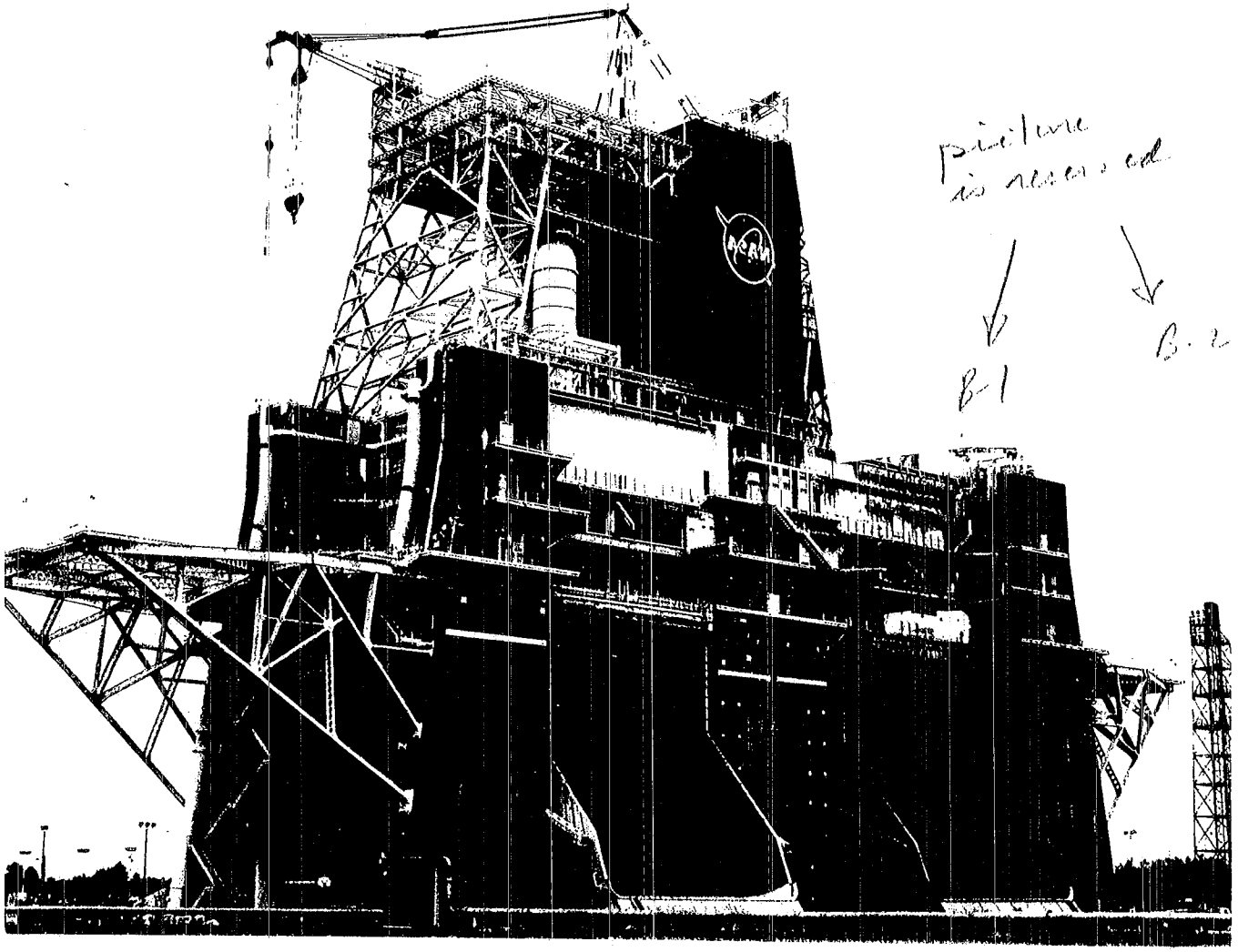

Fig. 2. "B" Test Complex at John C. Stennis Space Center (Courtesy of John C. Stennis Space Center, Stennis Space Center, Mississippi)

Another major assumption in the analysis involves the presence of different temperature regions. For analysis purposes, the impingement region is divided into four regions. These regions will experience peak plume temperatures of 6538°R (3632 K), 5400°R (3000 K), 3600°R (2000 K), and 1800°R (1000 K). The region experiencing the most severe conditions will be the region directly impacted by the plume's centerline. The other three regions will extend out as shown in Figure 3.

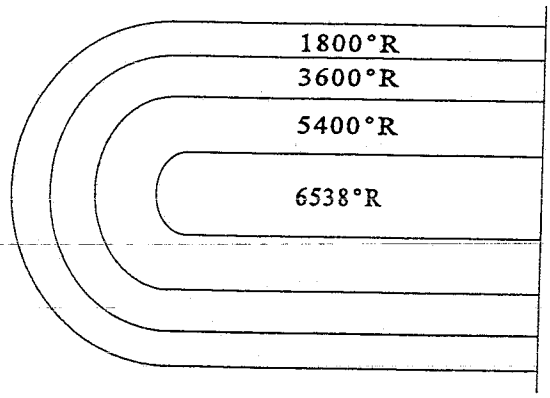

Fig. 3. Impingement Temperature Regions

Backface Condition

In the absence of service temperatures, a restriction was placed on the material surface indicating that the temperature of the material must not exceed 75% of the melting temperature. This limiting temperature is referred to herein as the critical temperature, T_{crit}. The determination of the appropriate backface condition was dependent upon which condition would transfer the most heat away from the surface of the material, therefore

providing lower surface temperatures for the material under consideration. A comparison of the various modes of heat transfer in Table 1 showed that the most effective condition would be a boiling water backface [16].

Table 1. Approximate Values of Convection Heat Transfer Coefficients [16]

Mode	h ($W/m^2 \cdot °C$)	h ($Btu/hr \cdot ft^2 \cdot °R$)
Free convection, $\Delta T = 30°C$		
Vertical plate 0.3 m (1 ft) high in air	4.5	0.79
Horizontal cylinder, 5 cm diameter, in air	6.5	1.14
Horizontal cylinder, 2 cm diameter, in water	890	157
Forced convection		
Airflow at 2 m/s over 0.2 m square plate	12	2.1
Airflow at 35 m/s over 0.75 m square plate	75	13.2
Air at 2 atm flowing in 2.5 cm diameter tube at 10 m/s	65	11.4
Water at 0.5 kg/s flowing in 2.5 cm diameter tube	3500	616
Airflow across 5 cm diameter cylinder with velocity of 50 m/s	180	32
Boiling water		
In a pool or container	2500 - 35,000	440 - 6200
Flowing in a tube	5000 - 100,000	880 - 17,600

Table 1. (Continued)

Mode	h ($W/m^2 \cdot °C$)	h ($Btu/hr \cdot ft^2 \cdot °R$)
Condensation of water vapor, 1 atm		
Vertical surfaces	4000 - 11,300	700 - 2000
Outside horizontal tubes	9500 - 25,000	1700 - 4400

Plane Wall Solution

If a solid body is suddenly subjected to a change in environment, some time must elapse before an equilibrium or steady state temperature condition is reached. In transient heating or cooling processes which take place in the interim period before equilibrium is established, the analysis must take into account the change in internal energy of the body with time, and the boundary conditions must match the physical situation which is apparent in the unsteady state heat transfer problem. With the aid of analytical methods, the unsteady state temperature distribution as a function of time and material depth was formulated in order to select viable candidates as tile insulators [17].

The solution was obtained by treating the system as a plane wall boundary value problem with a convective frontface boundary condition. In the system under consideration, the backface temperature, T_{bf}, will be held at 672°R (373 K), which is the boiling backface condition. The plane wall of thickness L is initially at temperature T_i, and at time = 0 the surface at x = 0 is suddenly changed to T_{bf} and the surface at x = L is exposed to convection (where $h < \infty$) with an ambient temperature of T_∞. A simple energy balance at x = L, which is shown in Appendix A, illustrates that all the energy that is

convected to the surface is conducted through the material and convected to the boiling water. The actual formulation of the solution given below is found in Appendix A.

$$u(x,\theta)=1-\frac{H}{1+H}\left(\frac{x}{L}\right)+2\sum_{n=1}^{\infty}\frac{C(\lambda_n+H\sin\lambda_n)-\lambda_n}{\lambda_n^2+H\sin^2\lambda_n}\sin\lambda_n\left(\frac{x}{L}\right)e^{-\lambda_n^2\theta} \qquad (2)$$

where

u = Nondimensional temperature = $(T - T_\infty)/(T_{bf} - T_\infty)$

H = Biot number = hL/k

h = Heat transfer coefficient

k = Thermal conductivity

C = $(T_i - T_\infty)/(T_{bf} - T_\infty)$

T = Temperature

T_i = Initial temperature of the material

T_∞ = Ambient temperature

T_{bf} = Backface temperature

λ_n = Eigenvalue

x = Material depth

L = Material thickness

θ = Nondimensional time = $\alpha t/L^2$

α = Thermal diffusivity

t = time.

The heat transfer coefficient was taken to be 1800 Btu/hr•ft²•°R (10,221 W/m²•K) corresponding to the conditions at the nozzle exit plane [18]. This equation will be used in Chapter 4 to select candidate materials for potential use as a thermal protection system.

Parametric Study

An analysis was performed on certain parameters to illustrate their importance in the heat transfer through the material. The parameters under consideration included the thermal conductivity (k), the thickness of the material (L), and the nondimensional depth x/L. All calculations were made with the use of Equation 2.

One important variable in Equation 2 is the Biot number which is a function of h, L, and k. The heat transfer coefficient, h, is constant; therefore, only the two variables, L and k, can be varied. Figures 4 and 5 show the effect of varying the thermal conductivity from 40 to 2.5 Btu/hr•ft•°R (69 to 4.3 W/m•K), while keeping the thickness constant at 1 inch (0.03 meters). These values result in Biot numbers of 3.75 and 60, respectively. The figures show that the temperature as a function of time is lower for smaller values of H and higher for larger values of H. Since the thickness is constant, this means that, as the thermal conductivity of the material decreases, the temperature distribution in the material increases.

Figures 6 and 7 show the effect of varying the thickness from 2 to 12 inches (0.05 to 0.3 meters), while keeping the thermal conductivity constant at 30 Btu/hr•ft•°R (52 W/m•K). These values result in Biot numbers of 10 and 60, respectively. The figures

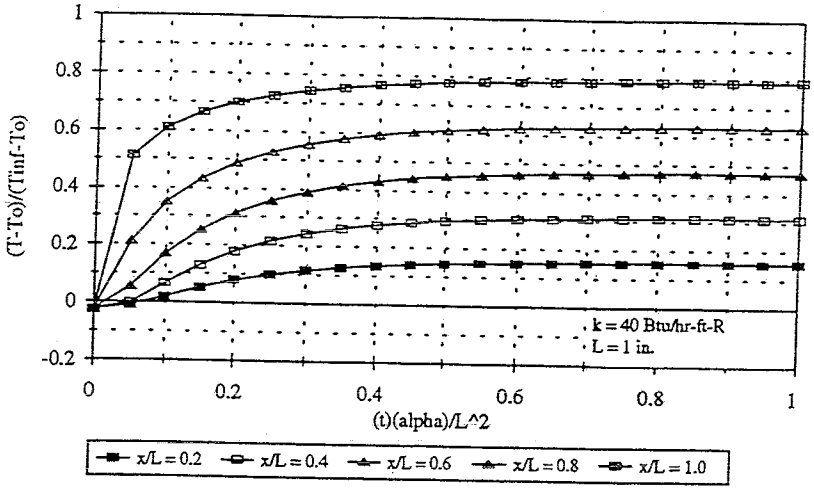

Fig. 4. Normalized Temperature Vs. Normalized Time at Several Depths for a Biot Number = 3.75

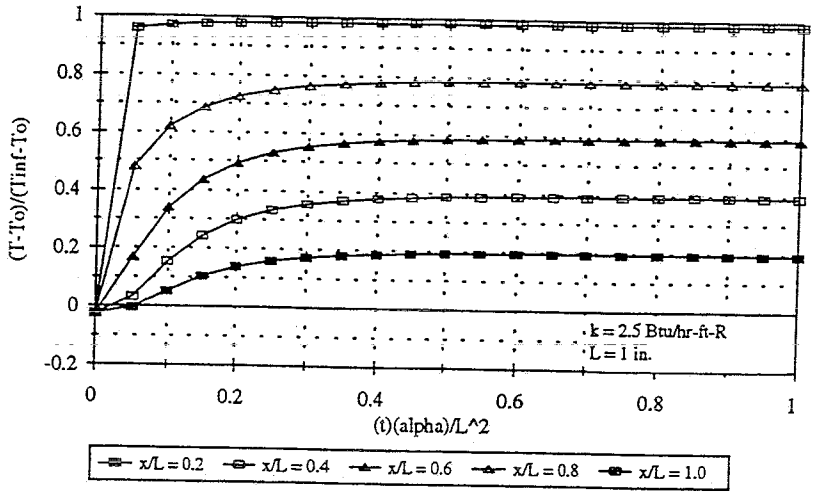

Fig. 5. Normalized Temperature Vs. Normalized Time at Several Depths for a Biot Number = 60

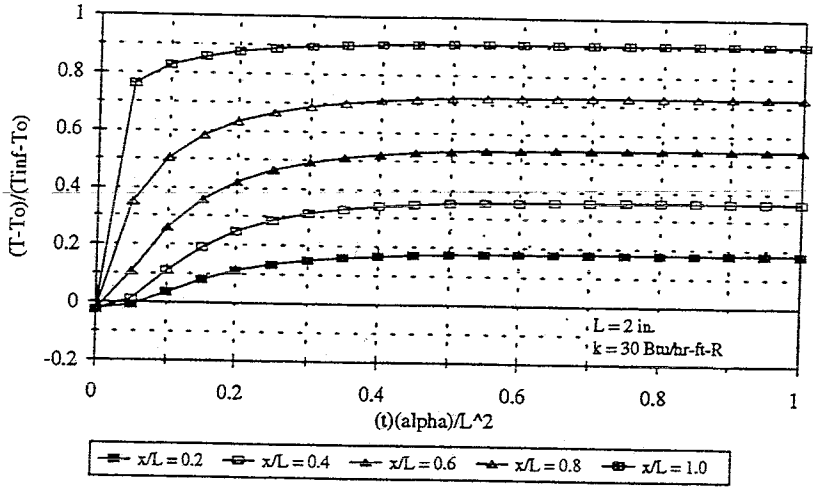

Fig. 6. Normalized Temperature Vs. Normalized Time at Several Depths for a Biot Number = 10

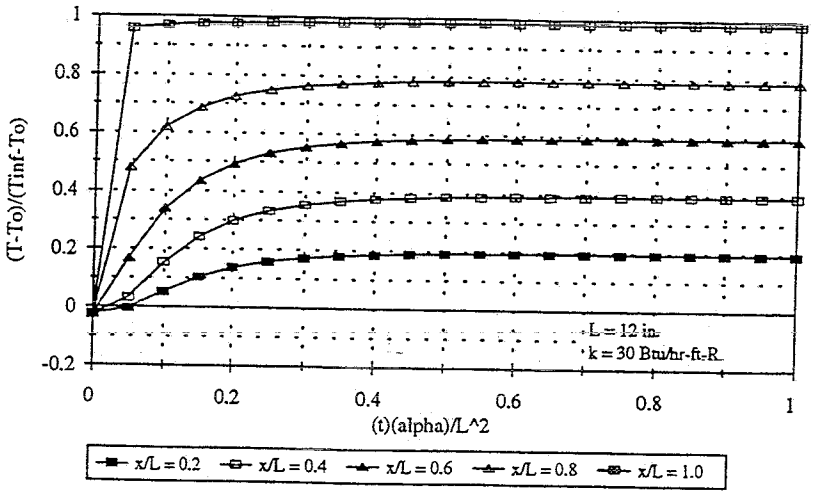

Fig. 7. Normalized Temperature Vs. Normalized Time at Several Depths for a Biot Number = 60

again show that the temperature as a function of time is lower for smaller values of H and higher for larger values of H. Since the thermal conductivity is constant, this means that as the thickness of the material increases the temperature distribution in the material increases.

The next analysis calculates the nondimensional temperature as a function of nondimensional time for several Biot numbers. Figures 8 and 9 show the effects of varying the Biot number at two depths in the material. Again, the graphs show that the temperature is lower for smaller values of H. As in any situation, the closer one gets to a surface in which heat is being applied, the higher the temperature.

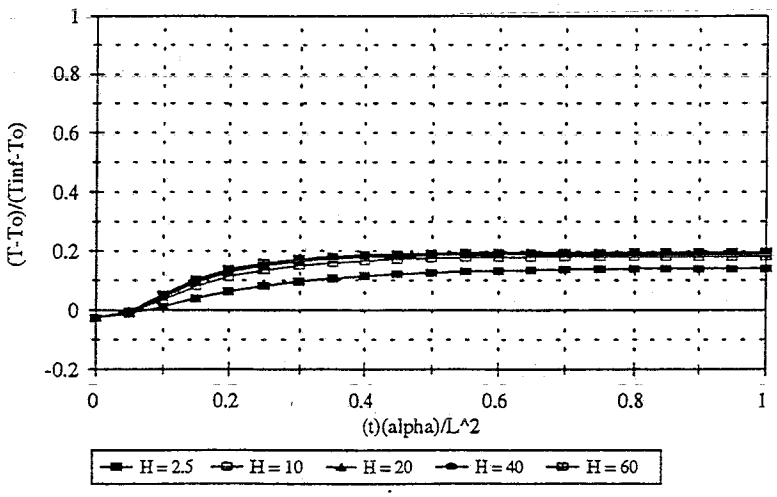

Fig. 8. Normalized Temperature Vs. Normalized Time at Several Biot Numbers for x/L = 0.2

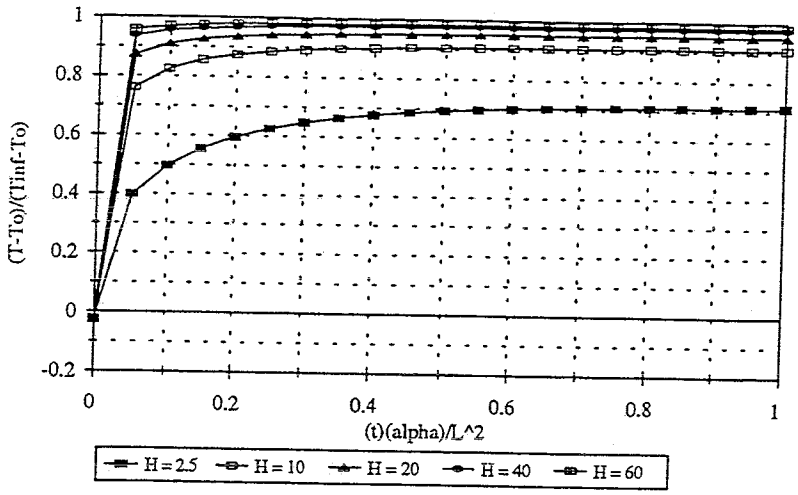

Fig. 9. Normalized Temperature Vs. Normalized Time at Several Biot Numbers for x/L = 1.0

The analyses show that the thermal conductivity and material thickness are important parameters in determining the temperature distribution in the material. These analyses indicate that the most desirable material for the boiling water backface condition should have a higher thermal conductivity and the thickness of the materials should be kept to a minimum in order to keep the temperatures low. The downside of this scenario, however, is the high cooling rates required to maintain the low backface temperature.

CHAPTER 4

TILE MATERIAL SELECTION

Introduction

There are three groups in which to find a suitable material for a tile protection system. These groups include metals and metal alloys, refractory metals and alloys, and ceramics. The most suitable candidate is the material that can be exposed to the conditions of the plume in the high heat region of 6538°R (3632 K) for the longest time before the surface temperature reaches its critical value. Since the length of time that the material is exposed to the plume is important in determining suitable candidates, Equation 2 was used to find the run times of the materials under consideration. A material thickness of two inches (0.05 meters) was chosen for subsequent calculations.

Metals and Metal Alloys

Equation 2 was used to illustrate the effectiveness of metals and their alloys for use as a thermal protection system. The four metals under consideration are aluminum, copper, titanium, and carbon steel (C = 1%), and their properties are given in Table 2. The properties shown in Table 2 include melting temperature, T_m, thermal diffusivity, α, density, ρ, specific heat, c, and thermal conductivity, k.

Table 2. Thermal Properties of Selected Metals.

Material	T_m (°R)	α (ft^2/s)	ρ (lbm/ft^3)	c (Btu/lbm•°R)	k (Btu/hr•ft•°R)
Aluminum	1680	1.01e-03	169	0.21	133
Copper	2441	1.27e-03	558	0.09	231
Steel (C = 1%)	3220	8.46e-05	487	0.11	17
Titanium	3492	9.68e-05	281	0.12	12

The temperature distributions for these four materials are shown in Figures 10 - 13.

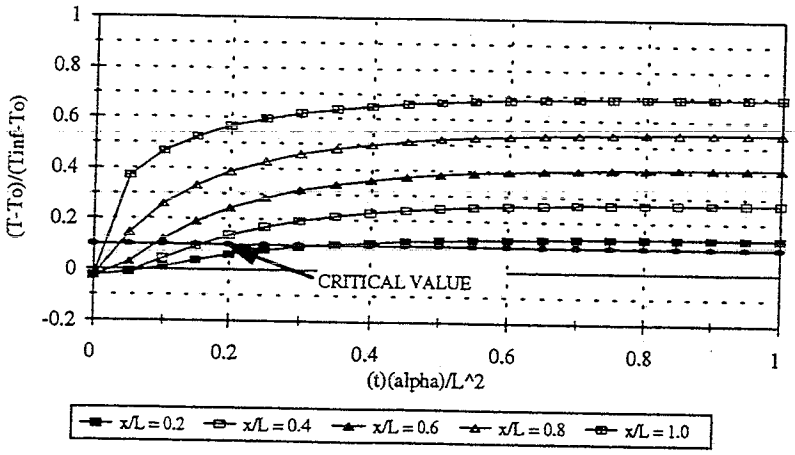

Fig. 10. Normalized Temperature Vs. Normalized Time at Several Depths for Aluminum with a Boiling Water Backface and $T_\infty = 6538°R$

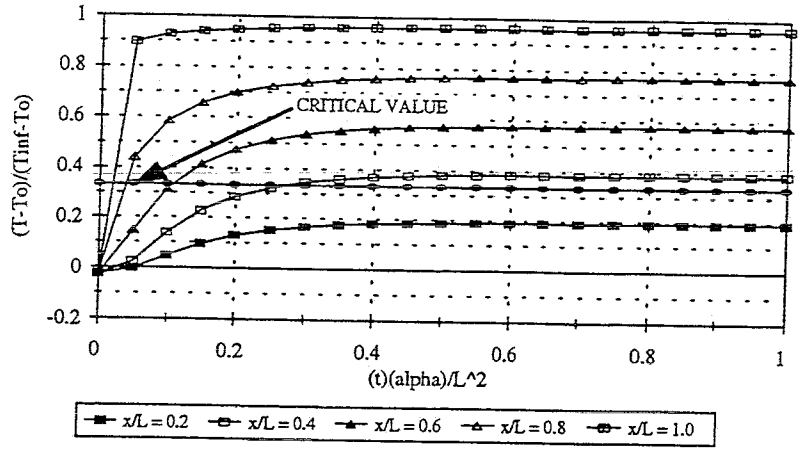

Fig. 11. Normalized Temperature Vs. Normalized Time at Several Depths for Titanium with a Boiling Water Backface and $T_\infty = 6538°R$

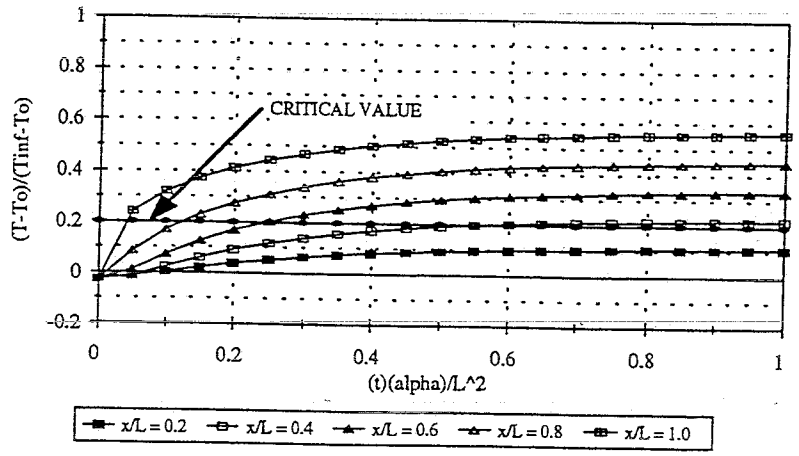

Fig. 12. Normalized Temperature Vs. Normalized Time at Several Depths for Copper with a Boiling Water Backface and $T_\infty = 6538°R$

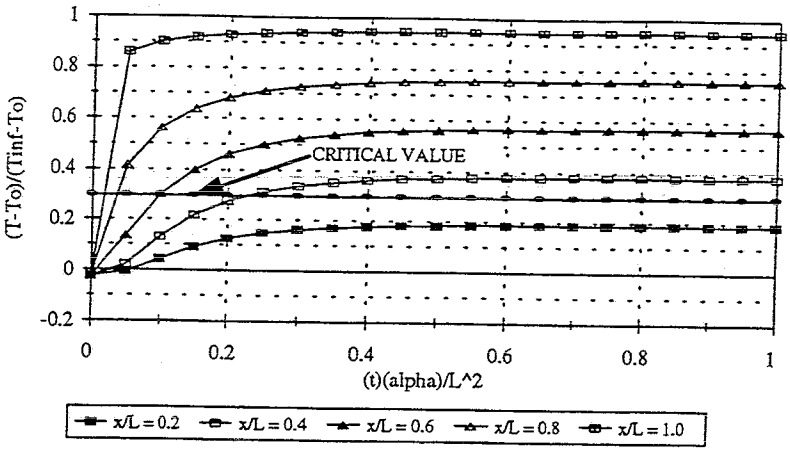

Fig. 13. Normalized Temperature Vs. Normalized Time at Several Depths for Carbon Steel (C = 1%) with a Boiling Water Backface and $T_\infty = 6538°R$

The graphs illustrate the unsuitability of all four metals. While aluminum and copper have lower temperature distributions because of their higher thermal conductivity, their low melting temperature make them unsuitable candidates for high temperature applications. On the other hand, steel and titanium have relatively high melting temperatures, but their high temperature distributions associated with their relatively low thermal conductivities also makes them unfit candidates for use in a thermal protection system. Table 3 shows that all four materials reach their critical temperatures at times much lower than one second.

Table 3. Maximum Run Times and Critical Temperatures for Selected Metals.

Material	t_{max} (s)	T_{crit} (°R)	H
Aluminum	0.08	1260	2.26
Copper	0.71	1831	1.30
Steel (C = 1%)	0.14	2415	17.90
Titanium	0.09	2619	24.72

Refractory Metals

To illustrate the effectiveness of refractory metals for potential use as a thermal protection system, Equation 2 was used. The four materials in this group are molybdenum, niobium, tantalum, and titanium. The properties of these refractory metals are shown in Table 4.

Table 4. Thermal Properties of Selected Refractory Metals.

Material	T_m (°R)	α (ft^2/s)	ρ (lbm/ft^3)	c (Btu/lbm•°R)	k (Btu/hr•ft•°R)
Molybdenum	5202	5.88e-04	637	0.06	81
Niobium	4932	2.41e-04	536	0.06	29
Tantalum	5922	3.87e-04	1043	0.03	48
Tungsten	6588	7.49e-04	1205	0.03	104

The temperature distributions of these four materials are shown in Figures 14 - 17. From observation of these graphs, it is apparent that no suitable candidate emerged from the refractory metal group. Since the temperatures near the surface quickly exceed the assumed service (critical) temperatures. While the thermal conductivity plays a significant

role in the performance of the materials, the melting temperatures of these refractory metals are still limiting.

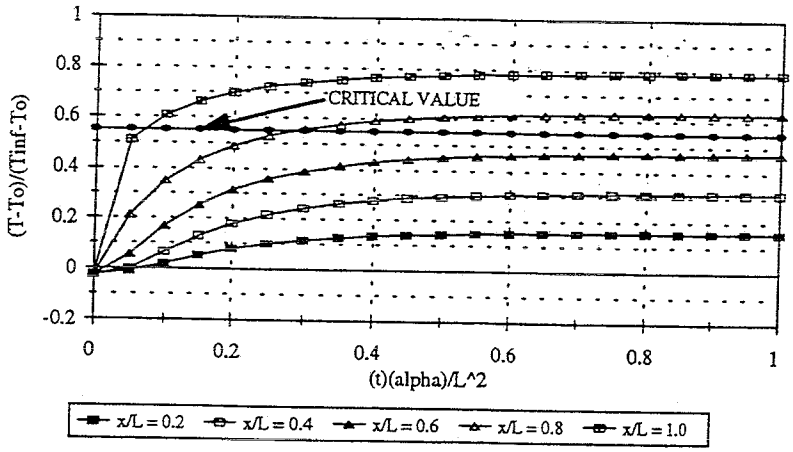

Fig. 14. Normalized Temperature Vs. Normalized Time at Several Depths for Molybdenum with a Boiling Water Backface and $T_\infty = 6538°R$

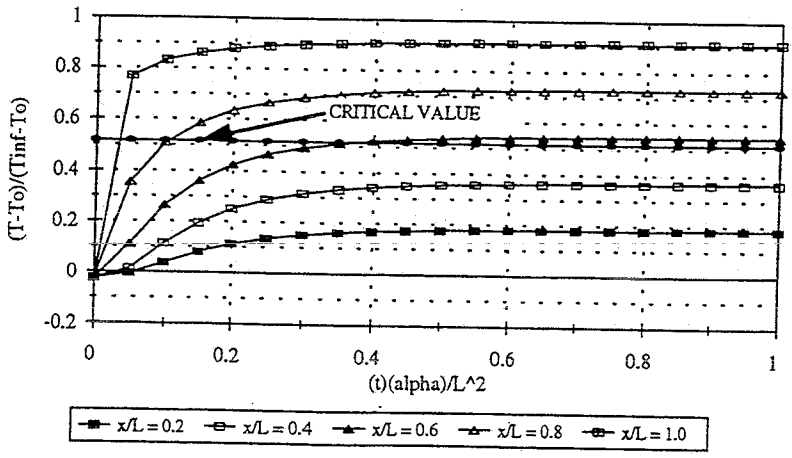

Fig. 15. Normalized Temperature Vs. Normalized Time at Several Depths for Niobium with a Boiling Water Backface and $T_\infty = 6538°R$

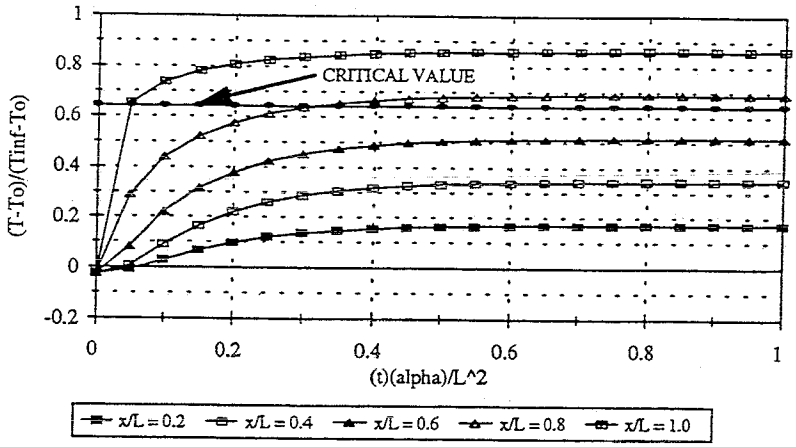

Fig. 16. Normalized Temperature Vs. Normalized Time at Several Depths for Tantalum with a Boiling Water Backface and $T_\infty = 6538°R$

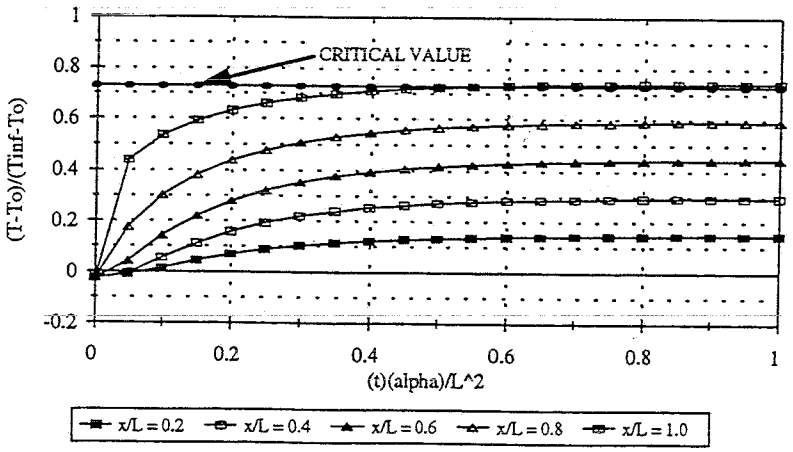

Fig. 17. Normalized Temperature Vs. Normalized Time at Several Depths for Tungsten with a Boiling Water Backface and $T_\infty = 6538°R$

The best material in the group, tungsten, with the highest service temperature will last less than 20 seconds when exposed to the conditions of the plume as shown in Table 5.

Table 5. Maximum Run Times and Critical Temperatures for Selected Refractory Metals.

Material	t_{max} (s)	T_{crit} (°R)	H
Molybdenum	3.16	3901	3.71
Niobium	0.77	3699	10.38
Tantalum	3.32	4441	6.26
Tungsten	19.78	4941	2.88

Ceramics

The ceramic family is the remaining group of materials to investigate to find a potential candidate for use as a thermal protection system. The primary source of information was the NASA Ames Thermal Protection Systems Expert and Material Properties Database (TPSX) software [8]. Using the Solid Species Database in the TPSX software, materials were chosen based on their melting temperature and thermal diffusivity. Only ceramics with a melting temperature, $T_m \geq 3240°R$ (1800 K), and a thermal diffusivity, α, on the order of 10^{-4} ft^2/s (10^{-5} m^2/s) were chosen for the first cut. Based on these criteria, 63 various ceramics were selected for further consideration. These materials along with their thermal properties are listed in Table 6. All 63 materials were evaluated with the use of Equation 2 to determine the time in which these materials reached their critical temperatures which was again taken to be 75% of the melting temperature. The results of this evaluation will be discussed in Chapter 5.

Table 6. Candidate Ceramic Materials for Insulation of Large Flame Buckets

Material	T_m (°R)	α (ft^2/s)	ρ (lbm/ft^3)	c (Btu/lbm·°R)	k (Btu/hr·ft·°R)
Aluminum Nitride	5040	1.47e-04	204	0.18	19.07
Aluminum Oxide	4180	1.33e-04	248	0.18	21.96
Aluminum Silicate	3822	2.63e-05	199	0.18	3.47
Barium Boride	4500	1.83e-04	270	0.12	20.80
Beryllium Carbide	4806	1.35e-04	152	0.39	28.89
Boron Carbide	4716	1.34e-04	157	0.23	17.34
Boron Nitride	4680	1.03e-04	140	0.19	9.82
Calcium Boride	4500	1.10e-04	152	0.22	13.29
Calcium Oxide	5197	1.20e-04	210	0.18	16.76
Calcium Zirconate	4698	1.39e-05	287	0.14	2.02
Cerium Boride	4428	1.53e-04	300	0.12	19.65
Cerium Oxide	4806	4.93e-05	454	0.09	6.93
Chromium Boride (CrB)	4277	7.32e-05	381	0.12	11.56
Chromium Boride (CrB_2)	4356	5.80e-05	350	0.17	12.71
Chromium Carbide ($Cr_{23}C_6$)	3330	5.68e-05	435	0.12	10.40
Chromium Carbide (Cr_3C_2)	3744	5.62e-05	415	0.13	10.98
Chromium Nitride	3456	5.95e-05	406	0.15	12.71
Chromium Silicide	3593	4.82e-05	366	0.10	6.36
Europium Boride	5130	1.09e-04	307	0.11	13.29
Gadolinium Boride	5004	9.24e-05	332	0.11	12.13
Gadolinium Oxide	4662	9.72e-06	479	0.07	1.16
Hafnium Carbide	7596	9.28e-05	793	0.05	12.71
Lanthanum Boride	5382	1.92e-04	295	0.14	27.73

Table 6. (Continued)

Material	T_m (°R)	α (ft^2/s)	ρ (lbm/ft^3)	c (Btu/lbm·°R)	k (Btu/hr·ft·°R)
Lanthanum Sulfide	4446	7.27e-05	353	0.08	7.51
Magnesium Aluminate	4335	4.43e-05	222	0.20	6.93
Magnesium Oxide	5580	1.95e-04	235	0.22	36.40
Magnesium Silicate	3906	1.97e-05	201	0.20	2.89
Molybdenum Beryllide	3456	1.63e-04	189	0.26	28.89
Molybdenum Carbide	5031	3.15e-05	568	0.07	4.62
Molybdenum Silicide	4176	1.84e-04	390	0.11	28.31
Neodymium Boride	5202	2.00e-04	310	0.12	26.58
Neodymium Sulfide	4338	5.46e-06	397	0.07	0.58
Niobium Boride	5958	6.24e-05	437	0.10	9.82
Niobium Carbide	7002	1.18e-04	486	0.08	17.34
Niobium Nitride	4680	1.48e-05	519	0.08	2.31
Praesodymium Boride	5184	1.83e-04	303	0.12	23.69
Samarium Boride	5130	6.17e-05	317	0.12	8.09
Scandium Nitride	5076	1.02e-04	277	0.15	15.60
Scandium Oxide	4806	3.35e-05	240	0.16	4.62
Silicon Carbide	5868	2.00e-04	201	0.16	23.11
Silicon Oxide	3593	5.48e-06	165	0.18	0.58
Silicon Nitride	3870	2.14e-04	199	0.17	26.00
Strontium Boride	4515	1.26e-04	214	0.16	15.02
Tantalum Carbide	7668	8.67e-05	905	0.05	12.71
Terbium Boride	4698	8.67e-05	336	0.11	11.56
Thorium Boride	4356	2.05e-04	443	0.08	26.58

Table 6. (Continued)

Material	T_m (°R)	α (ft^2/s)	ρ (lbm/ft^3)	c (Btu/lbm·°R)	k (Btu/hr·ft·°R)
Titanium Carbide	6012	1.96e-04	306	0.13	28.89
Titanium Nitride	5796	1.10e-04	336	0.14	19.07
Titanium Oxide	3852	4.03e-05	265	0.17	6.36
Titanium Silicide	4302	8.99e-05	273	0.10	8.67
Vanadium Carbide	5256	1.41e-04	348	0.13	22.54
Vanadium Nitride	4734	3.90e-05	380	0.14	7.51
Ytterbium Boride	4752	1.16e-04	347	0.10	14.45
Ytterbium Silicate	4860	2.56e-05	292	0.13	3.47
Yttrium Boride	5166	1.30e-04	231	0.16	16.76
Yttrium Oxide	4914	8.12e-05	314	0.11	9.82
Zirconium Beryllide	3960	1.42e-04	170	0.27	23.11
Zirconium Boride (ZrB_2)	6336	1.63e-04	381	0.10	23.11
Zirconium Boride (ZrB_{12})	4536	4.98e-05	225	0.19	7.51
Zirconium Carbide	6642	8.83e-05	411	0.09	11.56
Zirconium Nitride	5796	8.16e-05	455	0.09	12.13
Zirconium Oxide	5310	6.90e-05	360	0.11	9.82
Zirconium Silicate	4860	2.56e-05	292	0.13	3.47

CHAPTER 5

SINGLE LAYER TILE PROTECTION SYSTEM

Boiling Water Backface Condition

By comparison of the various types of convective coefficients, it was determined previously from the data in Table 1 that the most effective backface that could handle the imposed heat loads would be a boiling water backface. All calculations that have been previously made have been based on a single layer tile system which is the best case scenario for a constant temperature backface because it offers the least resistance to the flow of heat. As discussed in the previous chapter, the time that it takes for the surface of the material to reach its critical temperature is important in determining the appropriate candidate.

With the use of Equation 2, the 63 ceramic materials were evaluated in order to find the candidates that could withstand the conditions of the plume for the longest times before their critical temperatures which were again taken to be 75% of their melting temperatures were exceeded. A material thickness of 2 inches (0.05 meters) and a heat transfer coefficient of 1800 Btu/hr•ft^2•°R (10,221 W/m•K) were chosen for subsequent calculations [18]. From the list in Table 6, the 20 materials with the longest run times in the high heat region of 6538°R (3632 K) were chosen for further analysis. These 20 materials along with their maximum run times are listed in Table 7. The candidate

materials in this table are listed in decreasing order according to their maximum run times. Figures 18 - 20 show the temperature distributions of the top three candidate materials, and the figures of the remaining candidate materials are shown in Appendix B.

Table 7. Maximum Run Times for Candidate Materials for the Insulation of Large Flame Buckets for an Exhaust Temperature Region of 6538°R

Material	t_{max} (s)	Material	t_{max} (s)	Material	t_{max} (s)
Tantalum Carbide	10.12	Titanium Nitride	1.63	Zirconium Nitride	0.89
Hafnium Carbide	8.22	Silicon Carbide	1.42	Praesodymium Boride	0.86
Niobium Carbide	4.73	Lanthanum Boride	1.35	Calcium Oxide	0.66
Zirconium Boride (ZrB_2)	2.78	Beryllium Carbide	1.23	Aluminum Nitride	0.61
Magnesium Oxide	2.74	Vanadium Carbide	1.07	Scandium Nitride	0.60
Titanium Carbide	2.60	Neodymium Boride	1.00	Yttrium Boride	0.59
Zirconium Carbide	1.81	Niobium Boride	0.89		

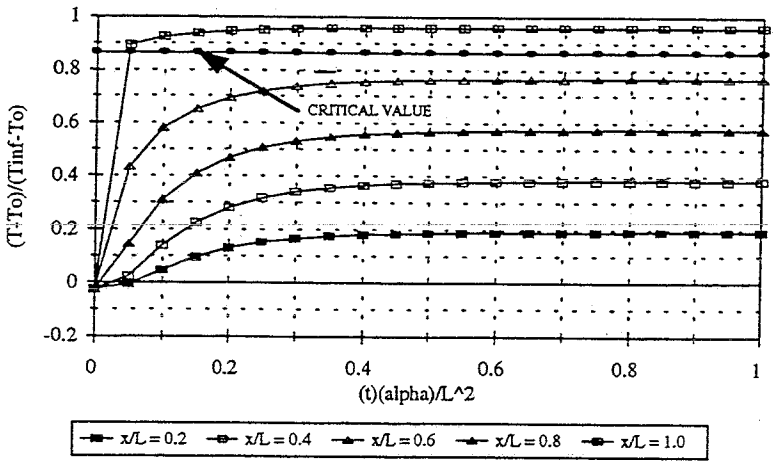

Fig. 18. Normalized Temperature Vs. Normalized Time at Several Depths for Tantalum Carbide with a Boiling Water Backface and T_∞ = 6538°R

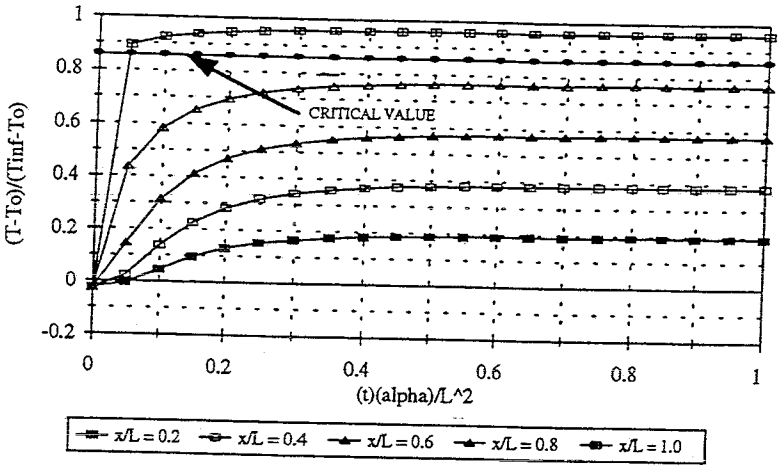

Fig. 19. Normalized Temperature Vs. Normalized Time at Several Depths for Hafnium Carbide with a Boiling Water Backface and $T_\infty = 6538°R$

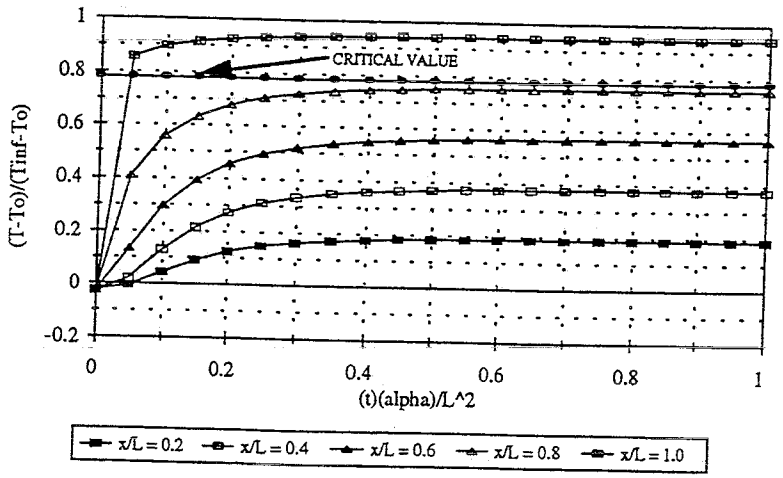

Fig. 20. Normalized Temperature Vs. Normalized Time at Several Depths for Niobium Carbide with a Boiling Water Backface and $T_\infty = 6538°R$

By inspection of the run times, it is evident that none of these materials would be suitable candidates for the high heat region of the flame bucket because all have temperatures near the heated surface that exceed the critical temperatures in a relatively short time. The problem with ceramics is that, while they do have high melting temperatures, their low thermal conductivity leads to high Biot numbers which means that the materials under consideration will have higher temperature distributions.

Even though these materials may not survive in the high heat region, there is a chance they can be utilized in the other three regions which have peak temperatures of 5400°R (3000 K), 3600°R (2000 K), and 1800°R (1000K). The materials in Table 6 were evaluated again for each of the three temperature regions.

In the temperature region of 5400°R (3000 K), the top 20 materials and their run times are listed in Table 8. Based on the data obtained, three materials with infinite run times emerge as suitable candidates for this temperature region. These materials are tantalum carbide (TaC), hafnium carbide (HfC), and niobium carbide (NbC), and they are shown in Figures 21 - 23. The temperature distributions of the remaining candidate materials are shown in Appendix C.

Table 8. Maximum Run Times for Candidate Materials for the Insulation of Large Flame Buckets for an Exhaust Temperature Region of 5400°R

Material	t_{max} (s)	Material	t_{max} (s)	Material	t_{max} (s)
Tantalum Carbide	∞	Titanium Nitride	6.02	Neodymium Boride	2.75
Hafnium Carbide	∞	Silicon Carbide	5.50	Praesodymium Boride	2.34
Niobium Carbide	∞	Lanthanum Boride	3.97	Calcium Oxide	1.81
Zirconium Carbide	19.67	Niobium Boride	3.71	Yttrium Boride	1.61
Zirconium Boride (ZrB_2)	17.07	Zirconium Nitride	3.29	Scandium Nitride	1.58
Titanium Carbide	11.26	Vanadium Carbide	3.00	Aluminum Nitride	1.58
Magnesium Oxide	8.86	Beryllium Carbide	2.96		

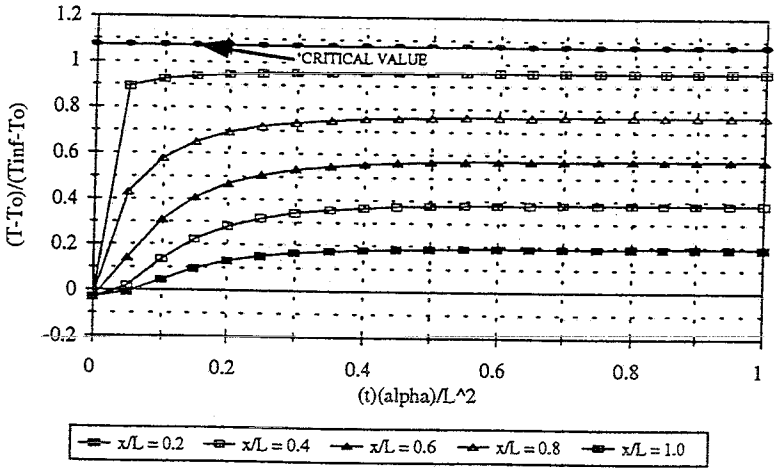

Fig. 21. Normalized Temperature Vs. Normalized Time at Several Depths for Tantalum Carbide with a Boiling Water Backface and T_∞ = 5400°R

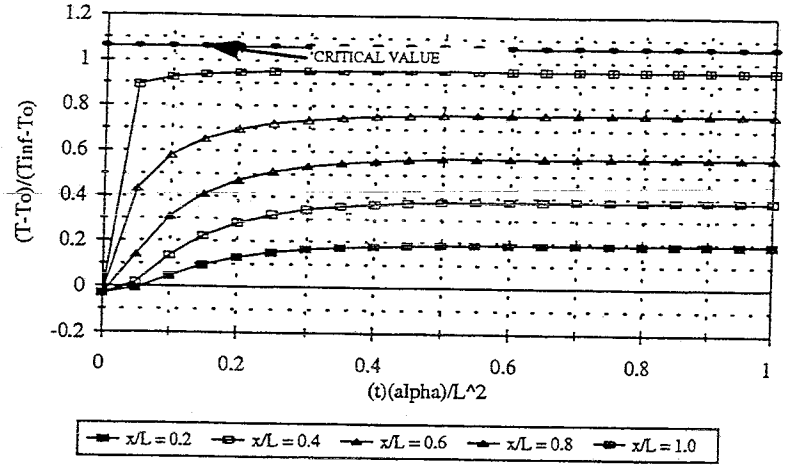

Fig. 22. Normalized Temperature Vs. Normalized Time at Several Depths for Hafnium Carbide with a Boiling Water Backface and $T_\infty = 5400°R$

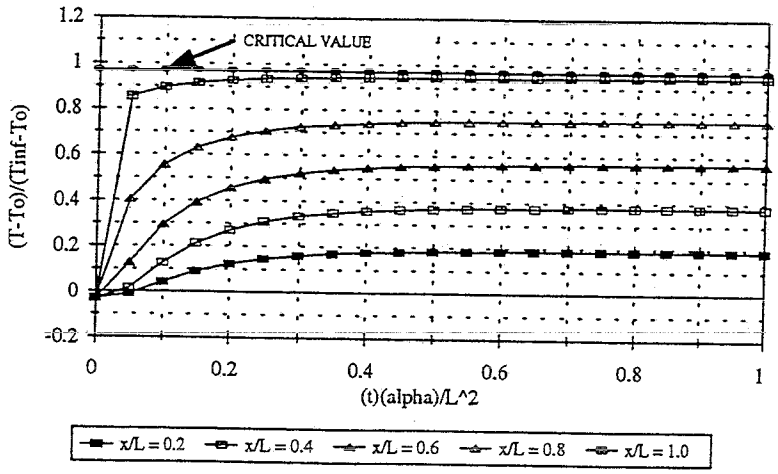

Fig. 23. Normalized Temperature Vs. Normalized Time at Several Depths for Niobium Carbide with a Boiling Water Backface and $T_\infty = 5400°R$

For the temperature region of 3600°R (2000 K), 37 materials and their run times are listed in Table 9. Of these 37 materials, 35 of them had infinite run times and therefore have the potential to be suitable candidates for this region. The 20 materials with the highest melting temperatures were chosen to illustrate the performance of the materials in this region. Three of these materials, tantalum carbide, hafnium carbide, and niobium carbide, are shown in Figures 24 - 26. The temperature distributions for the other candidate materials are shown in Appendix D.

Table 9. Maximum Run Times for Candidate Materials for the Insulation of Large Flame Buckets in an Exhaust Temperature Region of 3600°R

Material	t_{max} (s)	Material	t_{max} (s)	Material	t_{max} (s)
Aluminum Nitride	∞	Neodymium Boride	∞	Vanadium Nitride	∞
Beryllium Carbide	∞	Niobium Boride	∞	Ytterbium Boride	∞
Boron Carbide	∞	Niobium Carbide	∞	Ytterbium Silicate	∞
Boron Nitride	∞	Praesodymium Boride	∞	Yttrium Boride	∞
Calcium Oxide	∞	Samarium Boride	∞	Yttrium Oxide	∞
Cerium Oxide	∞	Scandium Nitride	∞	Zirconium Boride (ZrB_2)	∞
Europium Boride	∞	Scandium Oxide	∞	Zirconium Carbide	∞
Gadolinium Boride	∞	Silicon Carbide	∞	Zirconium Nitride	∞
Hafnium Carbide	∞	Tantalum Carbide	∞	Zirconium Oxide	∞
Lanthanum Boride	∞	Terbium Boride	∞	Zirconium Silicate	∞
Magnesium Oxide	∞	Titanium Carbide	∞	Molybdenum Silicide	169.65
Molybdenum Carbide	∞	Titanium Nitride	∞	Barium Boride	42.87

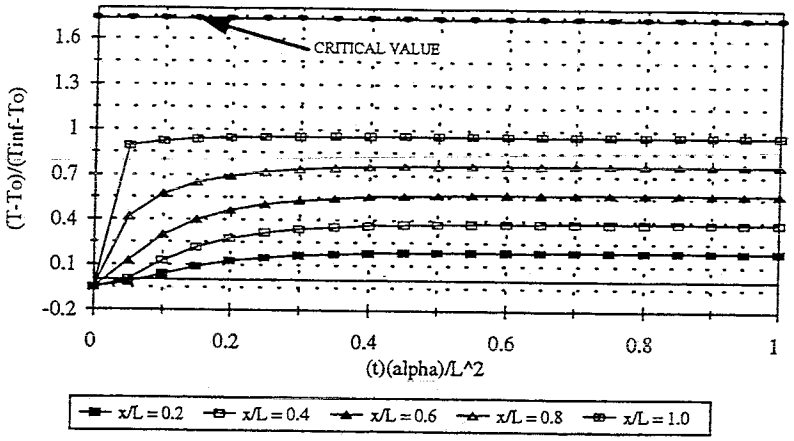

Fig. 24. Normalized Temperature Vs. Normalized Time at Several Depths for Tantalum Carbide with a Boiling Water Backface and $T_\infty = 3600°R$

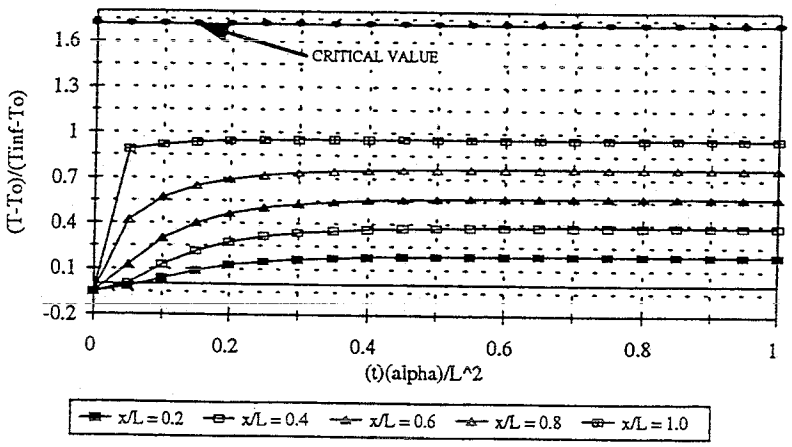

Fig. 25. Normalized Temperature Vs. Normalized Time at Several Depths for Hafnium Carbide with a Boiling Water Backface and $T_\infty = 3600°R$

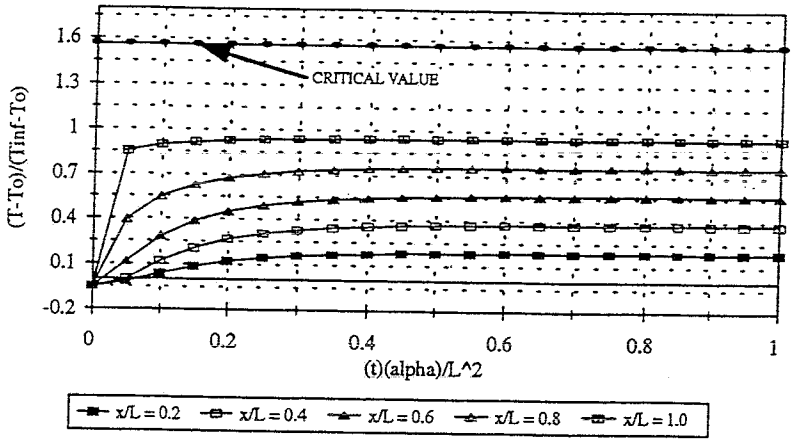

Fig. 26. Normalized Temperature Vs. Normalized Time at Several Depths for Niobium Carbide with a Boiling Water Backface and $T_\infty = 3600°R$

In the temperature region of 1800°R (1000 K), all 63 materials and their run times are listed in Table 10. These 63 materials have infinite run times and can be considered as potential candidates for this low temperature region. Again, the 20 materials with the highest melting temperatures were chosen to illustrate the performance of the materials in this region. Figures 27 - 29 are the temperature distributions for the same three materials shown in the previous temperature regions, tantalum carbide, hafnium carbide, and niobium carbide. The remaining temperature distributions of the candidate materials in this temperature region are shown in Appendix E.

Table 10. Maximum Run Time for Candidate Materials for the Insulation of Large Flame Buckets in an Exhaust Temperature Region of 1800°R

Material	t_{max} (s)	Material	t_{max} (s)	Material	t_{max} (s)
Aluminum Nitride	∞	Hafnium Carbide	∞	Strontium Boride	∞
Aluminum Oxide	∞	Lanthanum Boride	∞	Tantalum Carbide	∞
Aluminum Silicate	∞	Lanthanum Sulfide	∞	Terbium Boride	∞
Barium Boride	∞	Magnesium Aluminate	∞	Thorium Boride	∞
Beryllium Carbide	∞	Magnesium Oxide	∞	Titanium Carbide	∞
Boron Carbide	∞	Magnesium Silicate	∞	Titanium Nitride	∞
Boron Nitride	∞	Molybdenum Beryllide	∞	Titanium Oxide	∞
Calcium Boride	∞	Molybdenum Carbide	∞	Titanium Silicide	∞
Calcium Oxide	∞	Molybdenum Silicide	∞	Vanadium Carbide	∞
Calcium Zirconate	∞	Neodymium Boride	∞	Vanadium Nitride	∞
Cerium Boride	∞	Neodymium Sulfide	∞	Ytterbium Boride	∞
Cerium Oxide	∞	Niobium Boride	∞	Ytterbium Silicate	∞
Chromium Boride (CrB)	∞	Niobium Carbide	∞	Yttrium Boride	∞
Chromium Boride (CrB_2)	∞	Niobium Nitride	∞	Yttrium Oxide	∞
Chromium Carbide ($Cr_{23}C_6$)	∞	Praesodymium Boride	∞	Zirconium Beryllide	∞
Chromium Carbide (Cr_3C_2)	∞	Samarium Boride	∞	Zirconium Boride (ZrB_2)	∞
Chromium Nitride	∞	Scandium Nitride	∞	Zirconium Boride (ZrB_{12})	∞
Chromium Silicide	∞	Scandium Oxide	∞	Zirconium Carbide	∞
Europium Boride	∞	Silicon Carbide	∞	Zirconium Nitride	∞
Gadolinium Boride	∞	Silicon Oxide	∞	Zirconium Oxide	∞
Gadolinium Oxide	∞	Silicon Nitride	∞	Zirconium Silicate	∞

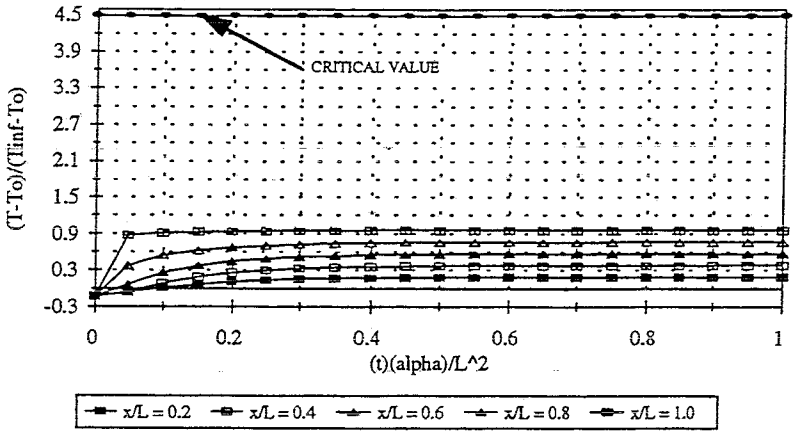

Fig. 27. Normalized Temperature Vs. Normalized Time at Several Depths for Tantalum Carbide with a Boiling Water Backface and $T_\infty = 1800°R$

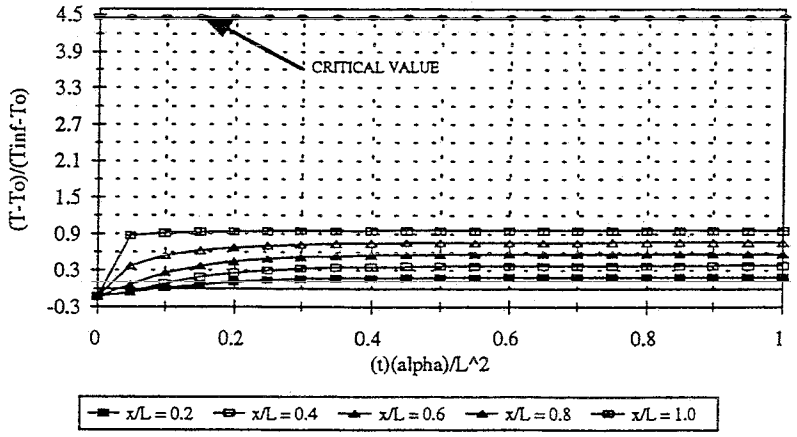

Fig. 28. Normalized Temperature Vs. Normalized Time at Several Depths for Hafnium Carbide with a Boiling Water Backface and $T_\infty = 1800°R$

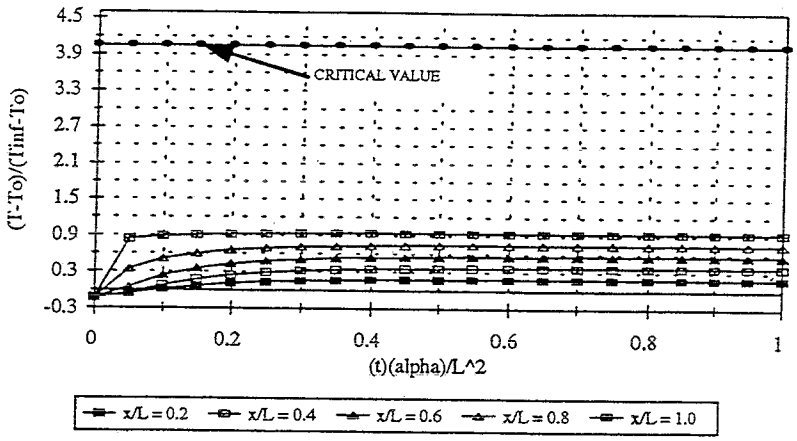

Fig. 29. Normalized Temperature Vs. Normalized Time at Several Depths for Niobium Carbide with a Boiling Water Backface and $T_\infty = 1800°R$

The minimum run time for the SSME test is 10 minutes [3], so any materials under consideration must be able to withstand those conditions for that amount of time. This study has shown that there are no materials known to the writers that can withstand the plume conditions in the high heat region of the flame bucket, but there are materials that can withstand the conditions in the other three regions.

Steady State Solution

Based on the temperature distributions of Figures 18 - 29, it is observed that the materials reach steady state rather quickly, so that it is the steady state solution that determines the surface temperatures of the materials and the heat loads that the materials must handle. The steady state solution is a linear equation with a convective frontface

boundary condition and a boiling water backface condition (T_{bf} = 672°R). Formulation of the steady state surface temperature equation given below can be found in Appendix F.

$$T_s = \frac{T_{bf} + \frac{hL}{k} T_\infty}{1 + \frac{hL}{k}} \qquad (3)$$

With the use of Equation 3, the steady state surface temperatures (T_s) of the candidate materials in all four regions were calculated and are shown in Tables 11 - 14. As before, the critical temperature is taken to be 75% of the melting temperature. The materials in Tables 11 and 12 are listed in descending order according to maximum run times while those in Tables 13 and 14 are listed alphabetically because all maximum run times are infinite except for two materials in Table 13. This equation is a strong function of the Biot number (H = hL/k), and as H increases so does the surface temperature of the material. Surface temperatures of materials with higher thermal conductivities, which means lower Biot numbers, are low while materials with lower thermal conductivities, which leads to higher Biot numbers, have higher surface temperatures. The data in these tables illustrate that materials with higher thermal conductivities are able to conduct heat away from the surface much faster than materials with lower conductivities resulting in lower surface temperatures.

Table 11. Steady State Surface Temperatures for an Exhaust Temperature Region of 6538°R for a Single Layer Tile Insulation System with a Boiling Water Backface

Material	H	T_{crit} (°R)	T_s (°R)
Tantalum Carbide	23.60	5751	6300
Hafnium Carbide	23.60	5697	6300
Niobium Carbide	17.31	5252	6218
Zirconium Boride (ZrB_2)	12.98	4752	6118
Magnesium Oxide	8.24	4185	5903
Titanium Carbide	10.38	4509	6023
Zirconium Carbide	25.96	4982	6320
Titanium Nitride	15.73	4347	6187
Silicon Carbide	12.98	4401	6118
Lanthanum Boride	10.82	4037	6042
Beryllium Carbide	10.38	3605	6023
Vanadium Carbide	13.31	3942	6128
Neodymium Boride	11.29	3902	6061
Niobium Boride	30.54	4469	6352
Zirconium Nitride	24.72	4347	6310
Praesodymium Boride	12.66	3888	6109
Calcium Oxide	17.90	3898	6228
Aluminum Nitride	15.73	3780	6187
Scandium Nitride	19.23	3807	6248
Yttrium Boride	17.90	3875	6228

Table 12. Steady State Surface Temperatures for an Exhaust Temperature Region of 5400°R for a Single Layer Tile Insulation System with a Boiling Water Backface

Material	H	T_{crit} (°R)	T_s (°R)
Tantalum Carbide	23.60	5751	5208
Hafnium Carbide	23.60	5697	5208
Niobium Carbide	17.31	5252	5142
Zirconium Carbide	25.96	4982	5225
Zirconium Boride (ZrB_2)	12.98	4752	5062
Titanium Carbide	10.38	4509	4985
Magnesium Oxide	8.24	4185	4888
Titanium Nitride	15.73	4347	5117
Silicon Carbide	12.98	4401	5062
Lanthanum Boride	10.82	4037	5000
Niobium Boride	30.54	4469	5250
Zirconium Nitride	24.72	4347	5216
Vanadium Carbide	13.31	3942	5070
Beryllium Carbide	10.38	3605	4985
Neodymium Boride	11.29	3902	5015
Praesodymium Boride	12.66	3888	5054
Calcium Oxide	17.90	3898	5150
Yttrium Boride	17.90	3875	5150
Scandium Nitride	19.23	3807	5166
Aluminum Nitride	15.73	3780	5117

Table 13. Steady State Surface Temperatures for an Exhaust Temperature Region of 3600°R for a Single Layer Tile Insulation System with a Boiling Water Backface

Material	H	T_{crit} (°R)	T_s (°R)
Aluminum Nitride	15.73	3780	3425
Beryllium Carbide	10.38	3605	3343
Boron Carbide	17.31	3537	3440
Boron Nitride	30.54	3510	3507
Calcium Oxide	17.90	3898	3445
Cerium Oxide	43.27	3605	3534
Europium Boride	22.57	2848	3476
Gadolinium Boride	24.72	3753	3486
Hafnium Carbide	23.60	5697	3481
Lanthanum Boride	10.82	4037	3352
Magnesium Oxide	8.24	4185	3283
Molybdenum Carbide	64.89	3773	3556
Neodymium Boride	11.29	3902	3362
Niobium Boride	30.54	4469	3507
Niobium Carbide	17.31	5252	3440
Praesodymium Boride	12.66	3888	3386
Samarium Boride	37.09	3848	3523
Scandium Nitride	19.23	3807	3455
Scandium Oxide	64.89	3605	3556
Silicon Carbide	12.98	4401	3391
Tantalum Carbide	23.60	5751	3481
Terbium Boride	25.96	3524	3491
Titanium Carbide	10.38	4509	3343
Titanium Nitride	15.73	4347	3425
Vanadium Carbide	13.31	3942	3395

Table 13. (Continued)

Material	H	T_{crit} (°R)	T_s (°R)
Vanadium Nitride	39.94	3551	3528
Ytterbium Boride	20.77	3564	3465
Ytterbium Silicate	86.53	3645	3567
Yttrium Boride	17.90	3875	3445
Yttrium Oxide	30.54	3686	3507
Zirconium Boride (ZrB_2)	12.98	4752	3391
Zirconium Carbide	25.96	4982	3491
Zirconium Nitride	24.72	4347	3486
Zirconium Oxide	30.54	3983	3507
Zirconium Silicate	86.53	3645	3567
Molybdenum Silicide	10.60	3132	3347
Barium Boride	14.42	3375	3410

Table 14. Steady State Surface Temperatures for an Exhaust Temperature Region of 1800°R for a Single Layer Tile Insulation System with a Boiling Water Backface

Material	H	T_{crit} (°R)	T_s (°R)
Aluminum Nitride	15.73	3780	1733
Aluminum Oxide	13.66	3135	1723
Aluminum Silicate	86.53	2866	1787
Barium Boride	14.42	3375	1727
Beryllium Carbide	10.38	3605	1701
Boron Carbide	17.31	3537	1738
Boron Nitride	30.54	3510	1764
Calcium Boride	22.57	3375	1752
Calcium Oxide	17.90	3898	1740
Calcium Zirconate	148.37	3524	1792
Cerium Boride	15.27	3321	1731
Cerium Oxide	43.27	3605	1775
Chromium Boride (CrB)	25.96	3208	1758
Chromium Boride (CrB_2)	23.60	3267	1754
Chromium Carbide ($Cr_{23}C_6$)	28.84	2498	1762
Chromium Carbide (Cr_3C_2)	27.33	2808	1760
Chromium Nitride	23.60	2592	1754
Chromium Silicide	47.20	2695	1777
Europium Boride	22.57	3848	1752
Gadolinium Boride	24.72	3753	1756
Gadolinium Oxide	259.52	3497	1796
Hafnium Carbide	23.60	5697	1754
Lanthanum Boride	10.82	4037	1705

Table 14. (Continued)

Material	H	T_{crit} (°R)	T_s (°R)
Lanthanum Sulfide	39.94	3335	1772
Magnesium Aluminate	43.27	3251	1775
Magnesium Oxide	8.24	4185	1678
Magnesium Silicate	103.84	2930	1789
Molybdenum Beryllide	10.38	2592	1701
Molybdenum Carbide	64.89	3773	1783
Molybdenum Silicide	10.60	3132	1703
Neodymium Boride	11.29	3902	1708
Neodymium Sulfide	519.03	3254	1798
Niobium Boride	30.54	4469	1764
Niobium Carbide	17.31	5252	1738
Niobium Nitride	129.81	3510	1791
Praesodymium Boride	12.66	3888	1717
Samarium Boride	37.09	3848	1770
Scandium Nitride	19.23	3807	1744
Scandium Oxide	64.89	3605	1783
Silicon Carbide	12.98	4401	1719
Silicon Oxide	519.03	2695	1798
Silicon Nitride	11.54	2903	1710
Strontium Boride	19.97	3386	1746
Tantalum Carbide	23.60	5751	1754
Terbium Boride	25.96	3524	1758
Thorium Boride	11.29	3267	1708
Titanium Carbide	10.38	4509	1701
Titanium Nitride	15.73	4347	1733
Titanium Oxide	47.20	2889	1777

Table 14. (Continued)

Material	H	T_{crit} (°R)	T_s (°R)
Titanium Silicide	34.61	3227	1768
Vanadium Carbide	13.31	3942	1721
Vanadium Nitride	39.94	3551	1772
Ytterbium Boride	20.77	3564	1748
Ytterbium Silicate	86.53	3645	1787
Yttrium Boride	17.90	3875	1740
Yttrium Oxide	30.54	3686	1764
Zirconium Beryllide	12.98	2970	1719
Zirconium Boride (ZrB_2)	12.98	4752	1719
Zirconium Boride (ZrB_{12})	39.94	3402	1772
Zirconium Carbide	25.96	4982	1758
Zirconium Nitride	24.72	4347	1756
Zirconium Oxide	30.54	3983	1764
Zirconium Silicate	86.53	3645	1787

The steady state heat rate equation was derived with the use of Fourier's law of heat conduction which is

$$\frac{q}{A} = -k\frac{\partial T}{\partial x} \tag{4}$$

After integration, the formula becomes

$$\frac{q}{A} = -k\frac{\Delta T}{\Delta x} \tag{5}$$

where

$\Delta T = T_s - T_{bf}$

$\Delta x = L$

Equation 3 is substituted into Equation 5 to obtain the heat rate equation where heat flow is positive from the hot plume into the insulation material.

$$\frac{q}{A} = \frac{h}{1+\frac{hL}{k}}(T_\infty - T_{bf}) \tag{6}$$

The nondimensional form of this equation, Equation 7, was used to construct the graph in Figure 30. Complete formulation of the steady state heat rate equation can be found in Appendix F.

$$\frac{q}{hAT_\infty} = \frac{1}{1+Bi}(1-\frac{T_{bf}}{T_\infty}) \tag{7}$$

Figure 30 illustrates the behavior of the nondimensional heat rate as a function of the ratio of the backface temperature to the plume temperature.

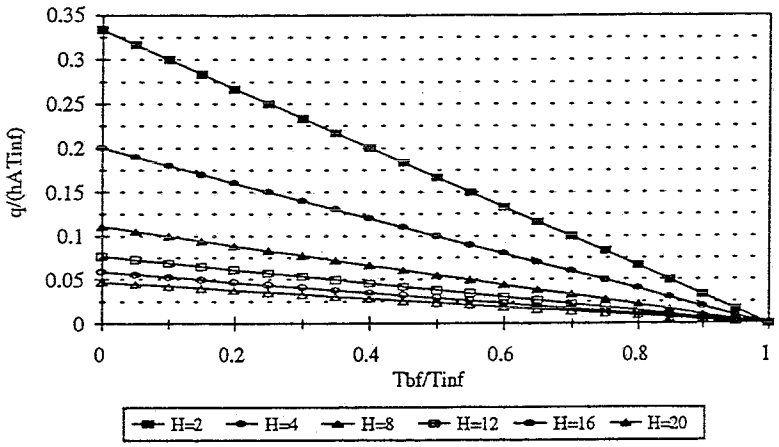

Fig. 30. Nondimensional Heat Rate Vs. Nondimensional Temperature Ratio at Several Biot Numbers

Depending on the temperature of the backface, the heat rate through the material can be calculated. The trends show that, as the backface temperature increases, the heat rate through the material decreases. The graph also shows that materials with higher Biot numbers have lower heat rates than materials with lower Biot numbers. A higher heat rate through the material leads to a higher water flowrate requirement across the backface.

The heat rate calculated from Equation 6 was then used to calculate the required water flowrate across the backface.

$$\frac{m}{A} = \frac{q}{A} \frac{1}{h_{fg}} \tag{8}$$

where

h_{fg} = enthalpy of water at the boiling point (≈ 970.22 Btu/lbm, 2256.7 kJ/kg).

Tables 15 - 18 show the heat rates and required water flowrates in all four regions for all the candidate materials. Materials with a higher thermal conductivity have higher heat rates; therefore, they require a larger water flowrate than materials with lower thermal conductivities.

After taking into account the area under consideration, the required water flowrate from Equation 8 can be directly compared with the current required water flowrate of 300,000 gpm (19 m^3/s). The decrease in water flowrate using a single layer tile protection system was calculated with the use of the following equation:

$$\%\ decrease = \frac{m_{current} - m_{bf}}{m_{current}} \qquad (9)$$

where

$m_{current}$ = current water flowrate requirement due to transpiration cooling (300,000 gpm, 19 m^3/s)

m_{bf} = water flowrate requirement for a system with a boiling water backface.

For candidate materials in the temperature region of 6538°R (3632 K), Table 15 shows that, if there was a material that could withstand the temperature of the plume in that region, the required water flowrate would be decreased by 87 - 95% from the current requirement. The materials in Table 15 are listed in descending order according to maximum run times.

Table 15. Heat Rates and Volumetric Flowrates for a Boiling Water Backface for an Exhaust Temperature Region of 6538°R

Material	H	q/A (Btu/hr•ft^2)	m/A (gal/min•ft^2)	m (gal/min)	% decrease in water flowrate
Tantalum Carbide	23.60	4.29e+05	0.88	18012	94
Hafnium Carbide	23.60	4.29e+05	0.88	18012	94
Niobium Carbide	17.31	5.77e+05	1.19	24208	92
Zirconium Boride (ZrB_2)	12.98	7.55e+05	1.55	31699	89
Magnesium Oxide	8.24	1.14e+06	2.35	47954	84
Titanium Carbide	10.38	9.28e+05	1.91	38927	87
Zirconium Carbide	25.96	3.92e+05	0.81	16437	95
Titanium Nitride	15.73	6.31e+05	1.30	26483	91
Silicon Carbide	12.98	7.55e+05	1.55	31699	89
Lanthanum Boride	10.82	8.94e+05	1.84	37501	87
Beryllium Carbide	10.38	9.28e+05	1.91	38927	87
Vanadium Carbide	13.31	7.38e+05	1.52	30961	90
Neodymium Boride	11.29	8.59e+05	1.77	36066	88
Niobium Boride	30.54	3.35e+05	0.69	14050	95
Zirconium Nitride	24.72	4.10e+05	0.84	17227	94
Praesodymium Boride	12.66	7.73e+05	1.59	32434	89
Calcium Oxide	17.90	5.59e+05	1.15	23443	92
Aluminum Nitride	15.73	6.31e+05	1.30	26483	91
Scandium Nitride	19.23	5.22e+05	1.07	21905	93
Yttrium Boride	17.90	5.59e+05	1.15	23443	92

If the present system remains in place only in the temperature region of 6538°R (3632 K) and the steel in the other three regions is replaced by a material that could withstand plume conditions up to 5400°R (3000 K), then there would still be significant savings. Table 16 shows the required flowrate for a system in which only the steel in the outer three regions was replaced by a suitable candidate material. If this system was implemented, the required water flowrate could be reduced by anywhere from 74 - 87%. Again, materials are listed in descending order according to maximum run times.

Another solution is to replace only the steel in the outer two regions. Based on the data in Table 17, the required water flowrate could be reduced by 67 - 70%. The materials are listed alphabetically since all but two materials have infinite run times.

The last alternative is to replace only the steel in the outer region of the flame bucket. Table 18 shows that the required water flowrate would be reduced by approximately 49%. Again, materials are listed alphabetically. Assuming that the cost of the replacement materials is low, any one of these alternatives would result in significant savings.

Insulated Backface Condition

An insulated backface is the most severe condition for the material. As the plume continuously impinges on the surface of the flame bucket, the temperature of a material with an insulated backface will continue to rise until melting or some other failure occurs; therefore, there is no steady state solution, so the transient case must be studied. The transient solution for the insulated backface condition was obtained by treating the system

Table 16. Heat Rates and Volumetric Flowrates for a Boiling Water Backface for an Exhaust Temperature Region of 5400°R

Material	H	q/A (Btu/hr•ft^2)	m/A (gal/min•ft^2)	m (gal/min)	% decrease in water flowrate
Tantalum Carbide	23.60	3.46e+05	0.71	38694	87
Hafnium Carbide	23.60	3.46e+05	0.71	38694	87
Niobium Carbide	17.31	4.65e+05	0.96	43083	86
Zirconium Carbide	25.96	3.16e+05	1.00	43777	85
Zirconium Boride (ZrB_2)	12.98	6.09e+05	1.92	60345	80
Titanium Carbide	10.38	7.48e+05	2.36	68191	77
Magnesium Oxide	8.24	9.21e+05	2.91	77991	74
Titanium Nitride	15.73	5.09e+05	1.60	54683	82
Silicon Carbide	12.98	6.09e+05	1.92	60345	80
Lanthanum Boride	10.82	7.20e+05	2.27	66643	78
Niobium Boride	30.54	2.70e+05	0.85	41186	86
Zirconium Nitride	24.72	3.31e+05	1.04	44635	85
Vanadium Carbide	13.31	5.95e+05	1.88	59544	80
Beryllium Carbide	10.38	7.48e+05	2.36	68191	77
Neodymium Boride	11.29	6.93e+05	2.19	65086	78
Praesodymium Boride	12.66	6.23e+05	1.97	61143	80
Calcium Oxide	17.90	4.50e+05	1.42	51383	83
Yttrium Boride	17.90	4.50e+05	1.42	51383	83
Scandium Nitride	19.23	4.21e+05	1.33	49714	83
Aluminum Nitride	15.73	5.09e+05	1.60	54683	82

Table 17. Heat Rates and Volumetric Flowrates for a Boiling Water Backface for an Exhaust Temperature Region of 3600°R

Material	H	q/A (Btu/hr•ft^2)	m/A (gal/min•ft^2)	m (gal/min)	% decrease in water flowrate
Aluminum Nitride	15.73	3.15e+05	0.65	96387	68
Beryllium Carbide	10.38	4.63e+05	0.95	100026	67
Boron Carbide	17.31	2.88e+05	0.59	95721	68
Boron Nitride	30.54	1.67e+05	0.34	92750	69
Calcium Oxide	17.90	2.79e+05	0.57	95497	68
Cerium Oxide	43.27	1.19e+05	0.25	91569	69
Europium Boride	22.57	2.24e+05	0.46	94139	69
Gadolinium Boride	24.72	2.05e+05	0.42	93679	69
Hafnium Carbide	23.60	2.14e+05	0.44	93909	69
Lanthanum Boride	10.82	4.46e+05	0.92	99609	67
Magnesium Oxide	8.24	5.70e+05	1.17	102666	66
Molybdenum Carbide	64.89	8.00e+04	0.16	90608	70
Neodymium Boride	11.29	4.29e+05	0.88	99189	67
Niobium Boride	30.54	1.67e+05	0.34	92750	69
Niobium Carbide	17.31	2.88e+05	0.59	95721	68
Praesodymium Boride	12.66	3.86e+05	0.79	98127	67
Samarium Boride	37.09	1.38e+05	0.28	92044	69
Scandium Nitride	19.23	2.61e+05	0.54	95048	68
Scandium Oxide	64.89	8.00e+04	0.16	90608	70
Silicon Carbide	12.98	3.77e+05	0.78	97912	67
Tantalum Carbide	23.60	2.14e+05	0.44	93909	69
Terbium Boride	25.96	1.96e+05	0.40	93448	69
Titanium Carbide	10.38	4.63e+05	0.95	100026	67

Table 17. (Continued)

Material	H	q/A (Btu/hr•ft^2)	m/A (gal/min•ft^2)	m (gal/min)	% decrease in water flowrate
Titanium Nitride	15.73	3.15e+05	0.65	96387	68
Vanadium Carbide	13.31	3.68e+05	0.76	97696	67
Vanadium Nitride	39.94	1.29e+05	0.27	91807	69
Ytterbium Boride	20.77	2.42e+05	0.50	94595	68
Ytterbium Silicate	86.53	6.02e+04	0.12	90122	70
Yttrium Boride	17.90	2.79e+05	0.57	95497	68
Yttrium Oxide	30.54	1.67e+05	0.34	92750	69
Zirconium Boride (ZrB_2)	12.98	3.77e+05	0.78	97912	67
Zirconium Carbide	25.96	1.96e+05	0.40	93448	69
Zirconium Nitride	24.72	2.05e+05	0.42	93679	69
Zirconium Oxide	30.54	1.67e+05	0.34	92750	69
Zirconium Silicate	86.53	6.02e+04	0.12	90122	70
Molybdenum Silicide	10.60	4.55e+05	0.94	99818	67
Barium Boride	14.42	3.42e+05	0.70	97045	68

Table 18. (Continued)

Material	H	q/A (Btu/hr•ft^2)	m/A (gal/min•ft^2)	m (gal/min)	% decrease in water flowrate
Thorium Boride	11.29	1.65e+05	0.34	153390	49
Titanium Carbide	10.38	1.78e+05	0.37	153551	49
Titanium Nitride	15.73	1.21e+05	0.25	152850	49
Titanium Oxide	47.20	4.21e+04	0.09	151876	49
Titanium Silicide	34.61	5.70e+04	0.12	152059	49
Vanadium Carbide	13.31	1.42e+05	0.29	153102	49
Vanadium Nitride	39.94	4.96e+04	0.10	151968	49
Ytterbium Boride	20.77	9.33e+04	0.19	152505	49
Ytterbium Silicate	86.53	2.32e+04	0.05	151643	49
Yttrium Boride	17.90	1.07e+05	0.22	152679	49
Yttrium Oxide	30.54	6.44e+04	0.13	152150	49
Zirconium Beryllide	12.98	1.45e+05	0.30	153144	49
Zirconium Boride (ZrB_2)	12.98	1.45e+05	0.30	153144	49
Zirconium Boride (ZrB_{12})	39.94	4.96e+04	0.10	151968	49
Zirconium Carbide	25.96	7.53e+04	0.16	152284	49
Zirconium Nitride	24.72	7.90e+04	0.16	152329	49
Zirconium Oxide	30.54	6.44e+04	0.13	152150	49
Zirconium Silicate	86.53	2.32e+04	0.05	151643	49

as a plane wall boundary problem with a convective boundary condition. The plane wall of thickness L is initially at temperature T_i and is insulated at x = 0. The surface at x = L is suddenly exposed to convection (where $h < \infty$) with an ambient temperature of T_∞. The formulation of the equation for the temperature distribution as a function of time is given in Appendix G. The solution is

$$u(x,\theta) = \sum_{n=1}^{\infty} \frac{2H\sin\lambda_n}{H\lambda_n + \lambda_n \sin^2\lambda_n} \cos\lambda_n \left(\frac{x}{L}\right) e^{-\lambda_n^2 \theta} \qquad \textbf{(10)}$$

This equation was derived in order to compare the best and worse case practical scenarios for backface conditions. Equation 10 was used to determine the run times at two different thicknesses for five selected materials. Tables 19 and 20 show the results of the comparison.

Table 19. Comparison of the Run Times of the Boiling Water and Insulated Backface Conditions for Selected Materials at a Thickness of 0.5 inches with $T_\infty = 6538°R$

Material	**H**	t (s) **for the insulated backface condition**	t (s) **for the boiling water backface condition**
Tantalum Carbide	5.90	8.31	∞
Hafnium Carbide	5.90	7.09	∞
Niobium Carbide	4.33	4.47	4.92
Zirconium Boride	3.25	2.72	2.76
Magnesium Oxide	2.06	2.65	2.73

Table 20. Comparison of the Run Times of the Boiling Water and Insulated Backface Conditions for Selected Materials at a Thickness of 2.0 inches with $T_\infty = 6538°R$

Material	**H**	t (s) **for the insulated backface condition**	t (s) **for the boiling water backface condition**
Tantalum Carbide	23.60	10.12	10.12
Hafnium Carbide	23.60	8.21	8.22
Niobium Carbide	17.04	4.73	4.73
Zirconium Boride	12.98	2.78	2.78
Magnesium Oxide	8.24	2.74	2.74

Based on the data in Tables 19 and 20, it appears that for small thicknesses the effect of the two different backfaces on the run times of the materials is quite significant for tantalum and hafnium carbide, but not important for the other materials. For sufficiently large thicknesses, the difference between the two backface conditions has little effect on the performance of the material, meaning there is no advantage or disadvantage to the various other backface conditions that could be chosen.

CHAPTER 6

COMPOSITE LAYER TILE PROTECTION SYSTEM

Introduction

A single layer tile protection system is an ideal system for the boiling water backface scenario because it offers the least resistance to the conduction of heat through the material, but it is not a practical solution because of the limiting properties of the candidate materials being considered for use. The metals and metal alloys have service temperatures that are too low for this application, the refractory metals and alloys have an oxidation problem at these temperatures, the coatings are too weak for prolonged usage, and the ceramics are too weak structurally because they are relatively weak in tension which means that they are also weak in bending. Thus, a compound material design is proposed using a ceramic as an insulation material and a strong, highly conductive metal as a support material. The backface of the support material will be convectively cooled with water in order to maintain the interface temperature below the service temperature of the metal. The thermal performance of candidate ceramic-metal combinations is analyzed in this chapter.

Steady State Solution

As previously demonstrated, the materials under consideration reach steady state in such a short time that the steady state solution must be used in order to model the

system. The steady state solution for this design involves a composite wall design with a convective frontface and a boiling water backface condition (T_{bf} = 672°R, 373 K). The four support materials under consideration for use in the thermal protection system are titanium, steel, aluminum, and copper. The frontface or surface temperature, T_s, and the interface temperature, T_{if}, between the insulation and the support material were calculated to find out if the temperatures exceed the critical temperatures of either material. This was done with the use of the following equations:

$$T_s = \frac{hT_\infty k_1 L_2 - hT_\infty k_1 L_1 + k_2 T_{bf} k_1 + hT_\infty L_1 k_2}{hk_1 L_2 - hk_1 L_1 + k_2 hL_1 + k_2 k_1} \qquad \textbf{(11)}$$

$$T_{if} = \frac{hT_\infty k_1 L_2 - hT_\infty k_1 L_1 + k_2 T_{bf} hL_1 + k_2 T_{bf} k_1}{hk_1 L_2 - hk_1 L_1 + k_2 hL_1 + k_2 k_1} \qquad \textbf{(12)}$$

where

k_1 = thermal conductivity of the insulation material, Btu/hr•ft•°R

k_2 = thermal conductivity of the support material, Btu/hr•ft•°R

L_1 = distance from the surface to the interface, ft

L_2 = distance from the interface to the backface, ft.

The formulation of these equations is presented in Appendix H.

Performance of Candidate Materials

Equations 11 and 12 were used to determine the most effective support material to use and to calculate the steady state surface and interface temperatures for all the

candidate materials in the four regions. Table 21 shows the surface and interface temperatures for candidate insulation materials with aluminum as the support material in the temperature region of 6538°R (3632 K). The remaining tables which show the surface and interface temperatures for candidate insulation materials with titanium, steel, and copper as the support materials are shown in Appendix I. From these tables it is observed that the steady state surface temperature exceeds the critical (service) temperature for all insulation materials. This conclusion was anticipated from the single layer tile analysis in Chapter 5.

Surface and interface temperatures for candidate insulation materials with aluminum as the support material in the temperature region of 5400°R (3000 K) are shown in Table 22. The tables illustrating the surface and interface temperatures for candidate materials with titanium, steel, and copper as the support material are shown in Appendix J. For titanium and steel support materials, the data show that the only insulation materials that do not exceed the critical surface temperatures are tantalum and hafnium carbide, but their interface temperatures do exceed the critical interface temperature. For aluminum and copper support materials, the data show that there are three materials that do not exceed the critical surface and interface temperatures. These materials are tantalum, hafnium, and niobium carbide. So, for the temperature region of 5400°R (3000 K), these three materials with either an aluminum or copper support material would make viable candidates.

Tables 23 shows the surface and interface temperatures for insulation materials with aluminum as the support material in a temperature region of 3600°R (2000 K).

Table 21. Steady State Surface and Interface Temperatures in an Exhaust Temperature Region of 6538°R for a Composite Wall Design with Aluminum as the Support Material with a Boiling Water Backface

Material	k (Btu/hr•ft•°R)	T_{crit} (°R)	T_s (°R)	T_{if} (°R)
Tantalum Carbide	12.71	5751	6320	1165
Hafnium Carbide	12.71	5697	6320	1165
Niobium Carbide	17.34	5252	6253	1316
Zirconium Boride (ZrB_2)	23.11	4752	6177	1487
Magnesium Oxide	36.40	4185	6028	1823
Titanium Carbide	28.89	4509	6108	1642
Zirconium Carbide	11.56	4982	6337	1125
Titanium Nitride	19.07	4347	6229	1369
Silicon Carbide	23.11	4401	6177	1487
Lanthanum Boride	27.73	4037	6121	1613
Beryllium Carbide	28.89	3605	6108	1642
Vanadium Carbide	22.54	3942	6184	1471
Neodymium Boride	26.58	3902	6135	1582
Niobium Boride	9.82	4469	6364	1063
Zirconium Nitride	12.13	4347	6328	1145
Praesodymium Boride	23.69	3888	6170	1503
Calcium Oxide	16.76	3898	6261	1297
Aluminum Nitride	19.07	3780	6229	1369
Scandium Nitride	15.60	3807	6277	1261
Yttrium Boride	16.76	3875	6261	1297

Table 22. Steady State Surface and Interface Temperatures in an Exhaust Temperature Region of 5400°R for a Composite Wall Design with Aluminum as the Support Material with a Boiling Water Backface

Material	k (Btu/hr•ft•°R)	T_{crit} (°R)	T_s (°R)	T_{if} (°R)
Tantalum Carbide	12.71	5751	5224	1069
Hafnium Carbide	12.71	5697	5224	1069
Niobium Carbide	17.34	5252	5170	1191
Zirconium Carbide	11.56	4982	5238	1037
Zirconium Boride (ZrB_2)	23.11	4752	5109	1329
Titanium Carbide	28.89	4509	5053	1454
Magnesium Oxide	36.40	4185	4989	1600
Titanium Nitride	19.07	4347	5151	1234
Silicon Carbide	23.11	4401	5109	1329
Lanthanum Boride	27.73	4037	5064	1430
Niobium Boride	9.82	4469	5260	987
Zirconium Nitride	12.13	4347	5231	1053
Vanadium Carbide	22.54	3942	5115	1316
Beryllium Carbide	28.89	3605	5053	1454
Neodymium Boride	26.58	3902	5075	1406
Praesodymium Boride	23.69	3888	5103	1342
Calcium Oxide	16.76	3898	5177	1176
Yttrium Boride	16.76	3875	5177	1176
Scandium Nitride	15.60	3807	5190	1146
Aluminum Nitride	19.07	3780	5152	1234

Table 23. Steady State Surface and Interface Temperatures in an Exhaust Temperature Region of 3600°R for a Composite Wall Design with Aluminum as the Support Material with a Boiling Water Backface

Material	k (Btu/hr•ft•°R)	T_{crit} (°R)	T_s (°R)	T_{if} (°R)
Aluminum Nitride	19.07	3780	3446	1020
Beryllium Carbide	28.89	3605	3385	1156
Boron Carbide	17.34	3537	3458	993
Boron Nitride	9.82	3510	3513	867
Calcium Oxide	16.76	3898	3462	984
Cerium Oxide	6.93	3605	3537	814
Europium Boride	13.29	2848	3487	928
Gadolinium Boride	12.13	3753	3495	908
Hafnium Carbide	12.71	5697	3491	918
Lanthanum Boride	27.73	4037	3392	1141
Magnesium Oxide	36.40	4185	3345	1247
Molybdenum Carbide	4.62	3773	3557	769
Neodymium Boride	26.58	3902	3399	1126
Niobium Boride	9.82	4469	3513	867
Niobium Carbide	17.34	5252	3458	993
Praesodymium Boride	23.69	3888	3416	1087
Samarium Boride	8.09	3848	3527	836
Scandium Nitride	15.60	3807	3470	966
Scandium Oxide	4.62	3605	3557	769
Silicon Carbide	23.11	4401	3420	1079
Tantalum Carbide	12.71	5751	3491	918
Terbium Boride	11.56	3524	3500	898
Titanium Carbide	28.89	4509	3385	1156

Table 23. (Continued)

Material	k (Btu/hr•ft•°R)	T_{crit} (°R)	T_s (°R)	T_{if} (°R)
Titanium Nitride	19.07	4347	3446	1020
Vanadium Carbide	22.54	3942	3423	1071
Vanadium Nitride	7.51	3551	3532	825
Ytterbium Boride	14.45	3564	3478	947
Ytterbium Silicate	3.47	3645	3567	745
Yttrium Boride	16.76	3875	3462	984
Yttrium Oxide	9.82	3686	3513	867
Zirconium Boride (ZrB_2)	23.11	4752	3420	1079
Zirconium Carbide	11.56	4982	3500	898
Zirconium Nitride	12.13	4347	3495	908
Zirconium Oxide	9.82	3983	3513	867
Zirconium Silicate	3.47	3645	3567	745
Molybdenum Silicide	28.31	3132	3388	1149
Barium Boride	20.80	3375	3434	1046

Variations of this table with titanium, steel, and copper as the support materials are found in Appendix K. With the exception of a few materials, most of the candidates in this region have surface temperatures that do not exceed their respective critical temperatures and interface temperatures that do not exceed the critical temperature of the support material. Thus, there are numerous viable candidates in this region.

Calculations for the surface and interface temperatures of the candidate insulation materials with aluminum as the support material in a temperature region of 1800°R (1000 K) are shown in Table 24. The remaining tables with titanium, steel, and copper as the support material are found in Appendix L. Based on the data shown, the temperatures of the plume are so low in this area that all of the materials have surface and interface temperatures that are well below the critical temperatures which means that all of the candidate materials could withstand the conditions in this region.

From the data shown in the tables, it is evident that the performance of the candidate insulation materials is dependent upon the support material. Support materials such as titanium and steel have low thermal conductivities which result in low surface and interface temperatures. Highly thermal conductive materials such as aluminum and copper conduct the heat away at faster rates which leads to lower surface and interface temperatures.

Tables 25 - 28 for aluminum as the support material and the corresponding tables for titanium, steel, and copper in Appendices M, N, O, and P illustrate these conclusions. Since it is not feasible to have a solution in which the entire bucket is replaced with a candidate material from this study, a new design involving partial replacement is

Table 24. Steady State Surface and Interface Temperatures in an Exhaust Temperature Region of 1800°R for a Composite Wall Design with Aluminum as the Support Material with a Boiling Water Backface

Material	k (Btu/hr•ft•°R)	T_{crit} (°R)	T_s (°R)	T_{if} (°R)
Aluminum Nitride	19.07	3780	1741	806
Aluminum Oxide	21.96	3135	1733	822
Aluminum Silicate	3.47	2866	1787	700
Barium Boride	20.80	3375	1736	816
Beryllium Carbide	28.89	3605	1717	858
Boron Carbide	17.34	3537	1745	796
Boron Nitride	9.82	3510	1767	747
Calcium Boride	13.29	3375	1756	770
Calcium Oxide	16.76	3898	1747	792
Calcium Zirconate	2.02	3524	1793	688
Cerium Boride	19.65	3321	1739	809
Cerium Oxide	6.93	3605	1776	726
Chromium Boride (CrB)	11.56	3208	1761	759
Chromium Boride (CrB_2)	12.71	3267	1758	767
Chromium Carbide ($Cr_{23}C_6$)	10.40	2498	1765	751
Chromium Carbide (Cr_3C_2)	10.98	2808	1763	755
Chromium Nitride	12.71	2592	1758	767
Chromium Silicide	6.36	2695	1778	722
Europium Boride	13.29	3848	1756	770
Gadolinium Boride	12.13	3753	1760	763
Gadolinium Oxide	1.16	3497	1796	681
Hafnium Carbide	12.71	5697	1758	766

Table 24. (Continued)

Material	k (Btu/hr•ft•°R)	T_{crit} (°R)	T_s (°R)	T_{lf} (°R)
Lanthanum Boride	27.74	4037	1720	853
Lanthanum Sulfide	7.51	3335	1774	731
Magnesium Aluminate	6.93	3251	1776	726
Magnesium Oxide	36.40	4185	1702	893
Magnesium Silicate	2.89	2930	1789	696
Molybdenum Beryllide	28.89	2592	1717	858
Molybdenum Carbide	4.62	3773	1783	709
Molybdenum Silicide	28.31	3132	1719	856
Neodymium Boride	26.58	3902	1722	847
Neodymium Sulfide	0.58	3254	1798	677
Niobium Boride	9.82	4469	1767	747
Niobium Carbide	17.34	5252	1745	796
Niobium Nitride	2.31	3510	1792	691
Praesodymium Boride	23.69	3888	1729	832
Samarium Boride	8.09	3848	1772	735
Scandium Nitride	15.60	3807	1750	785
Scandium Oxide	4.62	3605	1783	709
Silicon Carbide	23.11	4401	1731	829
Silicon Oxide	0.58	2695	1798	677
Silicon Nitride	26.00	2903	1724	844
Strontium Boride	15.02	3386	1751	781
Tantalum Carbide	12.71	5751	1758	766
Terbium Boride	11.56	3524	1761	759

Table 24. (Continued)

Material	k (Btu/hr•ft•°R)	T_{crit} (°R)	T_s (°R)	T_{if} (°R)
Titanium Carbide	28.89	4509	1717	858
Titanium Nitride	19.07	4347	1741	806
Titanium Oxide	6.36	2889	1778	722
Titanium Silicide	8.67	3227	1770	739
Vanadium Carbide	22.54	3942	1732	825
Vanadium Nitride	7.51	3551	1774	731
Ytterbium Boride	14.45	3564	1753	778
Ytterbium Silicate	3.47	3645	1787	700
Yttrium Boride	16.76	3875	1747	792
Yttrium Oxide	9.82	3686	1767	747
Zirconium Beryllide	23.11	2970	1731	829
Zirconium Boride (ZrB_2)	23.11	4752	1731	829
Zirconium Boride (ZrB_{12})	7.51	3402	1774	731
Zirconium Carbide	11.56	4982	1766	759
Zirconium Nitride	12.13	4347	1760	763
Zirconium Oxide	9.82	3983	1767	747
Zirconium Silicate	3.47	3645	1787	700

considered. Thus, the required water flowrates calculated in these tables represent the total water flowrates, which include the required water flowrate due to transpiration cooling plus the required water flowrate due to the boiling water backface. The equation is

$$m_{total} = m_{trans} + m_{bf} \quad \textbf{(13)}$$

The water flowrate for transpiration cooling was calculated based on the current flowrate per unit area, which was 10.5 gpm/ft^2 (0.007 m^3/s•m^2) [19]. Tables 25 - 28 and the tables in Appendices M, N, O, and P show that, as the thermal conductivity of the support material increases, the heat rate through the system increases and the flowrate of water required across the backface increases accordingly. These tables also show that, as the thermal conductivity of the candidate insulation material increases, which means a lower Biot number, the heat rate through the material also increases.

In Table 25 and its corresponding tables in Appendix M, the percent decrease in water flowrate represents the hypothetical situation where the entire flame bucket is replaced with an insulation material that can withstand a plume temperature of 6538°R (3632 K). This total area would be approximately 20,387 ft^2 (1984 m^2) [19]. If a viable material had been found, the amount of water needed would decrease between 87 - 95% depending on the specific insulation and support materials used. However, it is noted again that none of the materials studied could meet the thermal requirements.

The percent decrease in water flowrate in Table 26 and its corresponding tables in Appendix N shows the amount that the current system would decrease flowrate

Table 25. Heat Rates and Volumetric Flowrates in an Exhaust Temperature Region of 6538°R for a Composite Wall Design with Aluminum as the Support Material with a Boiling Water Backface

Material	H	T_{if} (°R)	q/A (Btu/hr•ft^2)	$(m/A)_{bf}$ (gal/min•ft^2)	m_{total} (gal/min)	% decrease in water flowrate
Tantalum Carbide	23.60	1165	3.93e+05	0.81	16498	95
Hafnium Carbide	23.60	1165	3.93e+05	0.81	16498	95
Niobium Carbide	17.31	1316	5.14e+05	1.06	21550	93
Zirconium Boride (ZrB_2)	12.98	1487	6.50e+05	1.34	27292	91
Magnesium Oxide	8.24	1823	9.18e+05	1.89	38540	87
Titanium Carbide	10.38	1642	7.74e+05	1.59	32485	89
Zirconium Carbide	25.96	1125	3.61e+05	0.74	15167	95
Titanium Nitride	15.73	1369	5.56e+05	1.14	23335	92
Silicon Carbide	12.98	1487	6.50e+05	1.34	27292	91
Lanthanum Boride	10.82	1613	7.50e+05	1.54	31486	90
Beryllium Carbide	10.38	1642	7.74e+05	1.59	32485	89
Vanadium Carbide	13.31	1471	6.37e+05	1.31	26743	91
Neodymium Boride	11.29	1582	7.26e+05	1.49	30468	90
Niobium Boride	30.54	1063	3.12e+05	0.64	13111	96
Zirconium Nitride	24.72	1145	3.77e+05	0.78	15837	95
Praesodymium Boride	12.66	1503	6.63e+05	1.37	27835	91
Calcium Oxide	17.90	1297	4.99e+05	1.03	20942	93
Aluminum Nitride	15.73	1369	5.56e+05	1.14	23335	92
Scandium Nitride	19.23	1261	4.70e+05	0.97	19706	93
Yttrium Boride	17.90	1297	4.99e+05	1.03	20942	93

Table 26. Heat Rates and Volumetric Flowrates in an Exhaust Temperature Region of 5400°R for a Composite Wall Design with Aluminum as the Support Material with a Boiling Water Backface

Material	H	T_{if} (°R)	q/A (Btu/hr•ft^2)	$(m/A)_{bf}$ (gal/min•ft^2)	m_{total} (gal/min)	% decrease in water flowrate
Tantalum Carbide	23.60	1069	3.17e+05	0.65	37622	87
Hafnium Carbide	23.60	1069	3.17e+05	0.65	37622	87
Niobium Carbide	17.31	1191	4.14e+05	0.85	41200	86
Zirconium Carbide	25.96	1037	2.91e+05	0.60	36678	88
Zirconium Boride (ZrB_2)	12.98	1329	5.24e+05	1.08	45267	85
Titanium Carbide	10.38	1454	6.24e+05	1.28	48946	84
Magnesium Oxide	8.24	1600	7.40e+05	1.52	53235	82
Titanium Nitride	15.73	1234	4.48e+05	0.92	42465	86
Silicon Carbide	12.98	1329	5.24e+05	1.08	45267	85
Lanthanum Boride	10.82	1430	6.05e+05	1.24	48238	84
Niobium Boride	30.54	987	2.52e+05	0.52	35223	88
Zirconium Nitride	24.72	1053	3.04e+05	0.63	37153	88
Vanadium Carbide	13.31	1316	5.14e+05	1.06	44879	85
Beryllium Carbide	10.38	1454	6.24e+05	1.28	48946	84
Neodymium Boride	11.29	1406	5.85e+05	1.20	47518	84
Praesodymium Boride	12.66	1342	5.35e+05	1.10	45652	85
Calcium Oxide	17.90	1176	4.02e+05	0.83	40770	86
Yttrium Boride	17.90	1176	4.02e+05	0.83	40770	86
Scandium Nitride	19.23	1146	3.78e+05	0.78	39894	87
Aluminum Nitride	15.73	1234	4.48e+05	0.92	42465	86

requirements if only the areas outside the impact area, which are the peak temperature regions of 5400°R (3000 K), 3600°R (2000 K), and 1800°R (1000 K), were replaced with an insulation material able to withstand a plume temperature of at least 5400°R (3000 K). The area under consideration for replacement is 17,917 ft^2 (1665 m^2). For the viable materials indicated in the tables, the amount of water used would decrease by 81 - 88% depending on the specific insulation and support materials.

In Table 27 and its corresponding tables in Appendix O, the percent decrease represents the amount that the current system flowrate requirements would decrease if only the areas enclosing the temperature regions of 3600°R (2000 K) and 1800°R (1000 K) were replaced with an insulation material able to withstand the plume temperature of at least 3600°R (2000 K). The area in question would be approximately 11,945 ft^2 (1110 m^2). If the solution were to involve a design of this type, the amount of water needed would be reduced by 66 - 70%.

The percent decrease in water flowrate in Table 28 and its corresponding tables in Appendix P reflects the amount that the flowrate requirements would be reduced by if the only the area encompassing the temperature region of 1800°R (1000 K) were replaced by an insulation material able to withstand a plume temperature of at least 1800°R (1000 K) in that region. In this case, the area would only be 5972 ft^2 (555 m^2), and the amount of water needed would decrease by almost 50%.

Table 27. Heat Rates and Volumetric Flowrates in an Exhaust Temperature Region of 3600°R for a Composite Wall Design with Aluminum as the Support Material with a Boiling Water Backface

Material	H	T_{if} (°R)	q/A (Btu/hr•ft^2)	$(m/A)_{bf}$ (gal/min•ft^2)	m_{total} (gal/min)	% decrease in water flowrate
Aluminum Nitride	15.73	1020	2.78e+05	0.57	95467	68
Beryllium Carbide	10.38	1156	3.86e+05	0.80	98142	67
Boron Carbide	17.31	993	2.56e+05	0.53	94944	68
Boron Nitride	30.54	867	1.56e+05	0.32	92476	69
Calcium Oxide	17.90	984	2.49e+05	0.51	94766	68
Cerium Oxide	43.27	814	1.13e+05	0.23	91427	70
Europium Boride	22.57	928	2.04e+05	0.42	93659	69
Gadolinium Boride	24.72	908	1.88e+05	0.39	93273	69
Hafnium Carbide	23.60	918	1.96e+05	0.40	93466	69
Lanthanum Boride	10.82	1141	3.75e+05	0.77	97850	67
Magnesium Oxide	8.24	1247	4.58e+05	0.94	99913	67
Molybdenum Carbide	64.89	769	7.73e+04	0.16	90543	70
Neodymium Boride	11.29	1126	3.62e+05	0.75	97552	67
Niobium Boride	30.54	867	1.56e+05	0.32	92476	69
Niobium Carbide	17.31	993	2.56e+05	0.53	94944	68
Praesodymium Boride	12.66	1087	3.31e+05	0.68	96782	68
Samarium Boride	37.09	836	1.31e+05	0.27	91854	69
Scandium Nitride	19.23	966	2.34e+05	0.48	94405	69
Scandium Oxide	64.89	769	7.73e+04	0.16	90543	70
Silicon Carbide	12.98	1079	3.25e+05	0.67	96623	68
Tantalum Carbide	23.60	918	1.96e+05	0.40	93466	69

Table 27. (Continued)

Material	H	T_{if} (°R)	q/A (Btu/hr•ft^2)	$(m/A)_{bf}$ (gal/min•ft^2)	m_{total} (gal/min)	% decrease in water flowrate
Terbium Boride	25.96	898	1.80e+05	0.37	93077	69
Titanium Carbide	10.38	1156	3.86e+05	0.80	98142	67
Titanium Nitride	15.73	1020	2.78e+05	0.57	95466	68
Vanadium Carbide	13.31	1071	3.18e+05	0.65	96463	68
Vanadium Nitride	39.94	825	1.22e+05	0.25	91642	69
Ytterbium Boride	20.77	947	2.19e+05	0.45	94036	69
Ytterbium Silicate	86.53	745	5.87e+04	0.12	90085	70
Yttrium Boride	17.90	984	2.49e+05	0.51	94766	68
Yttrium Oxide	30.54	867	1.56e+05	0.32	92476	69
Zirconium Boride (ZrB_2)	12.98	1079	3.25e+05	0.67	96623	68
Zirconium Carbide	25.96	898	1.80e+05	0.37	93077	69
Zirconium Nitride	24.72	908	1.88e+05	0.39	93273	69
Zirconium Oxide	30.54	867	1.56e+05	0.32	92476	69
Zirconium Silicate	86.53	745	5.87e+04	0.12	90085	70
Molybdenum Silicide	10.60	1149	3.80e+05	0.78	97997	67
Barium Boride	14.42	1046	2.98e+05	0.61	95972	68

Table 28. Heat Rates and Volumetric Flowrates in an Exhaust Temperature Region of 1800°R for a Composite Wall Design with Aluminum as the Support Material with a Boiling Water Backface

Material	H	T_{if} (°R)	q/A (Btu/hr•ft^2)	$(m/A)_{bf}$ (gal/min•ft^2)	m_{total} (gal/min)	% decrease in water flowrate
Aluminum Nitride	15.73	806	1.07e+05	0.22	152673	49
Aluminum Oxide	13.66	822	1.20e+05	0.25	152834	49
Aluminum Silicate	86.53	700	2.26e+04	0.05	151636	49
Barium Boride	14.42	816	1.15e+05	0.24	152770	49
Beryllium Carbide	10.38	858	1.49e+05	0.31	153188	49
Boron Carbide	17.31	796	9.88e+04	0.20	152572	49
Boron Nitride	30.54	747	6.01e+04	0.12	152097	49
Calcium Boride	22.57	770	7.86e+04	0.16	152325	49
Calcium Oxide	17.90	792	9.60e+04	0.20	152538	49
Calcium Zirconate	148.37	688	1.34e+04	0.03	151523	49
Cerium Boride	15.27	809	1.10e+05	0.23	152706	49
Cerium Oxide	43.27	726	4.37e+04	0.09	151895	49
Chromium Boride (CrB)	25.96	759	6.95e+04	0.14	152213	49
Chromium Boride (CrB_2)	23.60	767	7.56e+04	0.16	152288	49
Chromium Carbide ($Cr_{23}C_6$)	28.84	751	6.33e+04	0.13	152136	49
Chromium Carbide (Cr_3C_2)	27.33	755	6.64e+04	0.14	152174	49
Chromium Nitride	23.60	767	7.56e+04	0.16	152288	49
Chromium Silicide	47.20	722	4.03e+04	0.08	151853	49
Europium Boride	22.57	770	7.86e+04	0.16	152325	49

Table 28. (Continued)

Material	H	T_{if} (°R)	q/A (Btu/hr•ft^2)	$(m/A)_{bf}$ (gal/min•ft^2)	m_{total} (gal/min)	% decrease in water flowrate
Gadolinium Boride	24.72	763	7.26e+04	0.15	152250	49
Gadolinium Oxide	259.52	681	7.73e+03	0.02	151453	50
Hafnium Carbide	23.60	766	7.56e+04	0.16	152288	49
Lanthanum Boride	10.82	853	1.44e+05	0.30	153132	49
Lanthanum Sulfide	39.94	731	4.70e+04	0.10	151936	49
Magnesium Aluminate	43.27	726	4.37e+04	0.09	151895	49
Magnesium Oxide	8.24	893	1.77e+05	0.36	153529	49
Magnesium Silicate	103.84	696	1.90e+04	0.04	151591	49
Molybdenum Beryllide	10.38	858	1.49e+05	0.31	153188	49
Molybdenum Carbide	64.89	709	2.98e+04	0.06	151724	49
Molybdenum Silicide	10.60	856	1.47e+05	0.30	153160	49
Neodymium Boride	11.29	847	1.40e+05	0.29	153075	49
Neodymium Sulfide	519.03	677	3.89e+03	0.01	151406	50
Niobium Boride	30.54	747	6.01e+04	0.12	152097	49
Niobium Carbide	17.31	796	9.88e+04	0.20	152572	49
Niobium Nitride	129.81	691	1.53e+04	0.03	151546	49
Praesodymium Boride	12.66	832	1.28e+05	0.26	152926	49
Samarium Boride	37.09	735	5.03e+04	0.10	151977	49

Table 28. (Continued)

Material	H	T_{if} (°R)	q/A (Btu/hr•ft^2)	$(m/A)_{bf}$ (gal/min•ft^2)	m_{total} (gal/min)	% decrease in water flowrate
Scandium Nitride	19.23	785	9.03e+04	0.19	152468	49
Scandium Oxide	64.89	709	2.98e+04	0.06	151724	49
Silicon Carbide	12.98	829	1.25e+05	0.26	152896	49
Silicon Oxide	519.03	677	3.89e+03	0.01	151406	50
Silicon Nitride	11.54	844	1.37e+05	0.28	153046	49
Strontium Boride	19.97	781	8.74e+04	0.18	152433	49
Tantalum Carbide	23.60	766	7.56e+04	0.16	152288	49
Terbium Boride	25.96	759	6.95e+04	0.14	152213	49
Thorium Boride	11.29	847	1.40e+05	0.29	153075	49
Titanium Carbide	10.38	858	1.49e+05	0.31	153188	49
Titanium Nitride	15.73	806	1.07e+05	0.22	152673	49
Titanium Oxide	47.20	722	4.03e+04	0.08	151853	49
Titanium Silicide	34.61	739	5.36e+04	0.11	152017	49
Vanadium Carbide	13.31	825	1.23e+05	0.25	152865	49
Vanadium Nitride	39.94	731	4.70e+04	0.10	151936	49
Ytterbium Boride	20.77	778	8.45e+04	0.17	152397	49
Ytterbium Silicate	86.53	700	2.26e+04	0.05	151636	49
Yttrium Boride	17.90	792	9.60e+04	0.20	152538	49
Yttrium Oxide	30.54	747	6.01e+04	0.12	152097	49
Zirconium Beryllide	12.98	829	1.25e+05	0.26	152896	49
Zirconium Boride (ZrB_2)	12.98	829	1.25e+05	0.26	152896	49
Zirconium Boride (ZrB_{12})	39.94	731	4.70e+04	0.10	151936	49

Table 28. (Continued)

Material	H	T_{if} (°R)	q/A (Btu/hr•ft^2)	$(m/A)_{bf}$ (gal/min•ft^2)	m_{total} (gal/min)	% decrease in water flowrate
Zirconium Carbide	25.96	759	6.95e+04	0.14	152213	49
Zirconium Nitride	24.72	763	7.26e+04	0.15	152250	49
Zirconium Oxide	30.54	747	6.01e+04	0.12	152097	49
Zirconium Silicate	86.53	700	2.26e+04	0.05	151636	49

CHAPTER 7

CONCLUSIONS AND RECOMMENDATIONS

The purpose of this research was to determine if the transpiration cooling process currently used for the flame buckets in SSME testing at NASA-SSC can be replaced by a thermal protection system that would result in significant operational savings. This was done by investigating the use of coatings, and metal and ceramic tiles in single layer and composite layer systems. Coatings were eliminated as a stand-alone system because of their compositional defects, lack of thickness control, and inadequate reliability and short effective lives caused by premature coating failures. Common metals and refractory metals were also considered but with the exception of tungsten they were excluded from further studies because of service temperatures that were below system requirements. Tungsten has the highest melting point of all metals, approximately 6590°R (3661 K), which made it a good candidate for this study, but it also has a few major disadvantages. These include brittleness at low temperatures and poor resistance to oxidation.

Ceramics were of great interest to this study because of their high melting temperatures, however, the stagnation conditions in the plume proved to be too extreme even for them. All the results lead to the conclusion that the heat loads in the highest temperature region were too large for any material in this study to withstand without reaching failure of some kind. The results also show that, while it will not be possible at

this time to replace the transpiration cooled system in the entire flame bucket, partial replacement would still result in a significant decrease in the amount of water needed to be pumped through the flame bucket.

Three materials emerged as viable candidates for use in temperature regions up to 5400°R (3000 K). These materials are tantalum carbide, hafnium carbide, and niobium carbide. If any one of these materials were used with aluminum or copper support materials, the amount of water needed would decrease from 300,000 gpm (19 m^3/s) to approximately 40,000 gpm (2.5 m^3/s). The total savings would depend on the cost of the insulation and support materials. In this study, the four support materials were titanium, steel, aluminum, and copper. In the composite layer system, it is important to keep the surface and interface temperatures lower than their respective critical temperatures. Because of its high thermal conductivity, the use of copper was the most effective in accomplishing this goal, but aluminum, which also has a high thermal conductivity, was also very effective. Thus, either aluminum or copper would make good support materials because they are able to handle such high heat loads, but because of the cost of copper, aluminum would be a less expensive option.

Data on the strength of carbides are very limited and vary so widely that it was impossible to perform a mechanical analysis on these three materials based on any published data. While tantalum, hafnium, and niobium carbide seem to be good candidates because of their thermal performance, their mechanical properties might prove to be a limitation even though ceramics are characterized by superior compressive strength.

It was shown that all materials studied either exceeded their service temperatures or reached steady state in less than 30 seconds, whereas, run times in excess of 10 minutes are required. Because of these material response characteristics, the specific heat and thermal diffusivity are not important parameters in material selection. The factors that are most important are the material service temperature and thermal conductivity, the tile thickness, and the backface boundary condition.

For sufficiently high material service temperatures, it is desired to have very low thermal conductivity to minimize heat flow through the material, and the tile thickness and backface boundary condition become irrelevant. However, for service temperatures below the expected plume temperatures, which is the case in the hotter portions of the plume for the materials studied, it is desired to have high material thermal conductivity to keep the surface temperature below the critical service temperature. In this case, a boiling water backface is required to handle the high heat transfer rates and it is desired that the tiles be as thin as structurally feasible.

Most of the equations used are developed in their nondimensional form in order to reduce the number of variables and to investigate which parameters are more important in determining the response of the system. The Biot number is shown to be a very significant parameter in that it contains the two important factors, which are material thermal conductivity and tile thickness. This is an important fact because as new materials become available the equations used in this study can be employed to readily predict the behavior of the material in order to find out if it would be a suitable material for use in a thermal protection system. Since the prime candidates for the insulation material are relatively

brittle, it is recommended that a two-layer design be used with a relatively strong metal as a support material. Specifically, aluminum is recommended because its high thermal conductivity results in temperatures at the interface between the insulation and support materials that are below its service temperature. Also, aluminum is sufficiently strong and relatively inexpensive.

In summary, this study has resulted in the following conclusions and recommendations:

1. Presently available coatings are not recommended due to their lack of durability under these severe thermal conditions.

2. Metals are not recommended as the exposed tile material because of their relatively low melting temperatures or, in the case of tungsten, poor resistance to oxidation and brittleness.

3. Refractory metals are not recommended as the exposed tile material due to inadequate service temperatures and/or poor resistance to oxidation.

4. The recommended design is a two-layer composite with a ceramic material supported by a metal. The ceramics with the highest thermal performance were tantalum carbide, hafnium carbide, and niobium carbide and the recommended metal is aluminum.

5. The three recommended design options are partial replacements of the existing transpiration cooled system with the two-layer composite system, resulting in the following reductions in cooling water flowrate from the current value of 300,000 gpm (19 m^3/s):

Replaced Area, ft^2	Nominal Flowrate, gpm
17,917	57,000
11,945	102,000
5,972	150,000

6. A structural analysis of the flame bucket configuration under plume dynamic loading is recommended to determine thicknesses of the two-layer composite design materials.

7. An economic analysis of the cost and availability of the identified insulation and support materials, as well as flame bucket structural modification requirements is recommended as a prerequisite to final design selection.

BIBLIOGRAPHY

1. "Propulsion Testing for the Future," John C. Stennis Space Center Brochure, National Aeronautics and Space Administration, 1995.

2. "SSME Rocket Application Output Summary," Thermo-Chemical Equilibrium Program, Software and Engineering Associates, Inc., 1995.

3. St Cyr, William W., Project Director, NASA - Stennis Space Center, Personal Communication, 1996.

4. Lasday, Stanley B., "Nature of Ceramic Coatings and Their Benefits in Thermal Processes," Engineering Applications of Ceramic Materials Source Book, American Society for Metals, Ohio, 1985.

5. National Research Council, High Temperature Oxidation Resistance Coatings, National Academy of Sciences, Washington D.C., 1970.

6. Jacobs, James A. and Thomas F. Kilduff, Engineering Materials Technology, Prentice-Hall, Inc., New Jersey, 1985.

7. Kalpakjian, Serope, Manufacturing Engineering and Technology, 2nd ed., Addison-Wesley Publishing Company, Massachusetts, 1992.

8. Squire, Thomas H. and Paul Kolodziej, "Thermal Protection Systems Expert and Material Properties Database," Ames Research Center, 1995

9. Schey, John A., Introduction to Manufacturing Processes, 2nd ed., McGraw-Hill, Inc., New York, 1987.

10. Burns, R. M., and W. W. Bradley, Protective Coatings for Metals, 3rd ed., Reinhold Publishing Corporation, New York, 1967.

11. Schwartz, Mel, Handbook of Structural Ceramics, McGraw-Hill, Inc., New York, 1992.

12. Schwartz, Mel M., ed., Engineering Applications of Ceramic Materials Source Book, American Society, Ohio, 1985.

13. Ashby, Michael F. and David R.H. Jones, Engineering Materials 2: An Introduction to Microstructures, Processing and Design, Pergamon Press, New York, 1986.

14. Schwartz, Mel M., ed., "General Characteristics of Ceramic Materials," Engineering Applications of Ceramic Materials Source Book, American Society for Metals, Ohio,
pp. 247 - 252, 1985.

15. Brady, George S, and Henry R. Clausen. Materials Handbook, 13th ed., McGraw-Hill, Inc., New York, 1991.

16. Holman, J.P., Heat Transfer, 7th ed., McGraw-Hill, New York, 1990.

17. Myers, Glen E., Analytical Methods in Conduction Heat Transfer, McGraw-Hill, New York, 1990.

18. Callens, E. Eugene, "Feasibility Study of an Impact Probe for Particle Characterization in Rocket Exhaust Plumes," Louisiana Tech University, 1994.

19. "Results of a Study of the Heating Rates, Pressure and Cooling Water Requirements for the MPTA Flame Bucket," Contract NAS8-32213, Lockheed Missiles & Space Company, Huntsville, Alabama, November 1976.

APPENDIX A

SOLUTION TO THE BOUNDARY VALUE PROBLEM WITH A BOILING WATER BACKFACE CONDITION

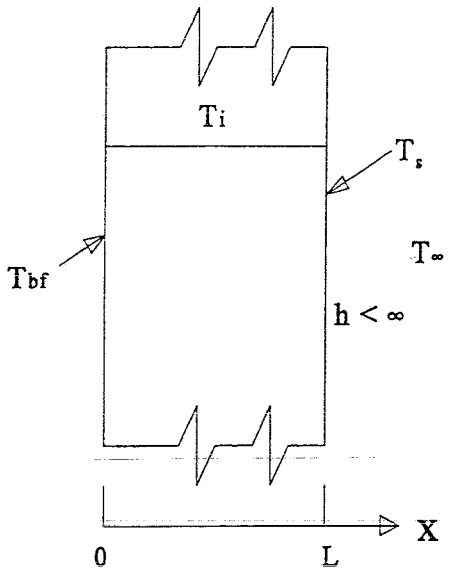

Fig. A1. Plane Wall Transient with a Convective Boundary Condition at x = L for the Boiling Water Backface Condition

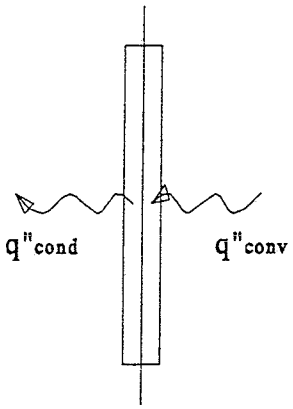

Fig. A2. System Boundary at Convective Surface for the Boiling Water Backface Condition

The governing equation for this problem is the unsteady heat conduction equation

$$\frac{\partial^2 T}{\partial x^2} = \frac{1}{\alpha}\frac{\partial T}{\partial t}$$

where

T = Temperature

x = Distance from the backface

α = Thermal diffusivity

t = Time

Energy balance across the system boundary

$q''_{conducted} = q''_{convected}$

Substitute the rate equations to obtain the first boundary condition at x = L

$$-k\frac{\partial T}{\partial x}=h(T_s-T_\infty)$$

where

h = heat transfer coefficient

or

$$\frac{\partial T}{\partial x}=-\frac{h}{k}(T_s-T_\infty)$$

The second boundary condition is that $T = T_{bf}$ at $x = 0$ or

$T(0,t) = T_{bf}$

The initial condition for this problem is that $T = T_i$ at $t = 0$ or

$T(x,0) = T_i$

In the form shown above, the first boundary condition is nonhomogeneous, but it can be made homogeneous by substituting $T = T - T_\infty$ in place of T. In addition, the problem is normalized by defining

$$u=\frac{T-T_\infty}{T_{bf}-T_\infty} \qquad \bar{x}=\frac{x}{L} \qquad \theta=\frac{\alpha t}{L^2}$$

so that the normalized problem is given by the partial differential equation

$$u_{xx} = u_\theta \tag{A1}$$

where the bars have been dropped for the x and θ.

The boundary conditions are

$$u(0, \theta) = 1 \tag{A2}$$

and

$$u_x(1, \theta) = -Hu(1, \theta) \tag{A3}$$

The initial condition is given by

$$u(x,0)=C \qquad where \ C=\frac{T_i-T_\infty}{T_{bf}-T_\infty} \tag{A4}$$

Since one of the boundary conditions is still nonhomogeneous (Equation A2), separation of variables cannot be used until the problem is converted to a homogeneous one using the method of partial solutions.

The method of partial solutions is based on the steady state solution; therefore, $u_\theta = 0$. If $\tilde{u}$ denotes the steady state solution then Equation A1 reduces to

$$\tilde{u}_{xx} = 0$$

$$\tilde{u}_x = c_1$$

$$\tilde{u} = c_1 x + c_2$$

The boundary conditions are used to evaluate c_1 and c_2.

$$\tilde{u}(0) = c_1(0) + c_2 = 1$$
$$\therefore c_2 = 1$$

$$\tilde{u}_x(1) = c_1 = -H\tilde{u}(1)$$
$$c_1 = -H(c_1 + c_2)$$
$$c_1 = -H(c_1 + 1)$$
$$c_1 + Hc_1 = -H$$

$\therefore$

$$c_1 = -\frac{H}{H+1}$$

Therefore, the steady-state solution is

$$\tilde{u} = -\frac{H}{H+1}x + 1$$

The next step is to form a homogeneous problem by writing $u(x, \theta)$ as the sum of the steady-state solution $\tilde{u}(x)$ and a transient term $v(x, \theta)$.

$$u(x, \theta) = \tilde{u}(x) + v(x, \theta) \qquad \text{(A5)}$$

or

$$v(x, \theta) = u(x, \theta) - \tilde{u}(x)$$

By substituting Equation A5 into Equation A1, the equation below is formed,

$$v_{xx} + \tilde{u}_{xx} = v_\theta + \tilde{u}_\theta$$

which reduces to the partial differential equation for v, because $\tilde{u}_{xx} = 0$ and $\tilde{u}_\theta = 0$.

$$v_{xx} = v_\theta$$

Next, the boundary conditions for v must be found

$$v(0,\theta) = u(0,\theta) - \tilde{u}(0) = 1 - \left(-\frac{H}{1+H}(0) + 1\right) = 1 - 1 = 0$$

$$v_x(1,\theta) = u_x(1,\theta) - \tilde{u}_x(1) = -Hu(1,\theta) + H\tilde{u}(1) = -H(u(1,\theta) - \tilde{u}(1)) = -Hv(1,\theta)$$

The initial condition becomes

$$v(x,0) = u(x,0) - \tilde{u}(x) = C + \frac{H}{1+H}x - 1$$

From Equation A5, the solution is given by

$$u(x,\theta) = -\frac{H}{1+H}x + 1 + v(x,\theta) \tag{A6}$$

and the new boundary value problem for $v(x, \theta)$ *is:*

$$v_{xx} = v_\theta \tag{A7}$$

$$v(0,\theta) = 0 \tag{A8}$$

$$v_x(1,\theta) = -Hv(1,\theta) \tag{A9}$$

with initial condition

$$v(x,0) = C + \frac{H}{1+H}x - 1 \tag{A10}$$

Since the problem has now been made homogeneous, the solution for $v(x, \theta)$ is found using separation of variables.

$$v(x,\theta) = X\theta$$

Equation A7 now becomes

$$X''\theta = X\theta'$$

$$\frac{X''}{X}=\frac{\theta'}{\theta}=-\lambda^2$$

This results in two ordinary differential equations. First,

$X'' + \lambda^2 X = 0$

whose solution is

$X = A\sin\lambda x + B\cos\lambda x$

And second,

$\theta' + \lambda^2\theta = 0$

whose solution is

$\theta = Ce^{-\lambda^2\theta}$

$X(0) = A\sin\lambda(0) + B\cos\lambda(0) = 0$

$\therefore B = 0$

$X = A\sin\lambda x$

$X'(x) = \lambda A\cos\lambda x$

$X'(1) = \lambda A\cos\lambda = -Ha\sin\lambda$

$\therefore \lambda\cot\lambda = -H$

$v_n = X\theta = A_n \sin\lambda_n x[e^{-\lambda_n^2\theta}]$ where $\lambda_n \cot\lambda_n = -H$

$$v(x,\theta)=\sum_{n=1}^{\infty} A_n \sin\lambda_n x[e^{-\lambda_n^2\theta}]$$

From the initial condition

$$v(x,0)=C+\frac{H}{1+H}x-1$$

$$v(x,0)=C+\frac{H}{1+H}x-1=\sum_{n=1}^{\infty}A_n\sin\lambda_n x$$

Multiply through by $\sin \lambda_m x\, dx$ and integrate between 0 and 1

$$\int_0^1(C+\frac{H}{1+H}x-1)\sin\lambda_m x dx=\sum_{n=1}^{\infty}A_n\int_0^1\sin\lambda_n x\sin\lambda_m x dx$$

When n = m, this equation becomes

$$\int_0^1(C+\frac{H}{1+H}x-1)\sin\lambda_m x dx=A_m\int_0^1\sin^2\lambda_m x dx$$

$$C\int_0^1\sin\lambda_m x dx+\frac{H}{1+H}\int_0^1 x\sin\lambda_m x dx-\int_0^1\sin\lambda_m x dx=A_m\int_0^1\sin^2\lambda_m x dx$$

$$-\frac{C}{\lambda_m}[\cos\lambda_m x]_0^1+\frac{H}{{\lambda_m}^2(1+H)}[\sin\lambda_m x-\lambda_m x\cos\lambda_m x]_0^1+\frac{1}{\lambda_m}[\cos\lambda_m x]_0^1=A_m(\frac{1}{\lambda_m}[\frac{\lambda_m x}{2}-\frac{1}{4}\sin 2\lambda_m x]_0^1)$$

$$-\frac{C}{\lambda_m}(\cos\lambda_m-1)+\frac{H}{{\lambda_m}^2(1+H)}(\sin\lambda_m-\lambda_m\cos\lambda_m)+\frac{1}{\lambda_m}(\cos\lambda_m-1)=A_m[\frac{1}{\lambda_m}(\frac{\lambda_m}{2}-\frac{1}{2}\sin\lambda_m\cos\lambda_m)]$$

substitute $\cos\lambda_m = -\frac{H}{\lambda_m}\sin\lambda_m$

$$A_m = \frac{-\frac{C}{\lambda_m}\left(-\frac{H}{\lambda_m}\sin\lambda_m - 1\right) + \frac{H}{\lambda_m{}^2(1+H)}\left(\sin\lambda_m + H\sin\lambda_m\right) + \frac{1}{\lambda_m}\left(-\frac{H}{\lambda_m}\sin\lambda_m - 1\right)}{\frac{1}{\lambda_m}\left(\frac{\lambda_m}{2} + \frac{H}{2\lambda_m}\sin^2\lambda_m\right)}$$

$$A_m = \frac{-C\ \left(-\frac{H}{\lambda_m}\sin\lambda_m - 1\right) + \frac{H}{\lambda_m(1+H)}\left(\sin\lambda_m + H\sin\lambda_m\right) + \left(-\frac{H}{\lambda_m}\sin\lambda_m - 1\right)}{\frac{\lambda_m}{2} + \frac{H}{2\lambda_m}\sin^2\lambda_m}$$

$$A_m = \frac{2C(H\sin\lambda_m + \lambda_m) + \frac{2H}{1+H}\left(\sin\lambda_m + H\sin\lambda_m\right) - 2H\sin\lambda_m - 2\lambda_m}{\lambda_m^2 + H\sin^2\lambda_m}$$

$$A_m = \frac{C\ \left(\frac{H}{\lambda_m}\sin\lambda_m + 1\right) + \frac{H}{\lambda_m(1+H)}\left(\sin\lambda_m + H\sin\lambda_m\right) - \frac{H}{\lambda_m}\sin\lambda_m - 1}{\frac{\lambda_m{}^2 + H\sin^2\lambda_m}{2\lambda_m}}$$

$$A_m = \frac{2C(Hsin\lambda_m + \lambda_m) + \dfrac{2Hsin\lambda_m + 2H^2\sin\lambda_m - 2Hsin\lambda_m - 2H^2\sin\lambda_m}{1+H} - 2\lambda_m}{\lambda_m^2 + Hsin^2\lambda_m}$$

$$A_m = \frac{2C(\lambda_m + Hsin\lambda_m) - 2\lambda_m}{\lambda_m^2 + Hsin^2\lambda_m}$$

$$v(x,\theta) = 2\sum_{n=1}^{\infty} \frac{C(\lambda_n + Hsin\lambda_n) - \lambda_n}{\lambda_-^2 + Hsin^2\lambda_-} \sin\lambda_n x e^{-\lambda_n^2\theta}$$

$$u(x,\theta) = 1 - \frac{H}{1+H}x + 2\sum_{n=1}^{\infty} \frac{C(\lambda_n + Hsin\lambda_n) - \lambda_n}{\lambda_n^2 + Hsin^2\lambda_n} \sin\lambda_n x e^{-\lambda_n^2\theta} \qquad \textbf{(A11)}$$

APPENDIX B

NORMALIZED TEMPERATURE VS. NORMALIZED TIME AT SEVERAL DEPTHS FOR CANDIDATE CERAMIC MATERIALS WITH A BOILING WATER BACKFACE AND $T_\infty = 6538°R$

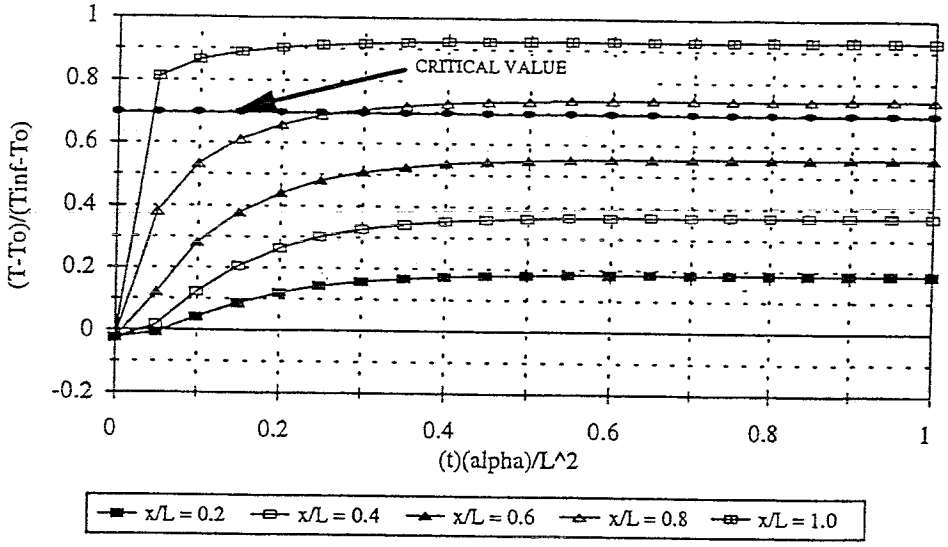

Fig. B1. Normalized Temperature Vs. Normalized Time at Several Depths for Zirconium Boride with a Boiling Water Backface and $T_\infty = 6538°R$

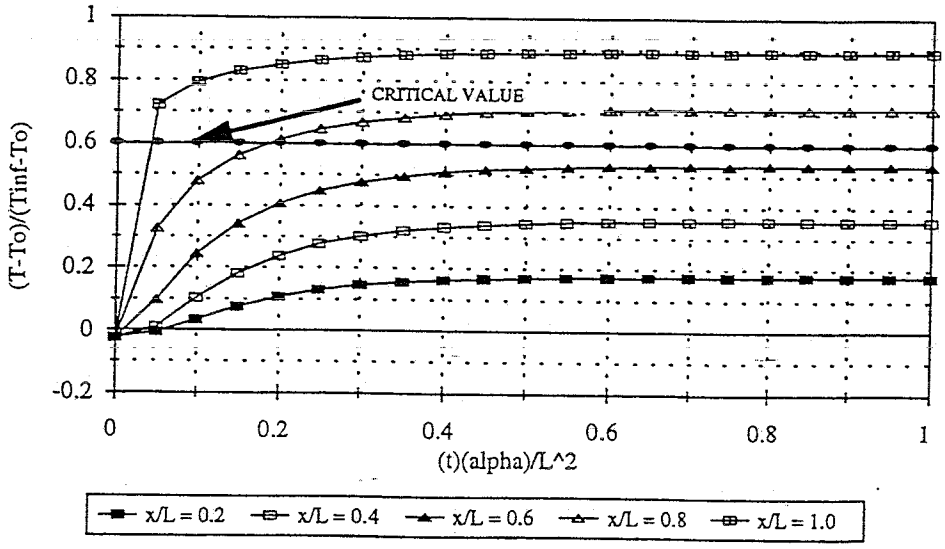

Fig. B2. Normalized Temperature Vs. Normalized Time at Several Depths for Magnesium Oxide with a Boiling Water Backface and $T_\infty = 6538°R$

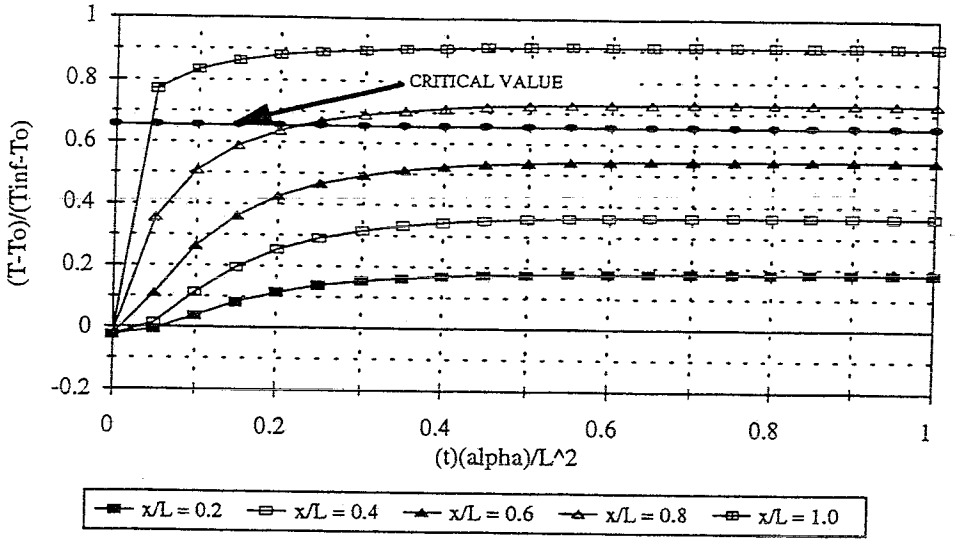

Fig. B3. Normalized Temperature Vs. Normalized Time at Several Depths for Titanium Carbide with a Boiling Water Backface and $T_\infty = 6538°R$

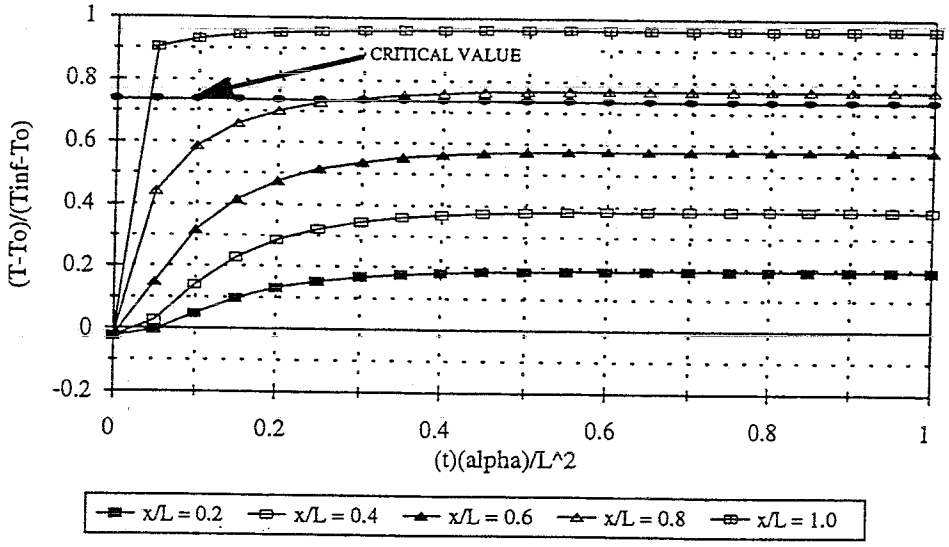

Fig. B4. Normalized Temperature Vs. Normalized Time at Several Depths for Zirconium Carbide with a Boiling Water Backface and $T_\infty = 6538°R$

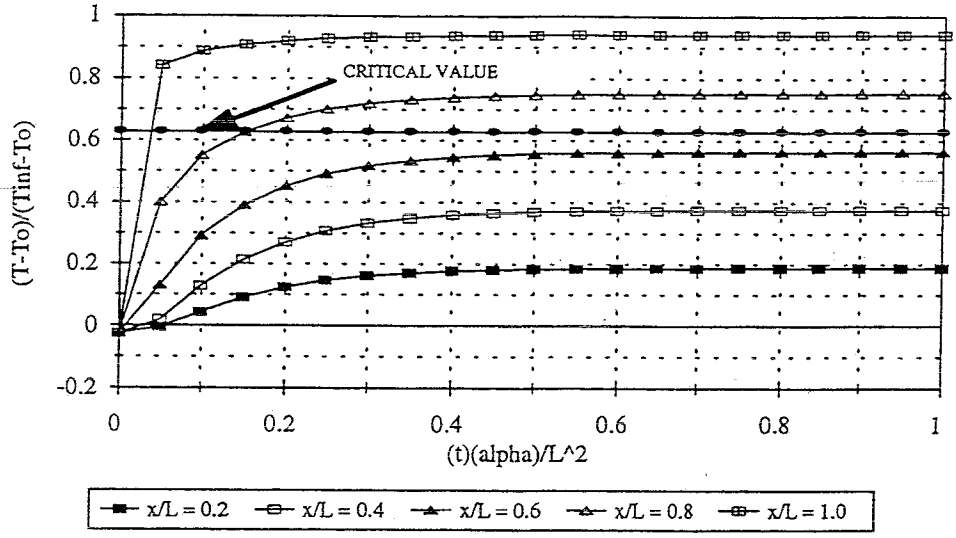

Fig. B5. Normalized Temperature Vs. Normalized Time at Several Depths for Titanium Nitride with a Boiling Water Backface and $T_\infty = 6538°R$

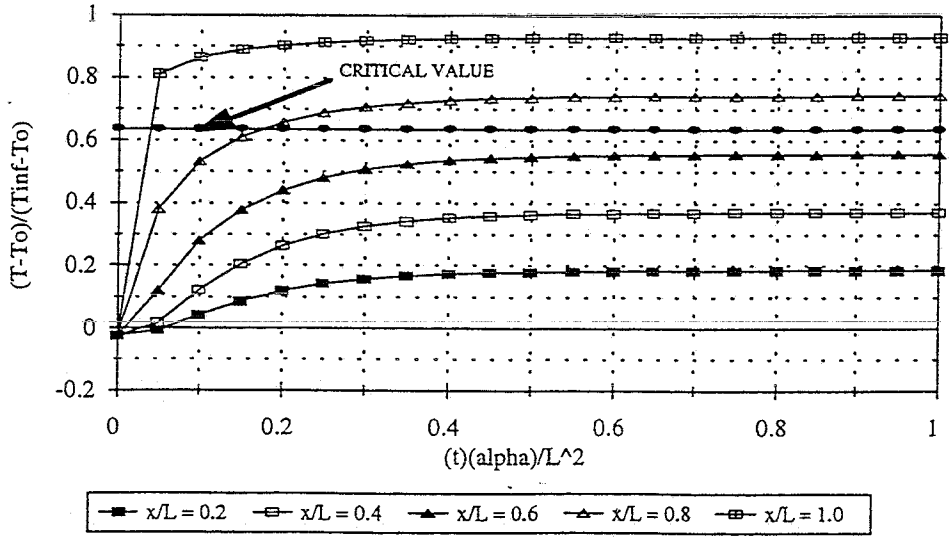

Fig. B6. Normalized Temperature Vs. Normalized Time at Several Depths for Silicon Carbide with a Boiling Water Backface and $T_\infty = 6538°R$

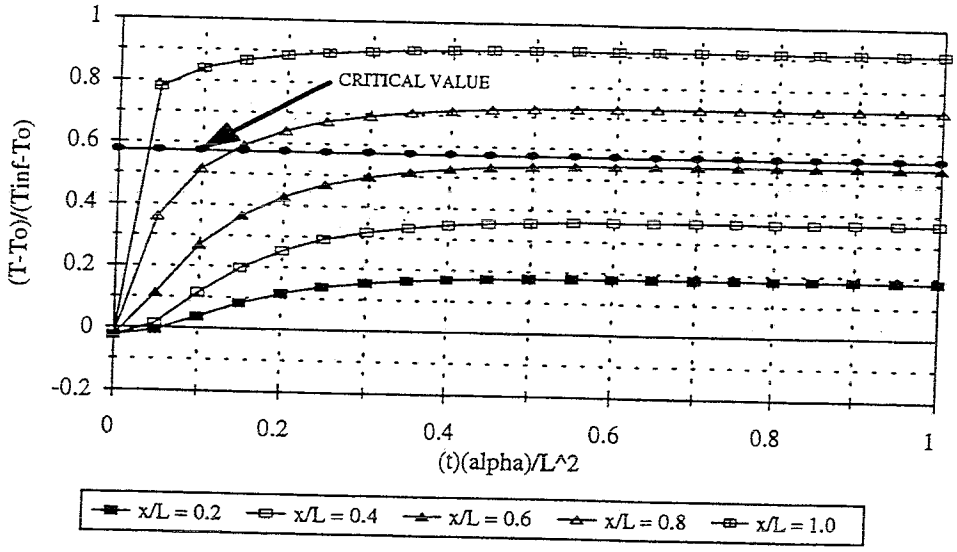

Fig. B7. Normalized Temperature Vs. Normalized Time at Several Depths for Lanthanum Boride with a Boiling Water Backface and $T_\infty = 6538°R$

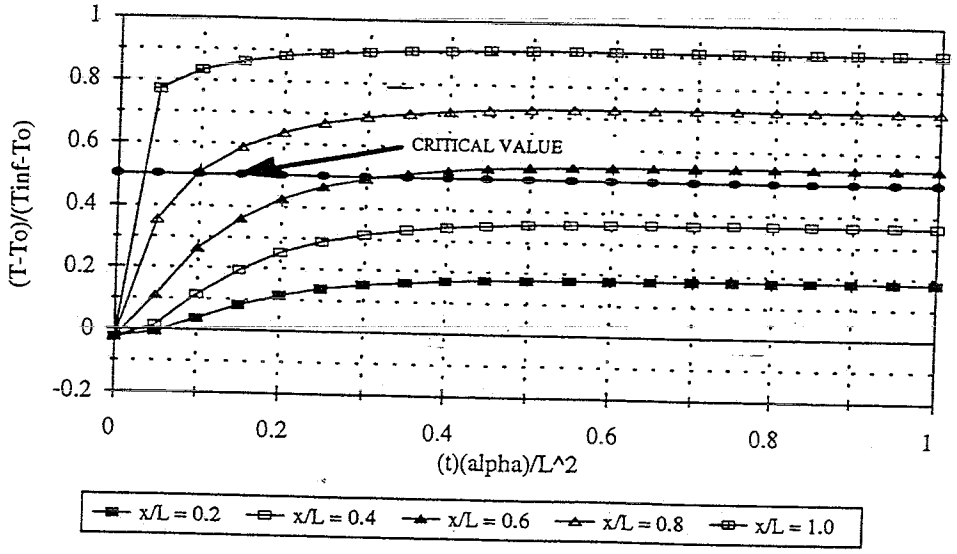

Fig. B8. Normalized Temperature Vs. Normalized Time at Several Depths for Beryllium Carbide with a Boiling Water Backface and $T_\infty = 6538°R$

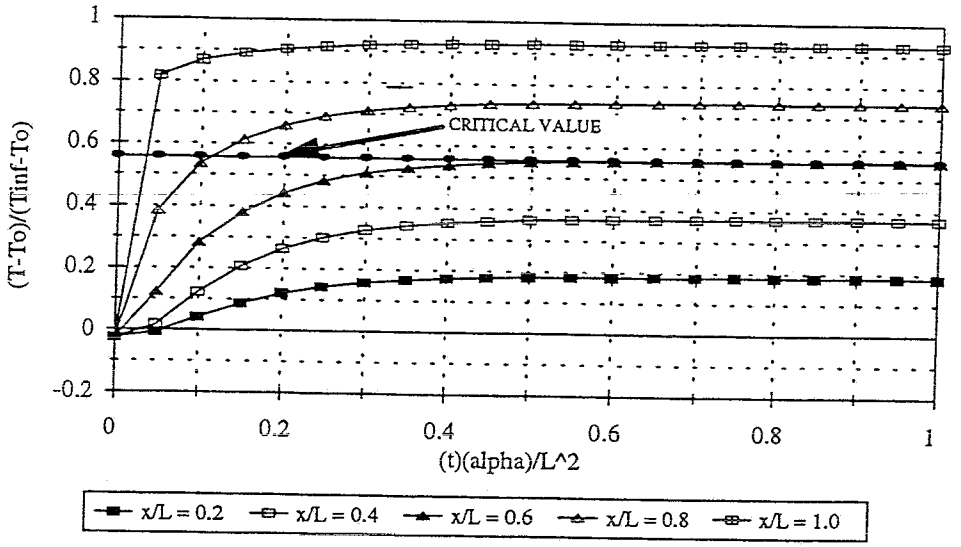

Fig. B9. Normalized Temperature Vs. Normalized Time at Several Depths for Vanadium Carbide with a Boiling Water Backface and $T_\infty = 6538°R$

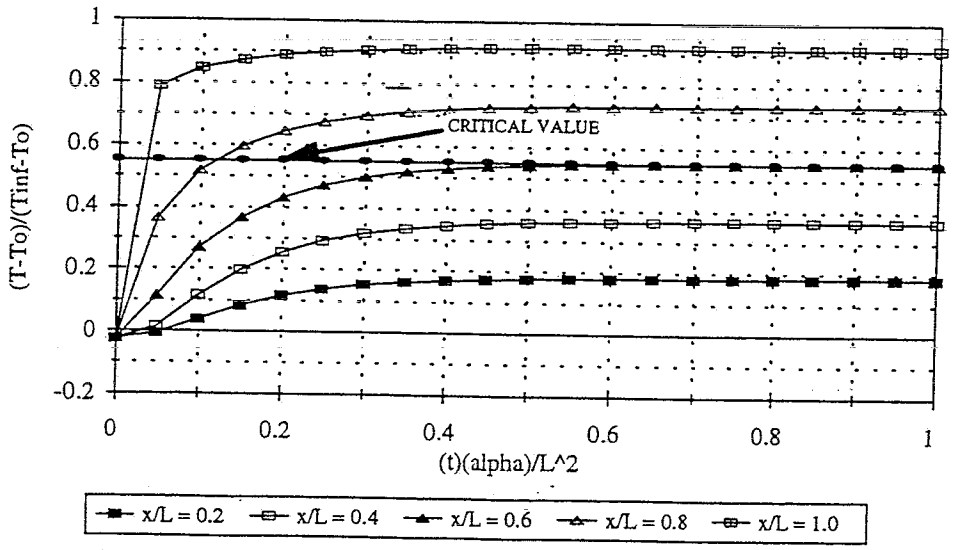

Fig. B10. Normalized Temperature Vs. Normalized Time at Several Depths for Neodymium Boride with a Boiling Water Backface and $T_\infty = 6538°R$

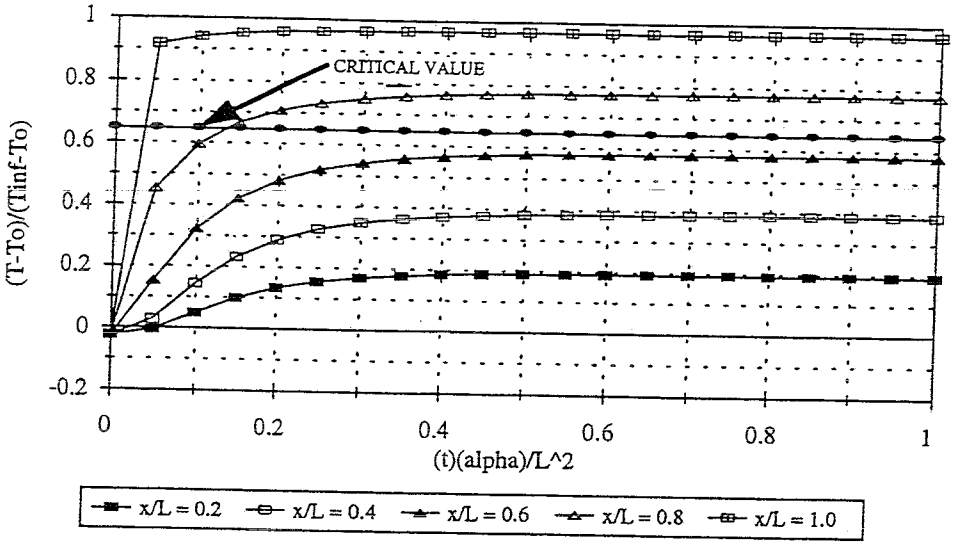

Fig. B11. Normalized Temperature Vs. Normalized Time at Several Depths for Niobium Boride with a Boiling Water Backface and $T_\infty = 6538°R$

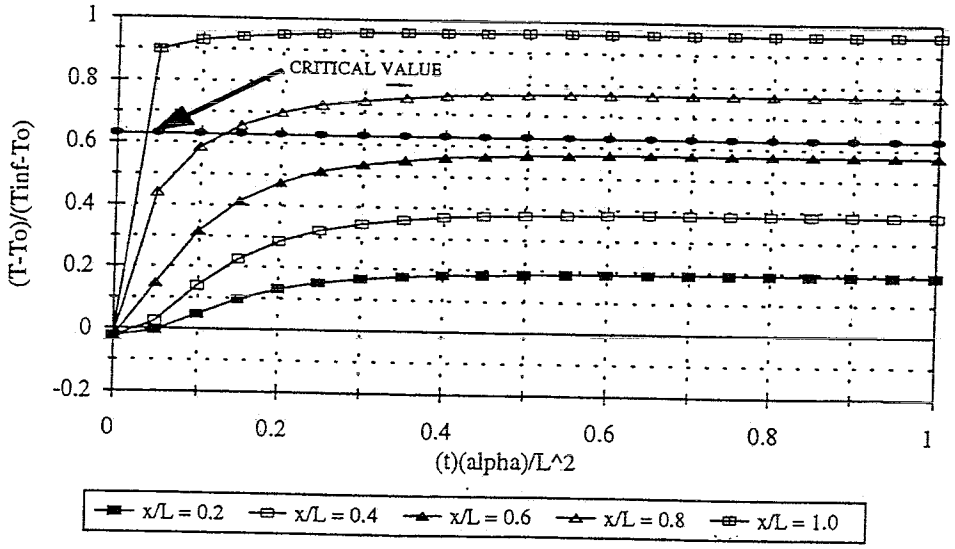

Fig. B12. Normalized Temperature Vs. Normalized Time at Several Depths for Zirconium Nitride with a Boiling Water Backface and $T_\infty = 6538°R$

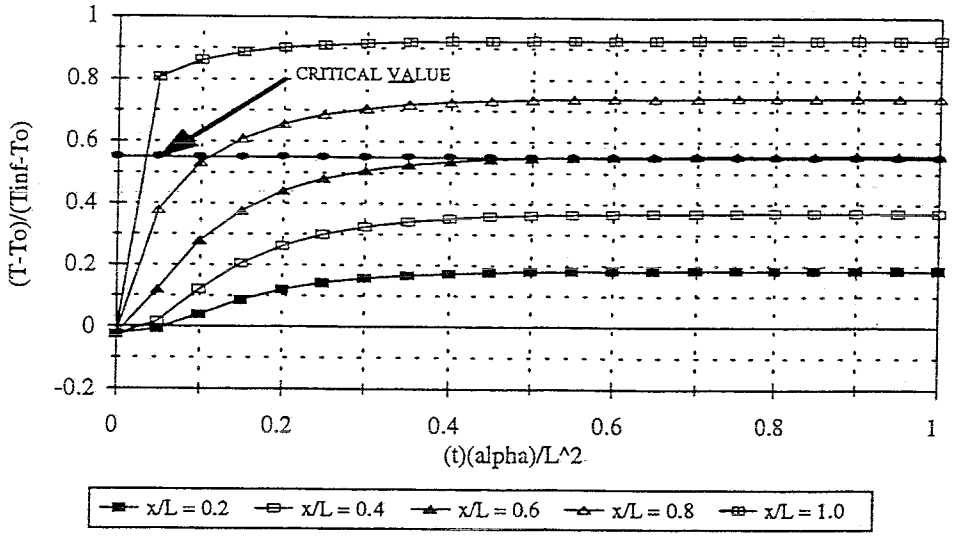

Fig. B13. Normalized Temperature Vs. Normalized Time at Several Depths for Praesodymium Boride with a Boiling Water Backface and $T_\infty = 6538°R$

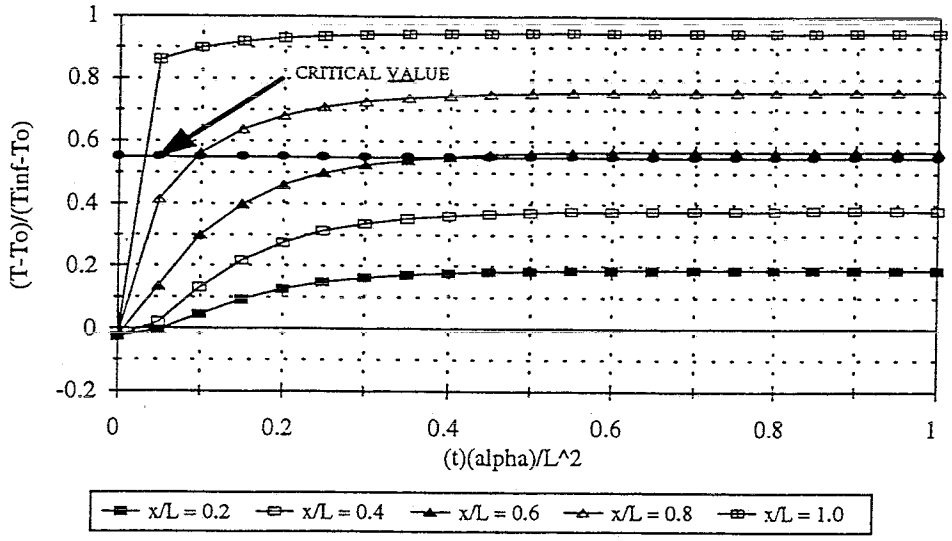

Fig. B14. Normalized Temperature Vs. Normalized Time at Several Depths for Calcium Oxide with a Boiling Water Backface and $T_\infty = 6538°R$

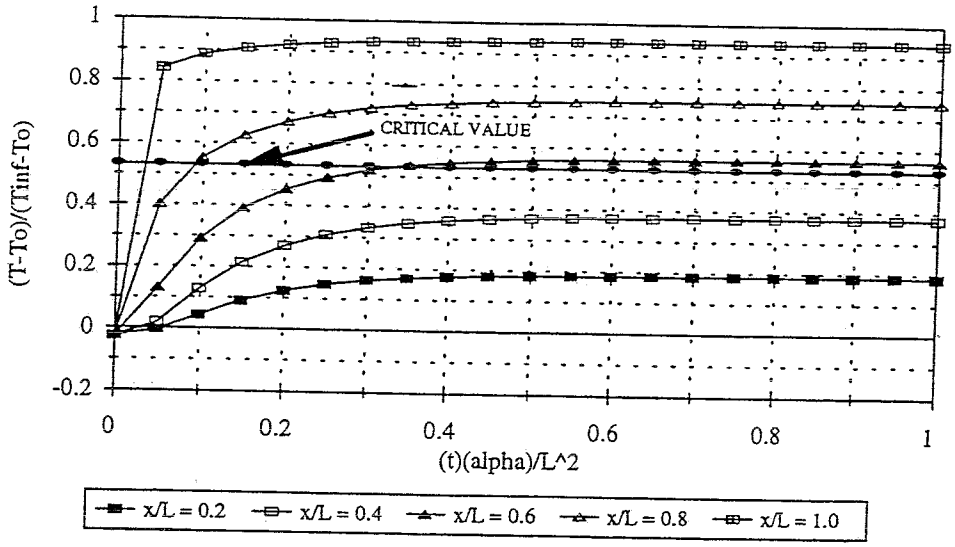

Fig. B15. Normalized Temperature Vs. Normalized Time at Several Depths for Aluminum Nitride with a Boiling Water Backface and $T_\infty = 6538°R$

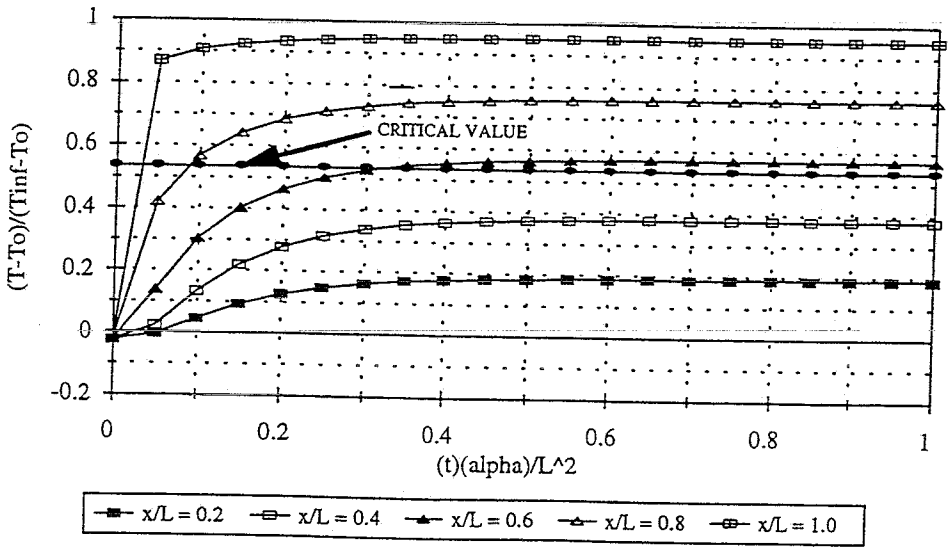

Fig. B16. Normalized Temperature Vs. Normalized Time at Several Depths for Scandium Nitride with a Boiling Water Backface and $T_\infty = 6538°R$

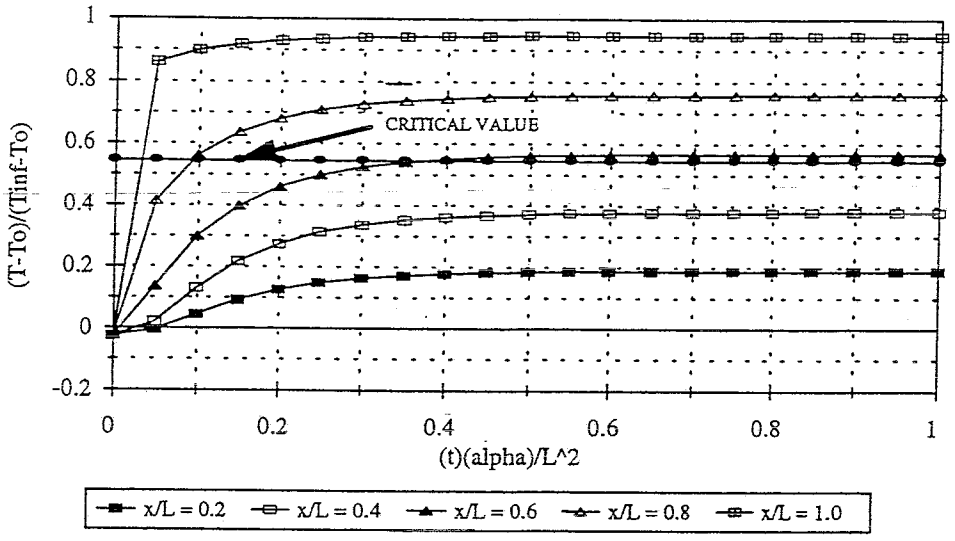

Fig. B17. Normalized Temperature Vs. Normalized Time at Several Depths for Yttrium Boride with a Boiling Water Backface and $T_\infty = 6538°R$

APPENDIX C

NORMALIZED TEMPERATURE VS. NORMALIZED TIME AT SEVERAL DEPTHS FOR CANDIDATE CERAMIC MATERIALS WITH A BOILING WATER BACKFACE AND $T_\infty = 5400°R$

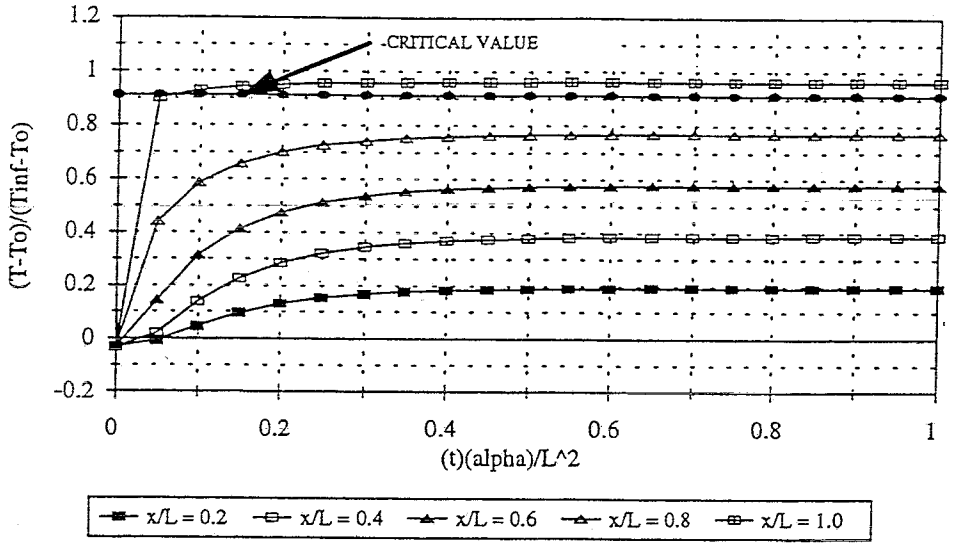

Fig. C1. Normalized Temperature Vs. Normalized Time at Several Depths for Zirconium Carbide with a Boiling Water Backface and T_∞ = 5400°R

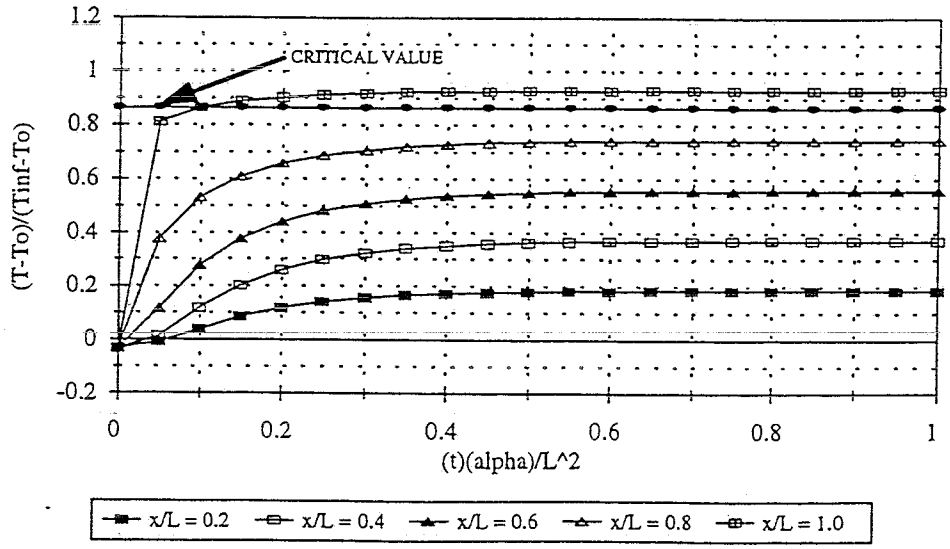

Fig. C2. Normalized Temperature Vs. Normalized Time at Several Depths for Zirconium Boride with a Boiling Water Backface and T_∞ = 5400°R

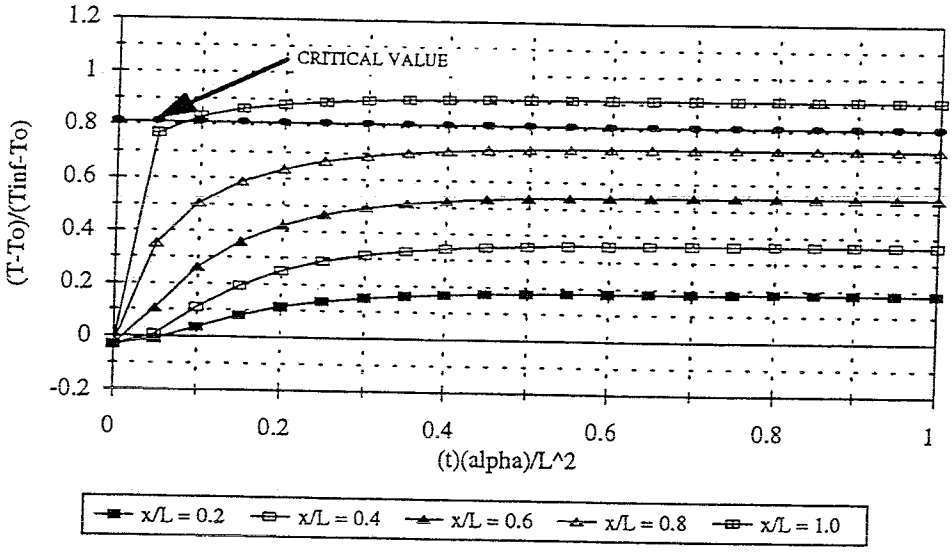

Fig. C3. Normalized Temperature Vs. Normalized Time at Several Depths for Titanium Carbide with a Boiling Water Backface and $T_\infty = 5400°R$

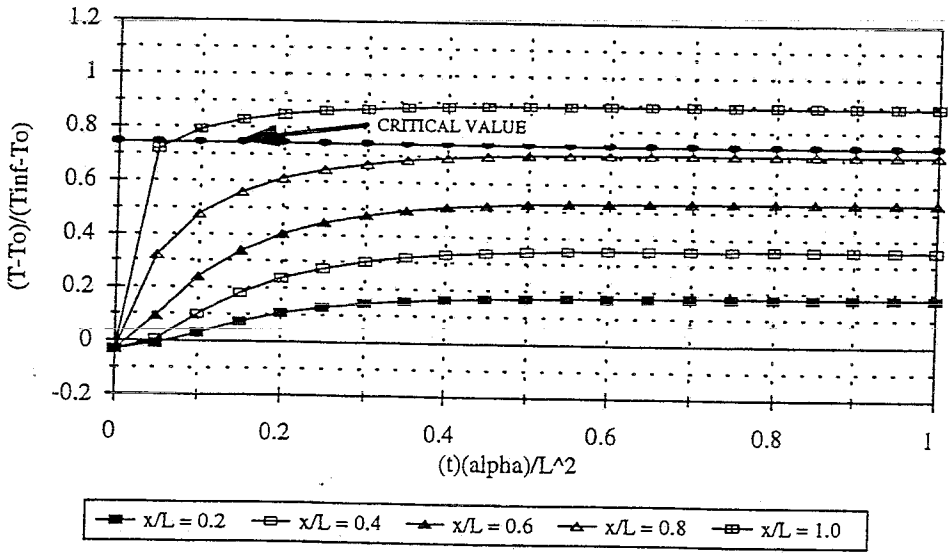

Fig. C4. Normalized Temperature Vs. Normalized Time at Several Depths for Magnesium Oxide with a Boiling Water Backface and $T_\infty = 5400°R$

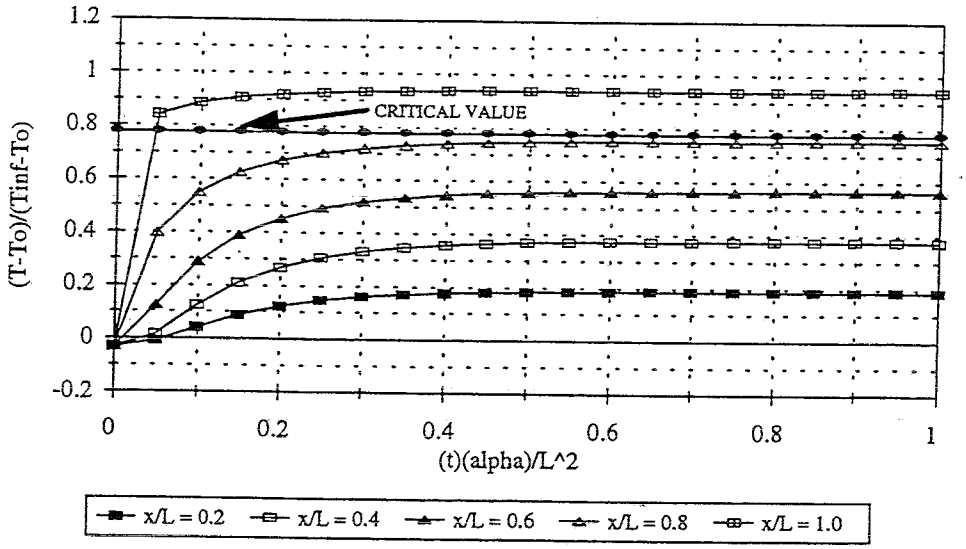

Fig. C5. Normalized Temperature Vs. Normalized Time at Several Depths for Titanium Nitride with a Boiling Water Backface and $T_\infty = 5400°R$

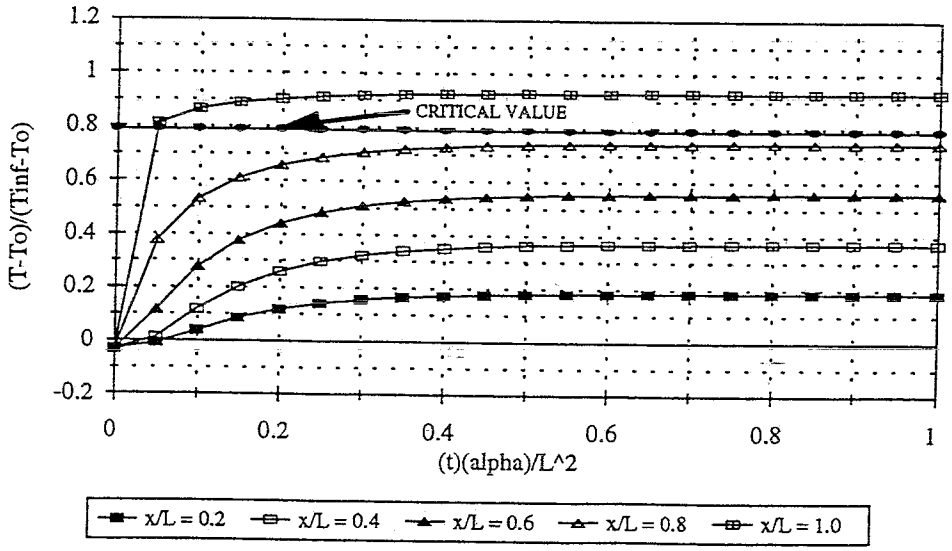

Fig. C6. Normalized Temperature Vs. Normalized Time at Several Depths for Silicon Carbide with a Boiling Water Backface and $T_\infty = 5400°R$

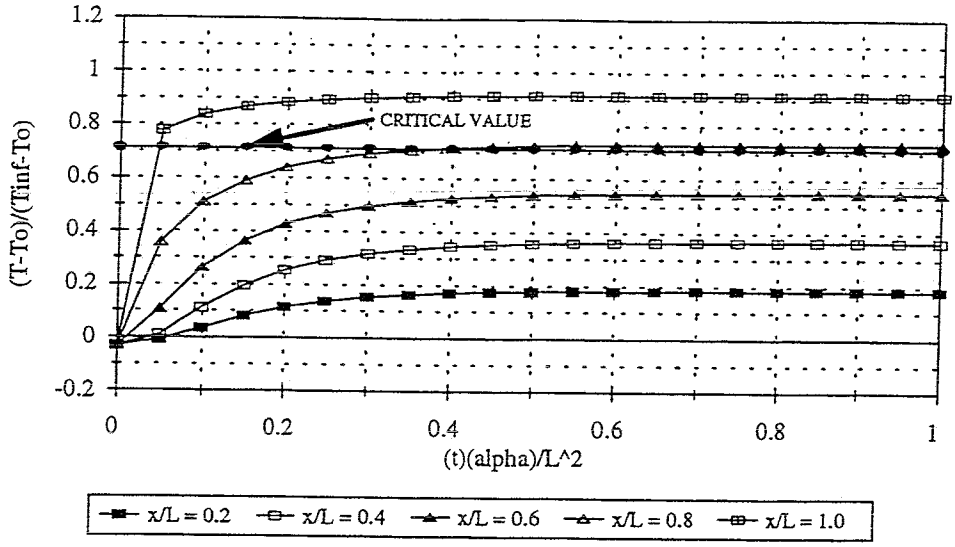

Fig. C7. Normalized Temperature Vs. Normalized Time at Several Depths for Lanthanum Boride with a Boiling Water Backface and $T_\infty = 5400°R$

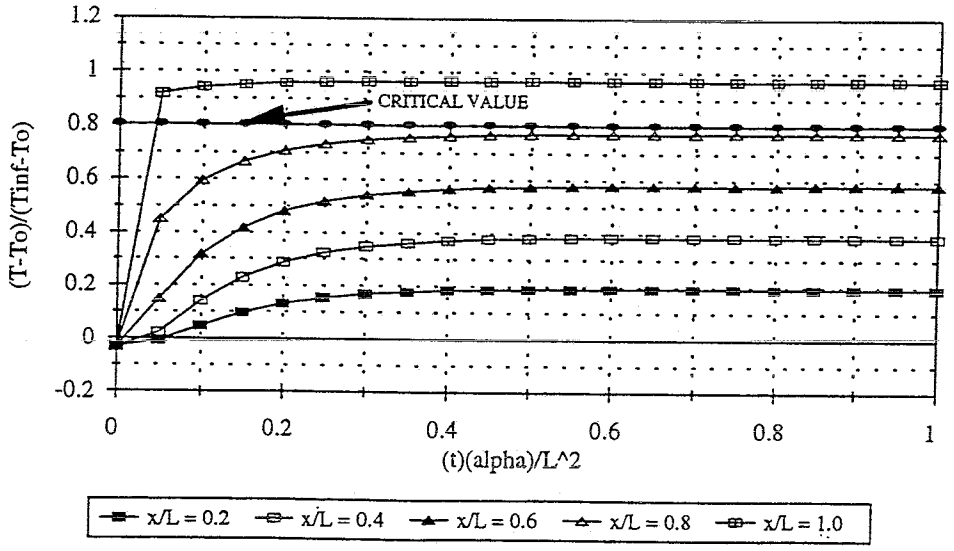

Fig. C8. Normalized Temperature Vs. Normalized Time at Several Depths for Niobium Boride with a Boiling Water Backface and $T_\infty = 5400°R$

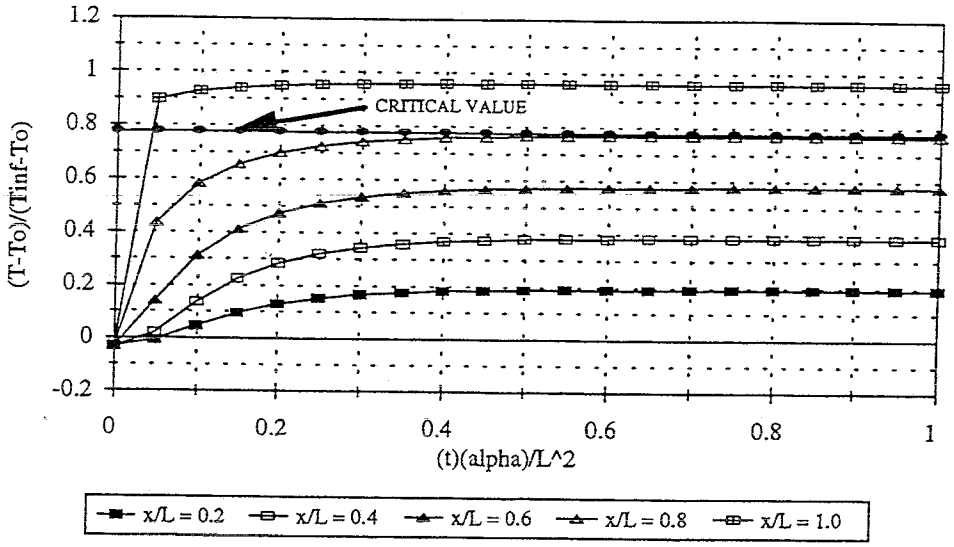

Fig. C9. Normalized Temperature Vs. Normalized Time at Several Depths for Zirconium Nitride with a Boiling Water Backface and $T_\infty = 5400°R$

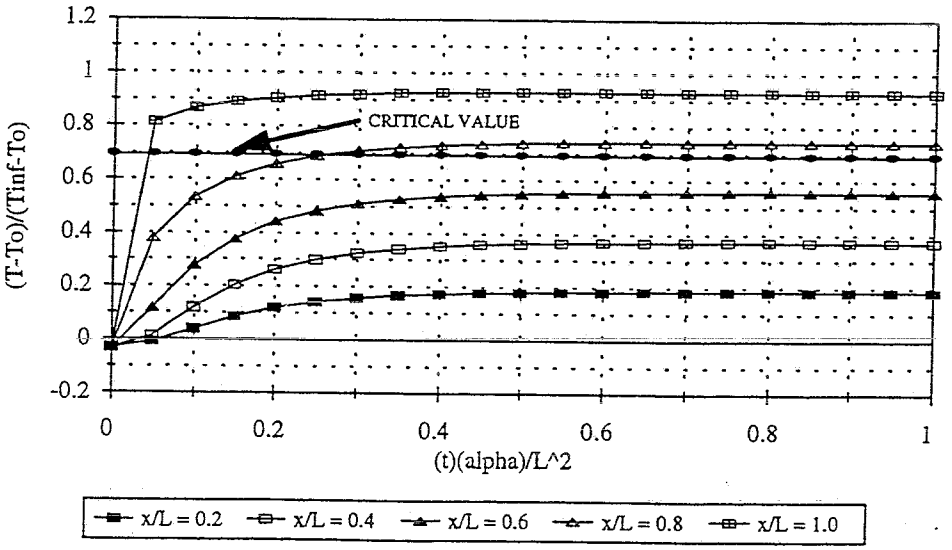

Fig. C10. Normalized Temperature Vs. Normalized Time at Several Depths for Vanadium Carbide with a Boiling Water Backface and $T_\infty = 5400°R$

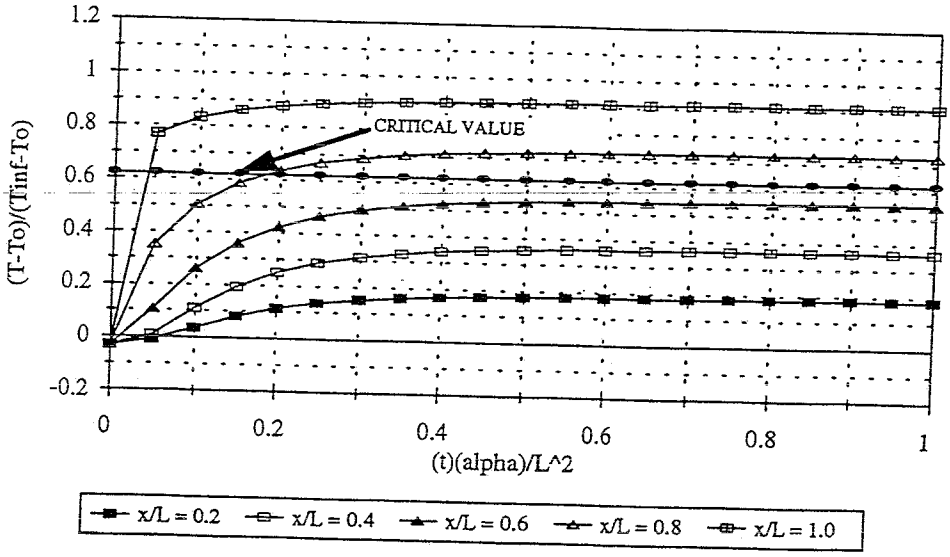

Fig. C11. Normalized Temperature Vs. Normalized Time at Several Depths for Beryllium Carbide with a Boiling Water Backface and $T_\infty = 5400°R$

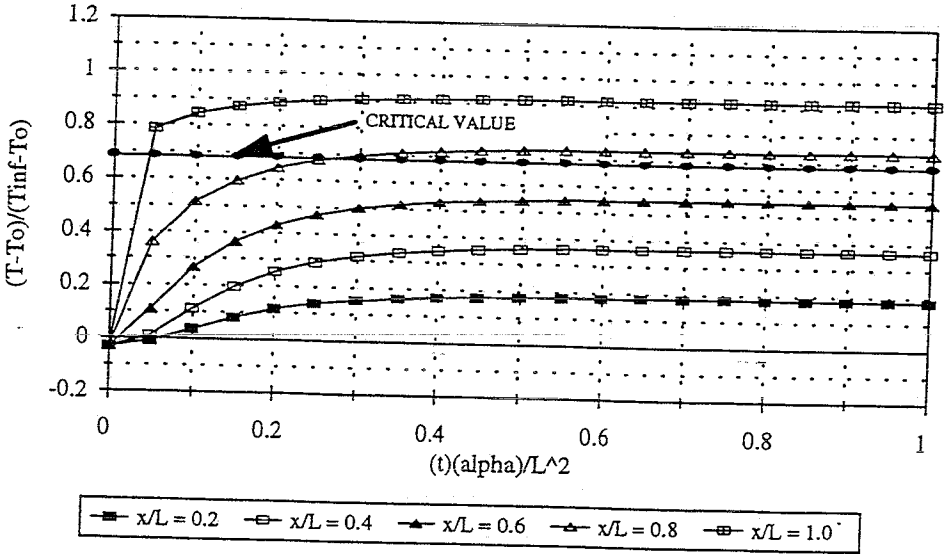

Fig. C12. Normalized Temperature Vs. Normalized Time at Several Depths for Neodymium Boride with a Boiling Water Backface and $T_\infty = 5400°R$

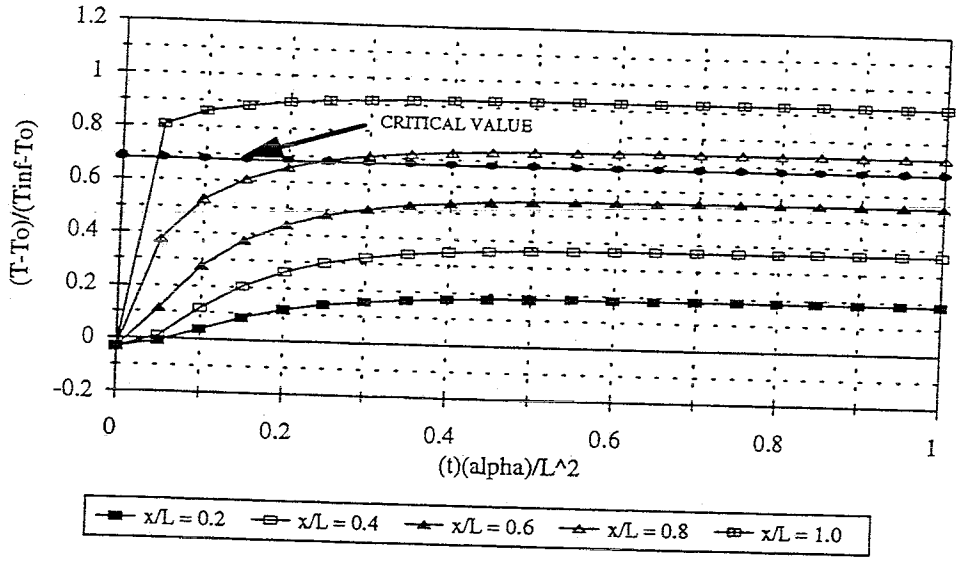

Fig. C13. Normalized Temperature Vs. Normalized Time at Several Depths for Praesodymium Boride with a Boiling Water Backface and $T_\infty = 5400°R$

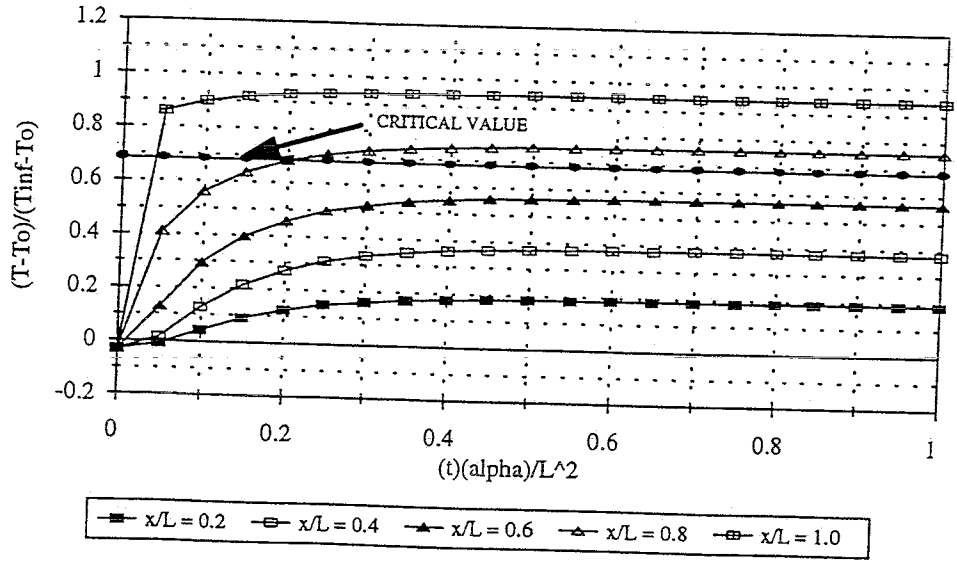

Fig. C14. Normalized Temperature Vs. Normalized Time at Several Depths for Calcium Oxide with a Boiling Water Backface and $T_\infty = 5400°R$

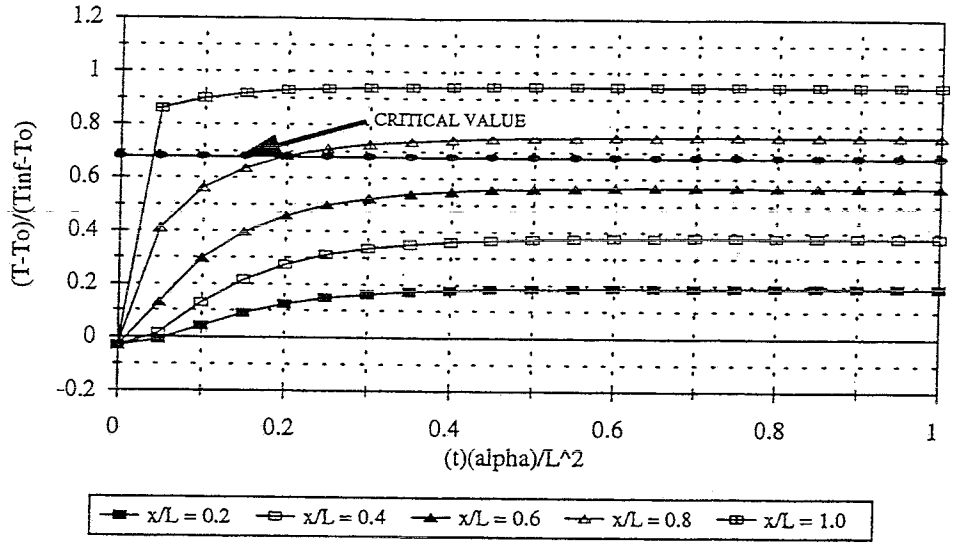

Fig. C15. Normalized Temperature Vs. Normalized Time at Several Depths for Yttrium Boride with a Boiling Water Backface and $T_\infty = 5400°R$

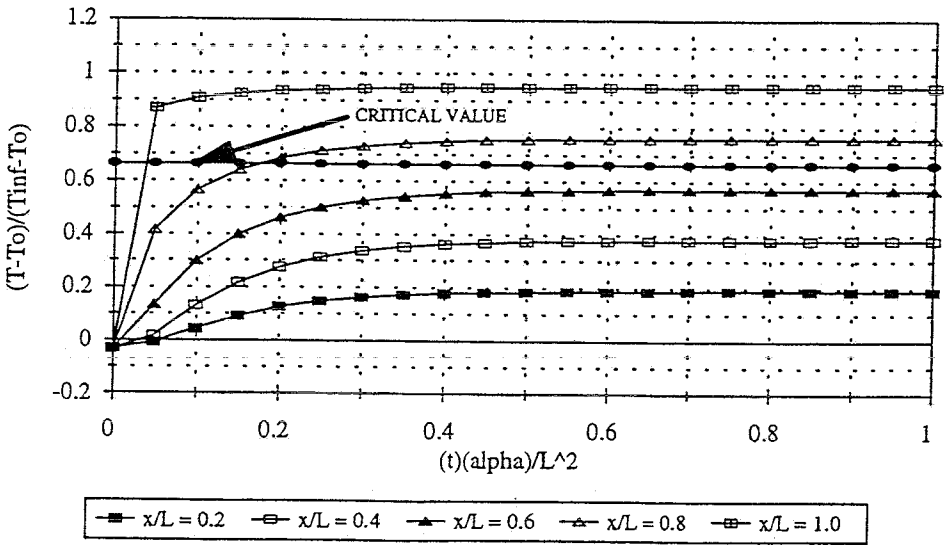

Fig. C16. Normalized Temperature Vs. Normalized Time at Several Depths for Scandium Nitride with a Boiling Water Backface and $T_\infty = 5400°R$

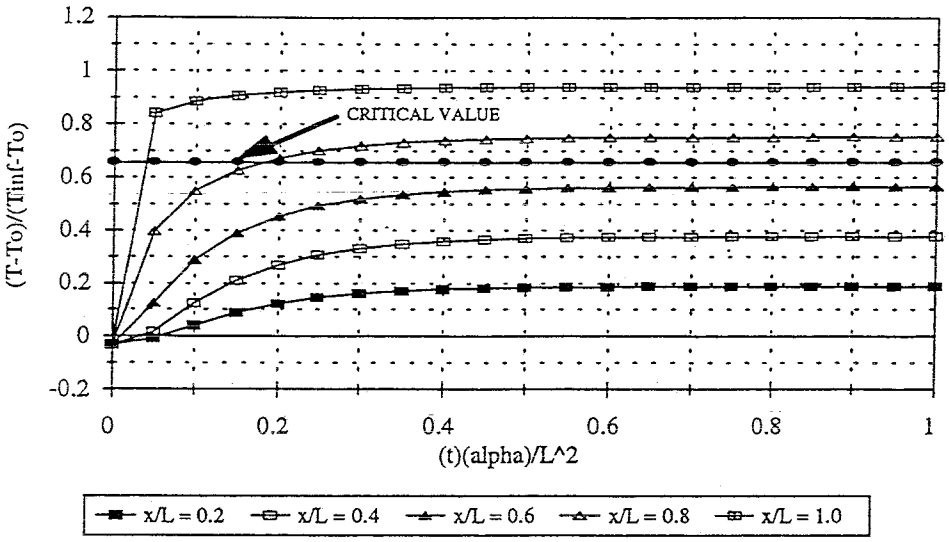

Fig. C17. Normalized Temperature Vs. Normalized Time at Several Depths for Aluminum Nitride with a Boiling Water Backface and $T_\infty = 5400°R$

APPENDIX D

NORMALIZED TEMPERATURE VS. NORMALIZED TIME AT SEVERAL DEPTHS FOR CANDIDATE CERAMIC MATERIALS WITH A BOILING WATER BACKFACE AND $T_\infty = 3600°R$

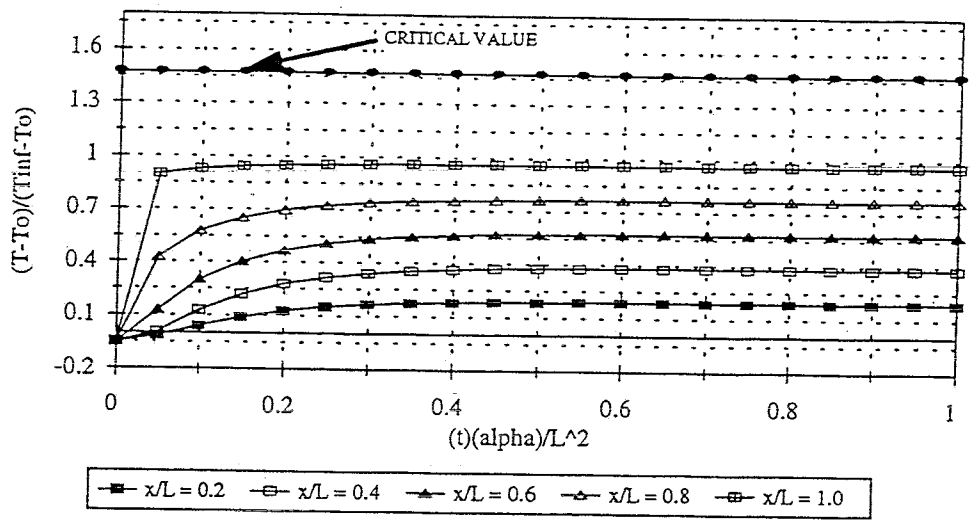

Fig. D1. Normalized Temperature Vs. Normalized Time at Several Depths for Zirconium Carbide with a Boiling Water Backface and $T_\infty = 3600°R$

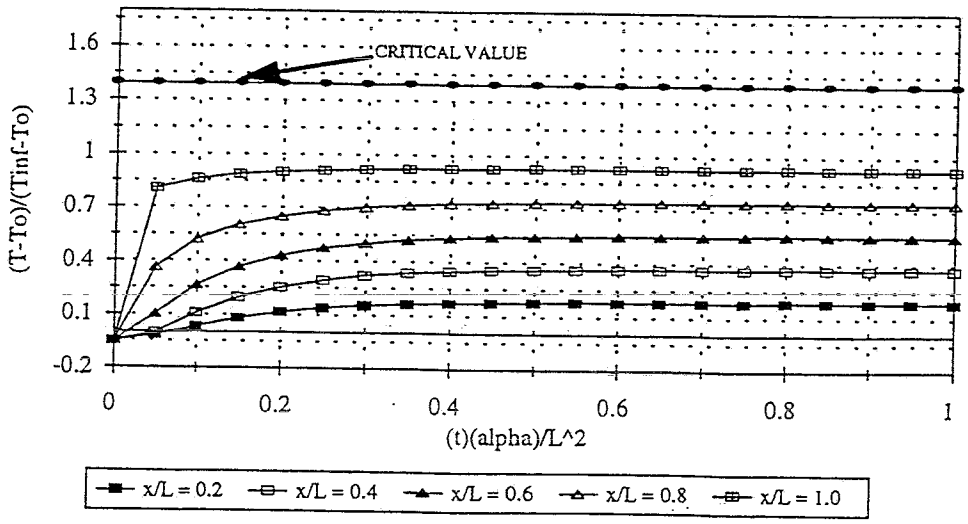

Fig. D2. Normalized Temperature Vs. Normalized Time at Several Depths for Zirconium Boride with a Boiling Water Backface and $T_\infty = 3600°R$

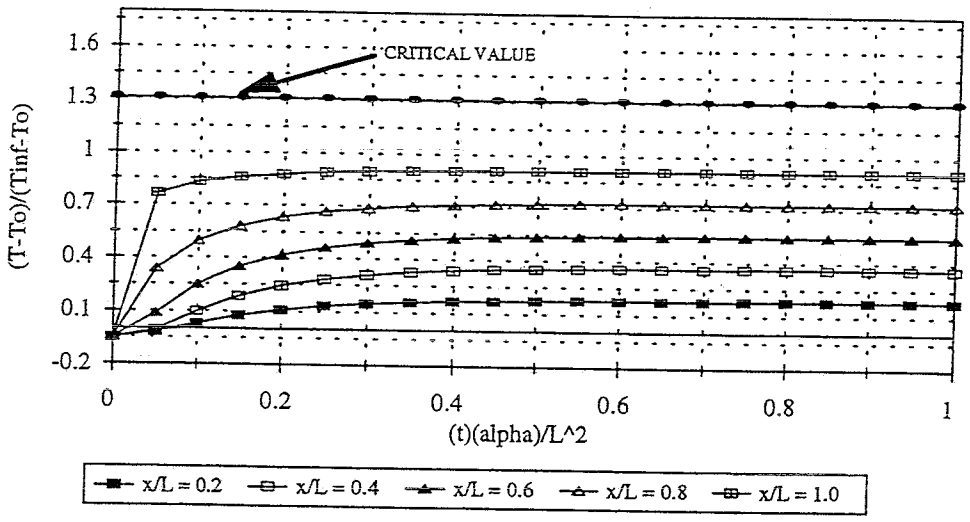

Fig. D3. Normalized Temperature Vs. Normalized Time at Several Depths for Titanium Carbide with a Boiling Water Backface and $T_\infty = 3600°R$

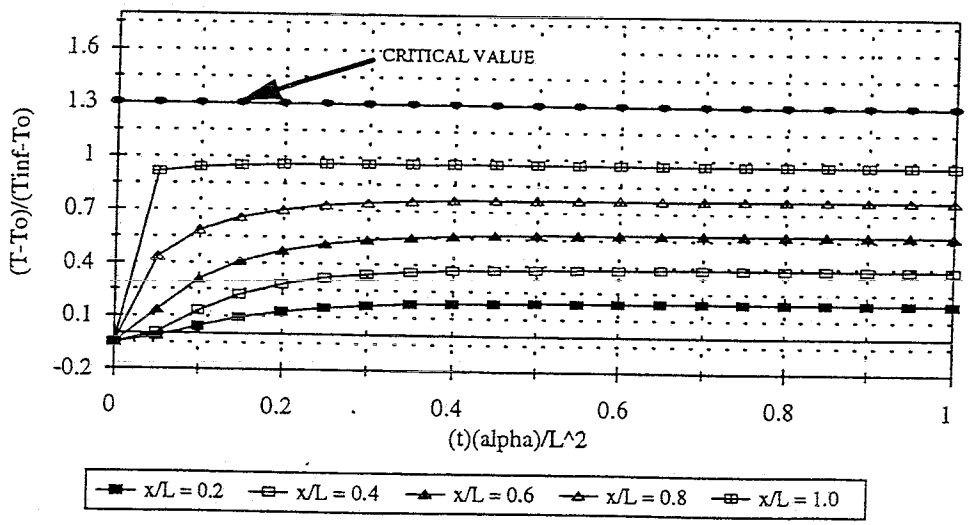

Fig. D4. Normalized Temperature Vs. Normalized Time at Several Depths for Niobium Boride with a Boiling Water Backface and $T_\infty = 3600°R$

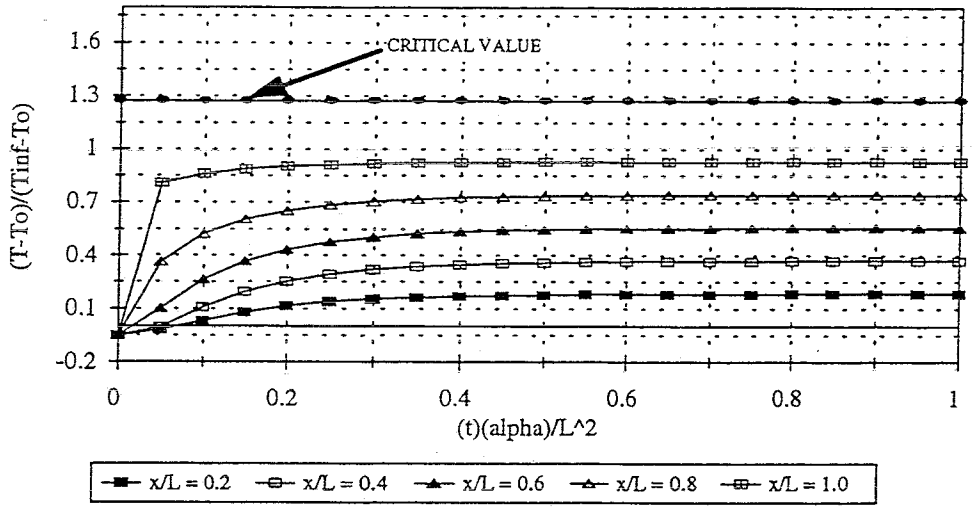

Fig. D5. Normalized Temperature Vs. Normalized Time at Several Depths for Silicon Carbide with a Boiling Water Backface and $T_\infty = 3600°R$

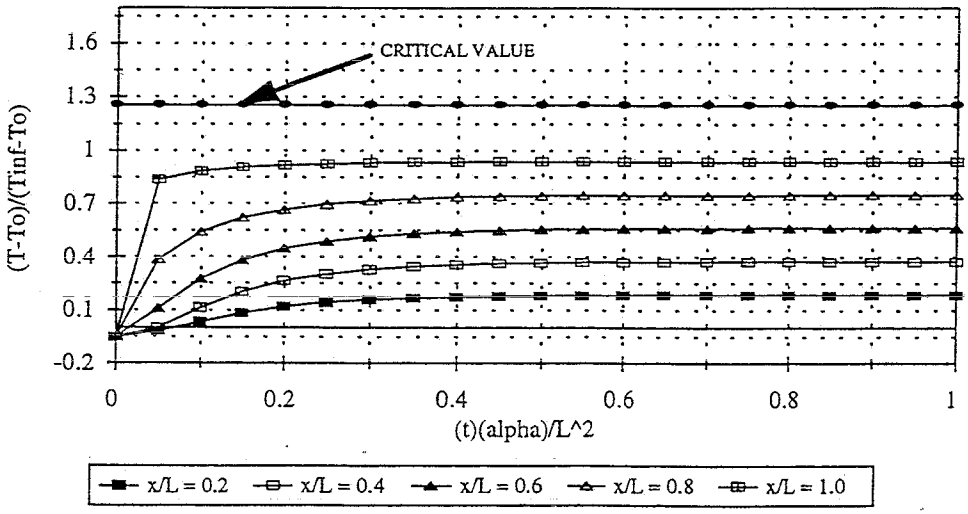

Fig. D6. Normalized Temperature Vs. Normalized Time at Several Depths for Titanium Nitride with a Boiling Water Backface and $T_\infty = 3600°R$

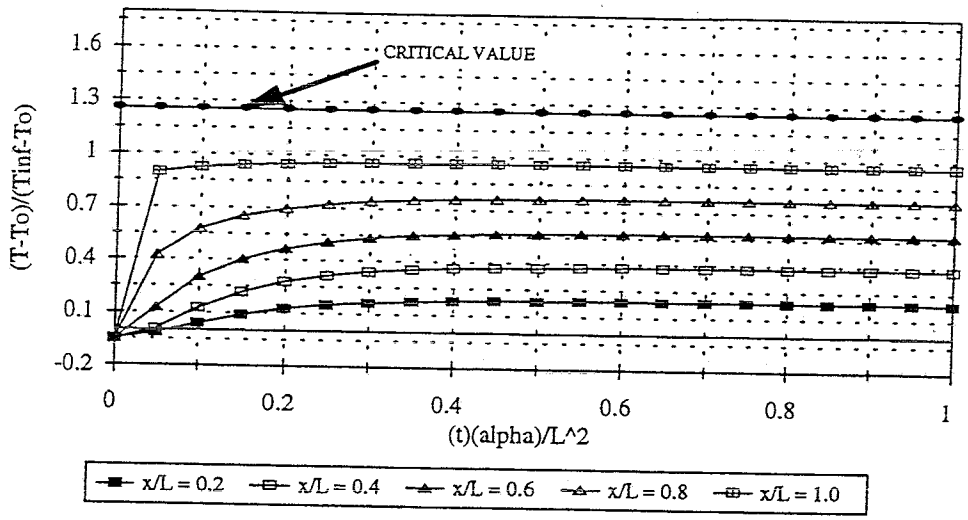

Fig. D7. Normalized Temperature Vs. Normalized Time at Several Depths for Zirconium Nitride with a Boiling Water Backface and $T_\infty = 3600°R$

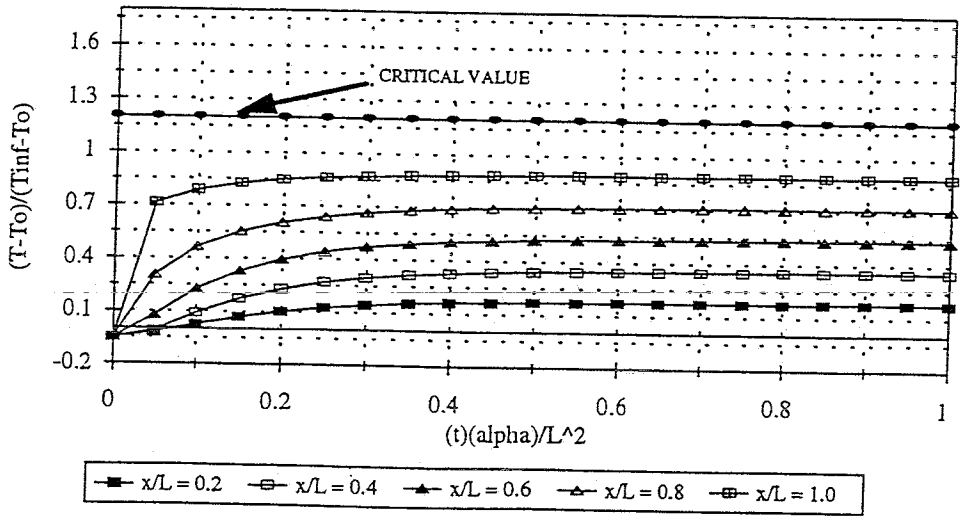

Fig. D8. Normalized Temperature Vs. Normalized Time at Several Depths for Magnesium Oxide with a Boiling Water Backface and $T_\infty = 3600°R$

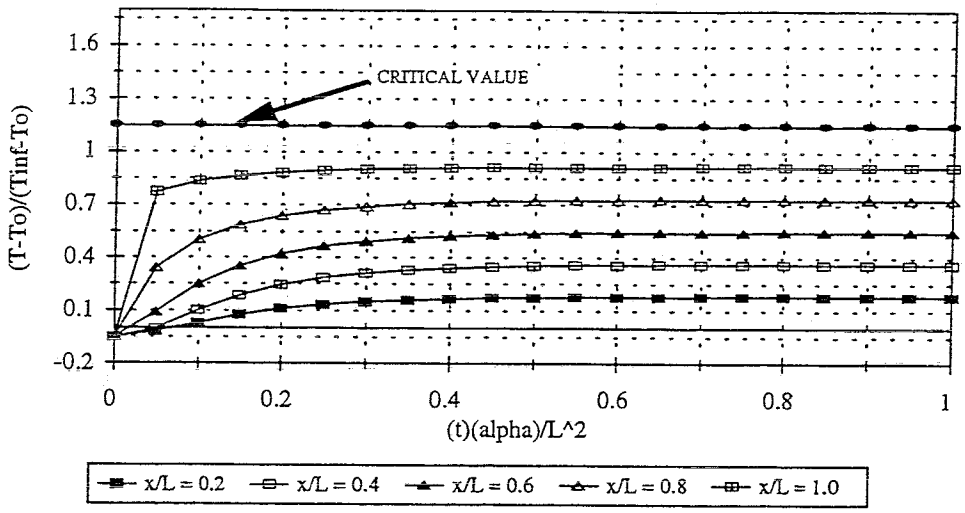

Fig. D9. Normalized Temperature Vs. Normalized Time at Several Depths for Lanthanum Boride with a Boiling Water Backface and $T_\infty = 3600°R$

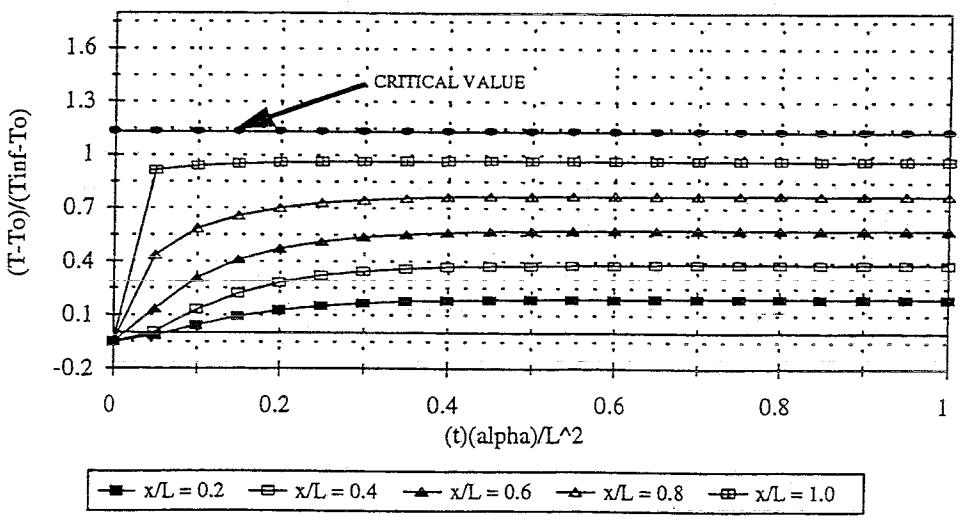

Fig. D10. Normalized Temperature Vs. Normalized Time at Several Depths for Zirconium Oxide with a Boiling Water Backface and $T_\infty = 3600°R$

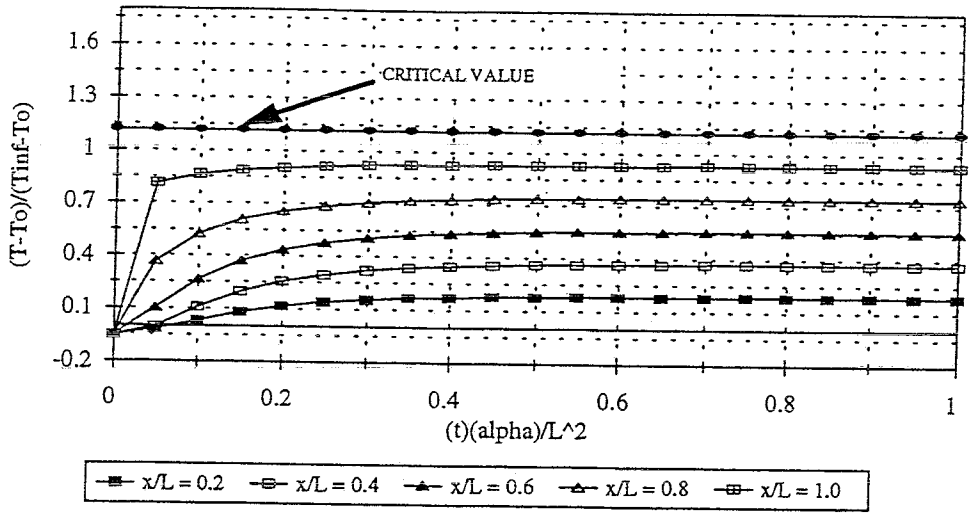

Fig. D11. Normalized Temperature Vs. Normalized Time at Several Depths for Vanadium Carbide with a Boiling Water Backface and $T_\infty = 3600°R$

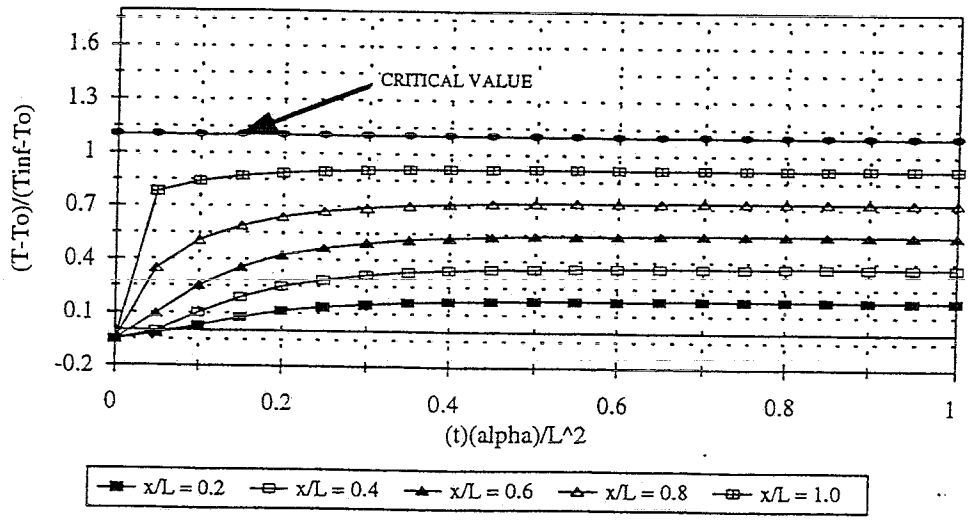

Fig. D12. Normalized Temperature Vs. Normalized Time at Several Depths for Neodymium Boride with a Boiling Water Backface and $T_\infty = 3600°R$

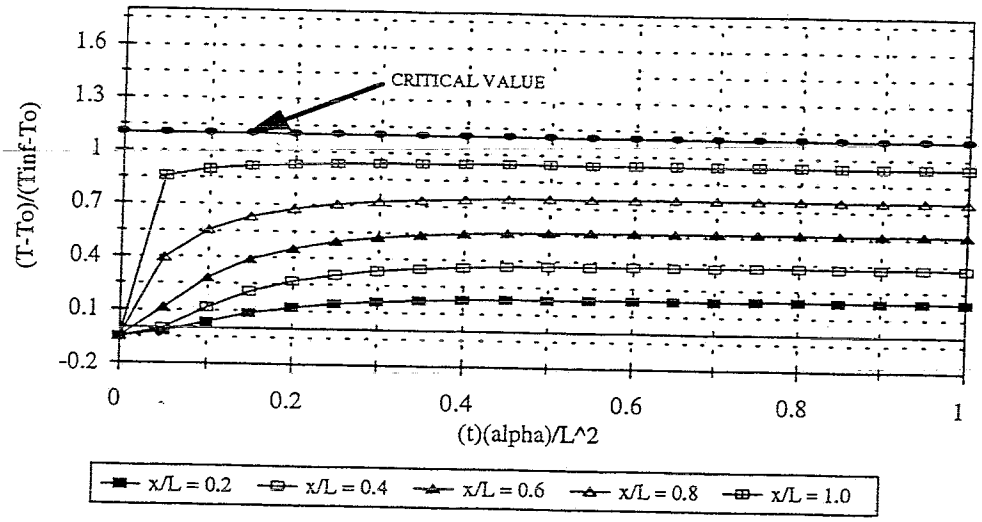

Fig. D13. Normalized Temperature Vs. Normalized Time at Several Depths for Calcium Oxide with a Boiling Water Backface and $T_\infty = 3600°R$

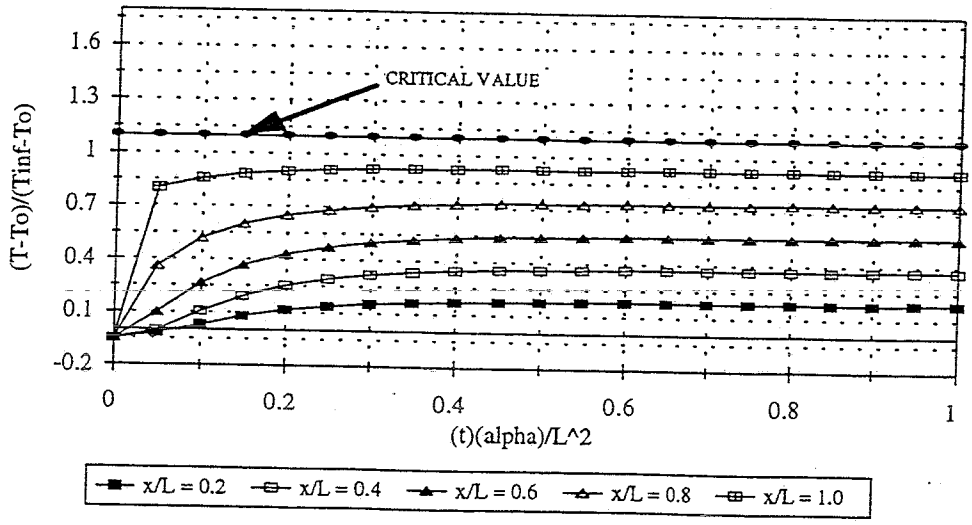

Fig. D14. Normalized Temperature Vs. Normalized Time at Several Depths for Praesodymium Boride with a Boiling Water Backface and $T_\infty = 3600°R$

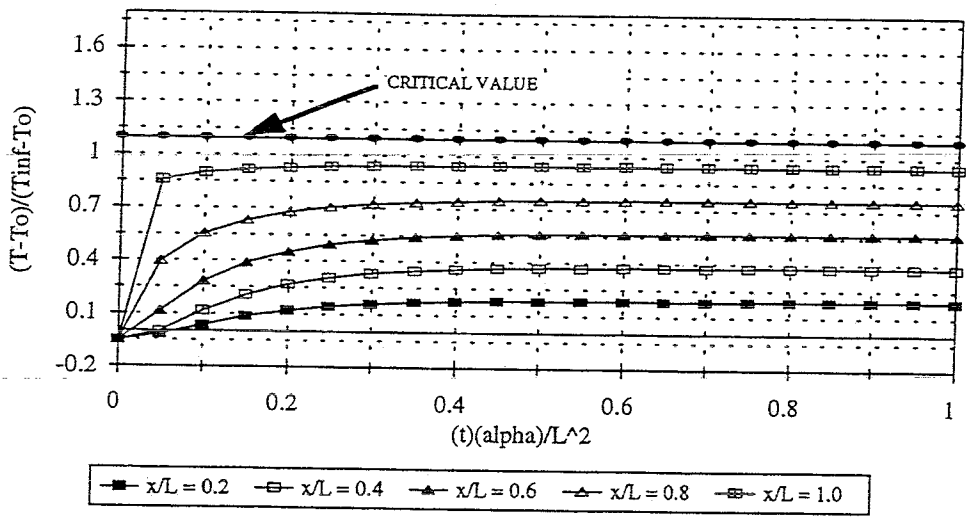

Fig. D15. Normalized Temperature Vs. Normalized Time at Several Depths for Yttrium Boride with a Boiling Water Backface and $T_\infty = 3600°R$

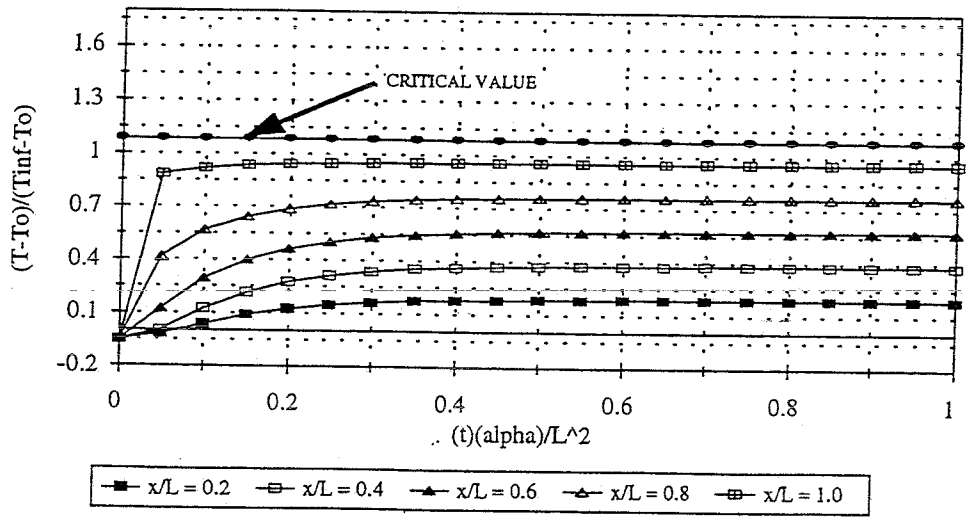

Fig. D16. Normalized Temperature Vs. Normalized Time at Several Depths for Europium Boride with a Boiling Water Backface and $T_\infty = 3600°R$

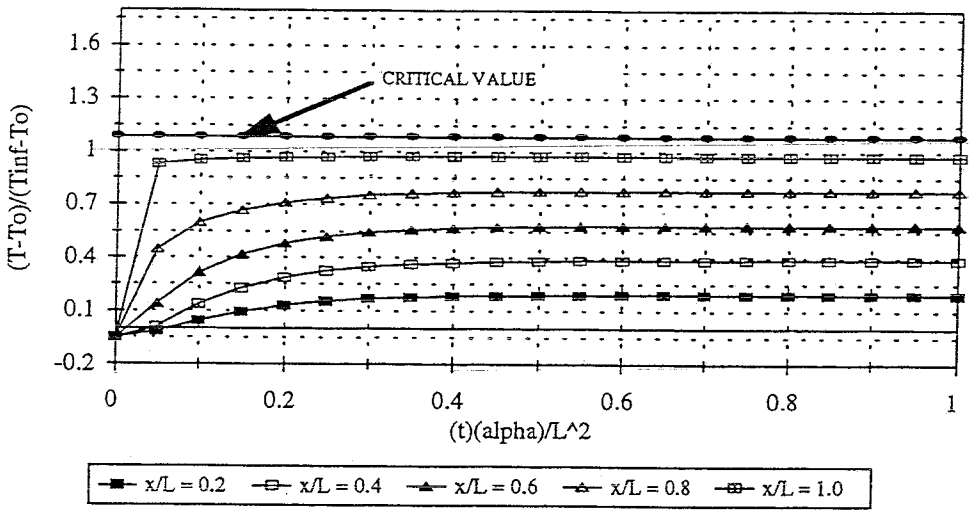

Fig. D17. Normalized Temperature Vs. Normalized Time at Several Depths for Samarium Boride with a Boiling Water Backface and $T_\infty = 3600°R$

APPENDIX E

NORMALIZED TEMPERATURE VS. NORMALIZED TIME AT SEVERAL DEPTHS FOR CANDIDATE CERAMIC MATERIALS WITH A BOILING WATER BACKFACE AND $T_\infty = 1800°R$

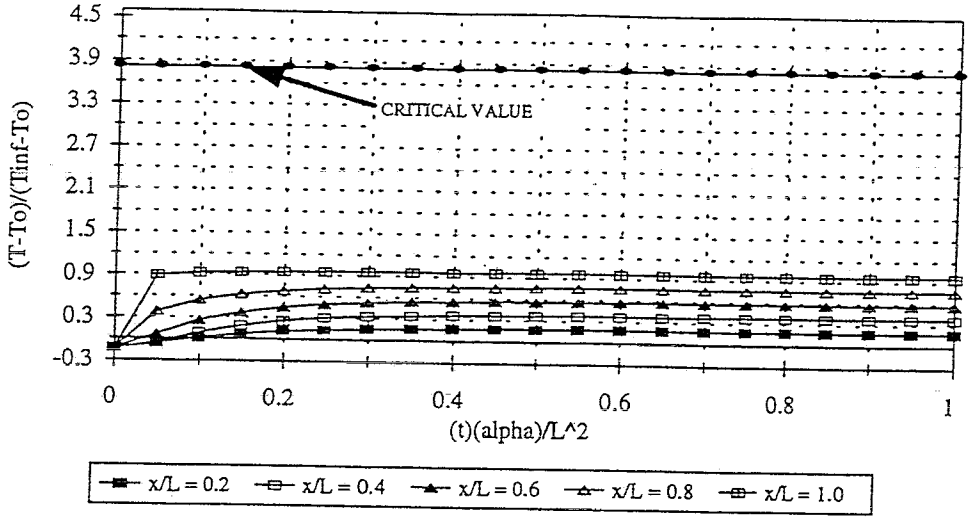

Fig. E1. Normalized Temperature Vs. Normalized Time at Several Depths for Zirconium Carbide with a Boiling Water Backface and T_∞ = 1800°R

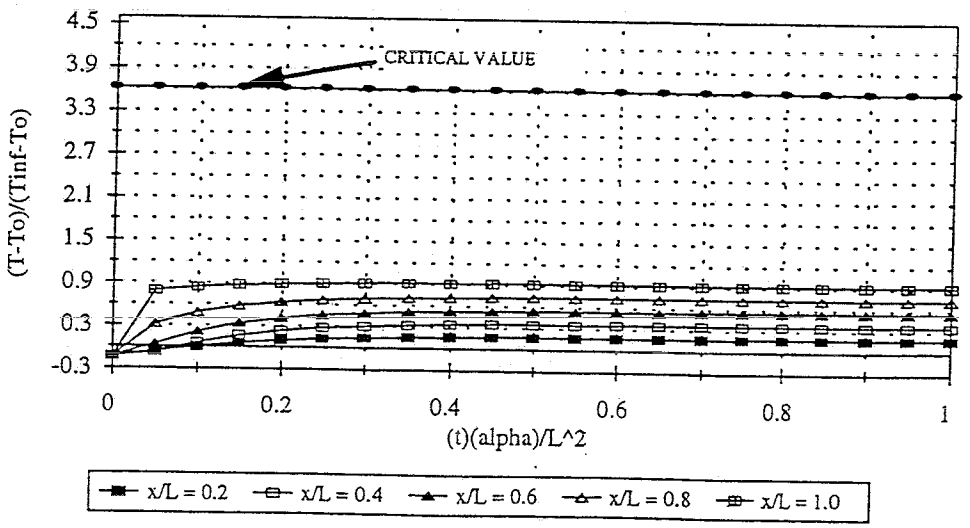

Fig. E2. Normalized Temperature Vs. Normalized Time at Several Depths for Zirconium Boride with a Boiling Water Backface and T_∞ = 1800°R

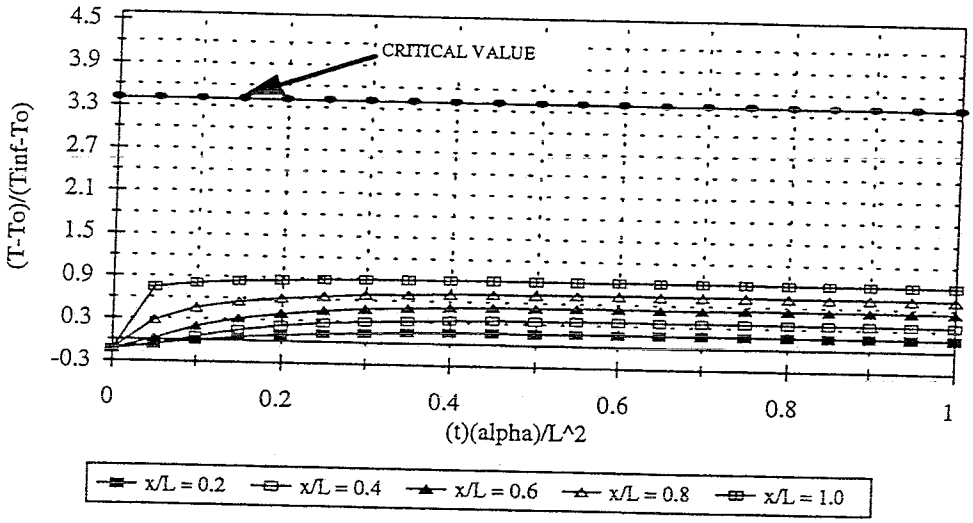

Fig. E3. Normalized Temperature Vs. Normalized Time at Several Depths for Titanium Carbide with a Boiling Water Backface and T_∞ = 1800°R

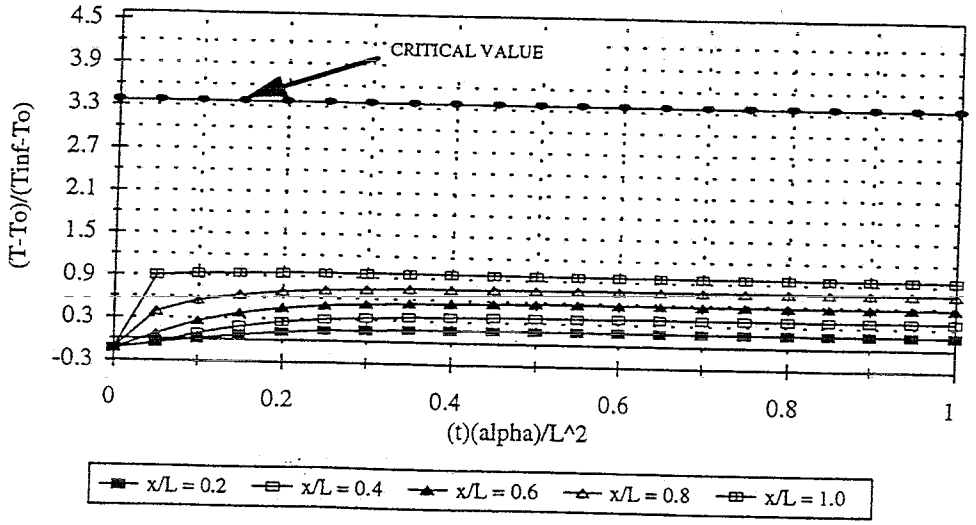

Fig. E4. Normalized Temperature Vs. Normalized Time at Several Depths for Niobium Boride with a Boiling Water Backface and T_∞ = 1800°R

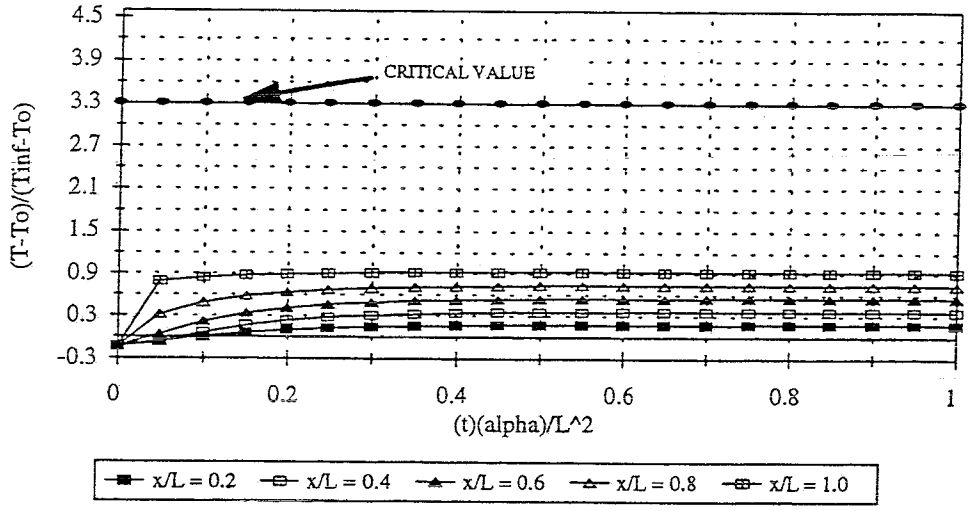

Fig. E5. Normalized Temperature Vs. Normalized Time at Several Depths for Silicon Carbide with a Boiling Water Backface and $T_\infty = 1800°R$

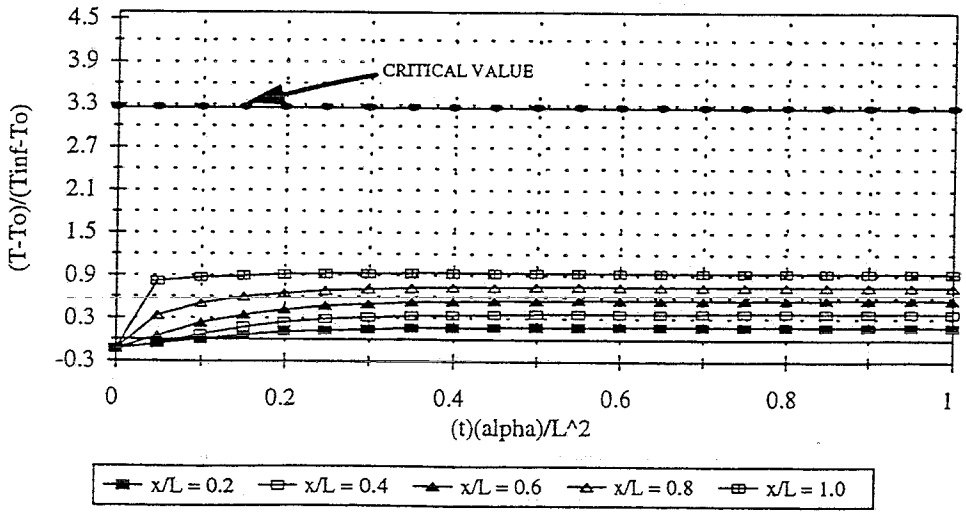

Fig. E6. Normalized Temperature Vs. Normalized Time at Several Depths for Titanium Nitride with a Boiling Water Backface and $T_\infty = 1800°R$

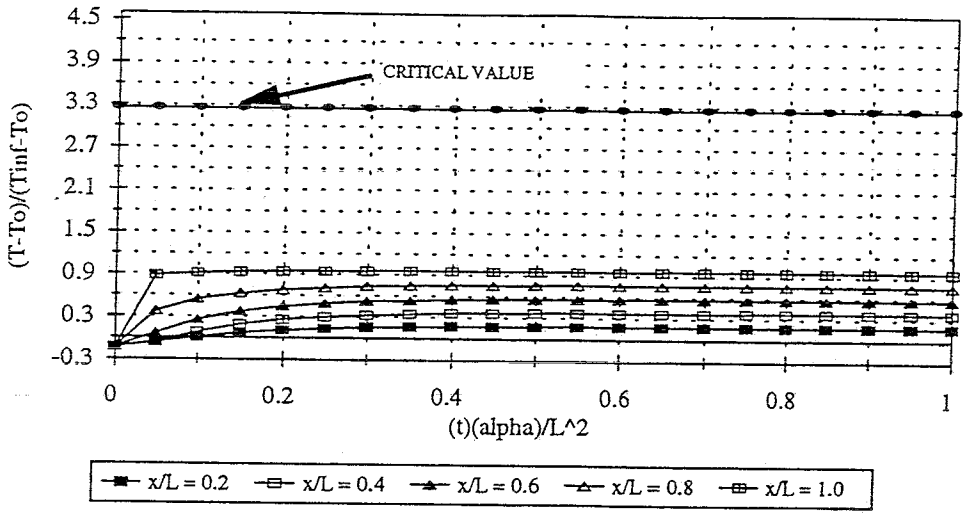

Fig. E7. Normalized Temperature Vs. Normalized Time at Several Depths for Zirconium Nitride with a Boiling Water Backface and T_∞ = 1800°R

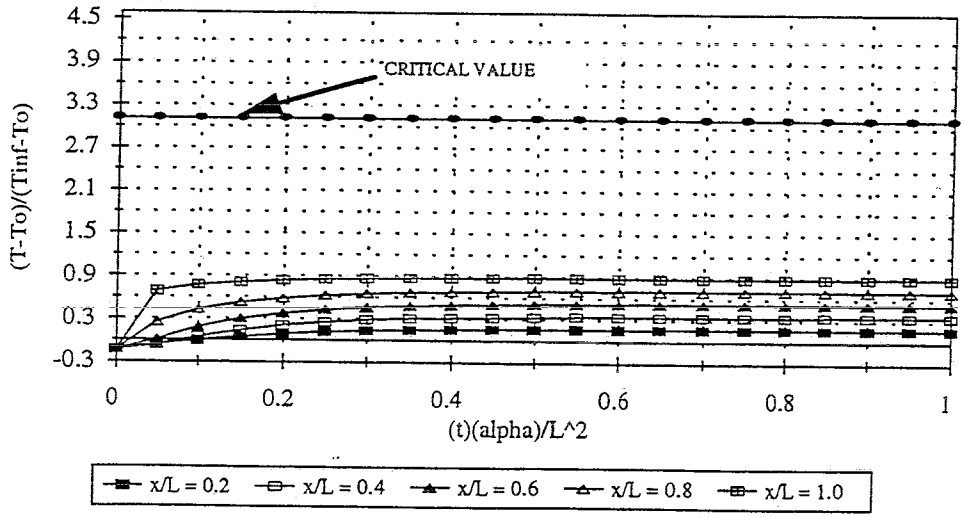

Fig. E8. Normalized Temperature Vs. Normalized Time at Several Depths for Magnesium Oxide with a Boiling Water Backface and T_∞ = 1800°R

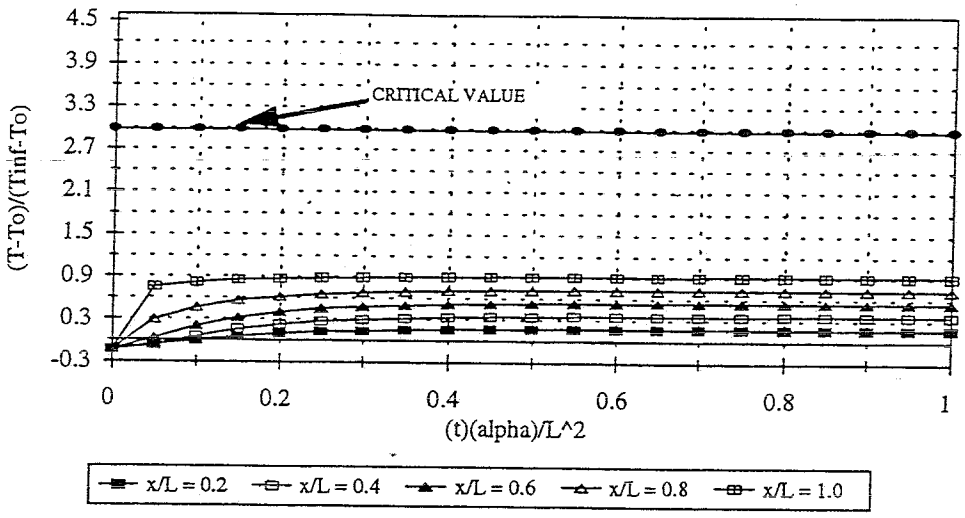

Fig. E9. Normalized Temperature Vs. Normalized Time at Several Depths for Lanthanum Boride with a Boiling Water Backface and $T_\infty = 1800°R$

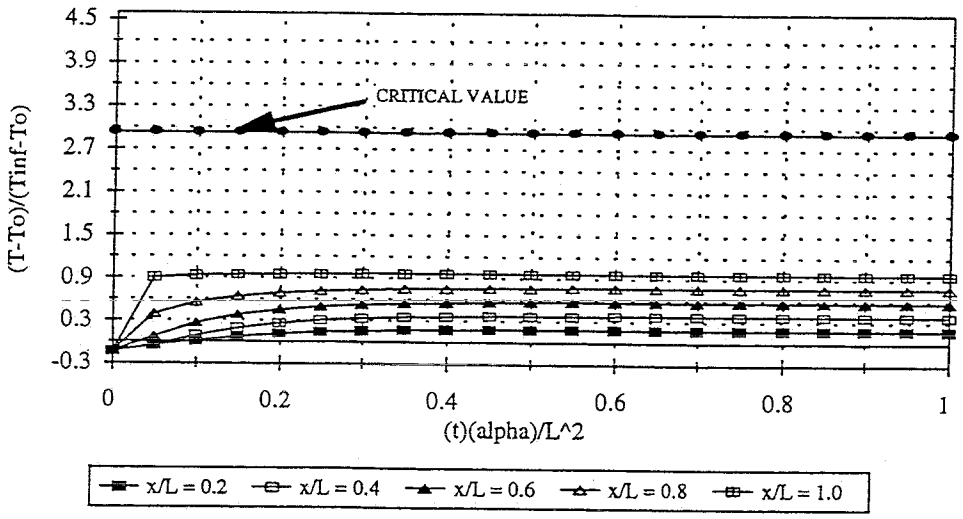

Fig. E10. Normalized Temperature Vs. Normalized Time at Several Depths for Zirconium Oxide with a Boiling Water Backface and $T_\infty = 1800°R$

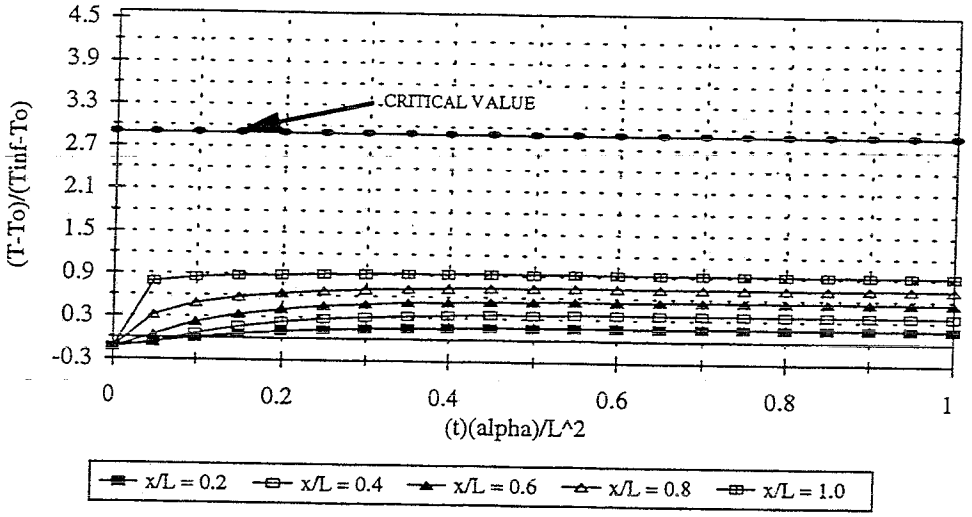

Fig. E11. Normalized Temperature Vs. Normalized Time at Several Depths for Vanadium Carbide with a Boiling Water Backface and $T_\infty = 1800°R$

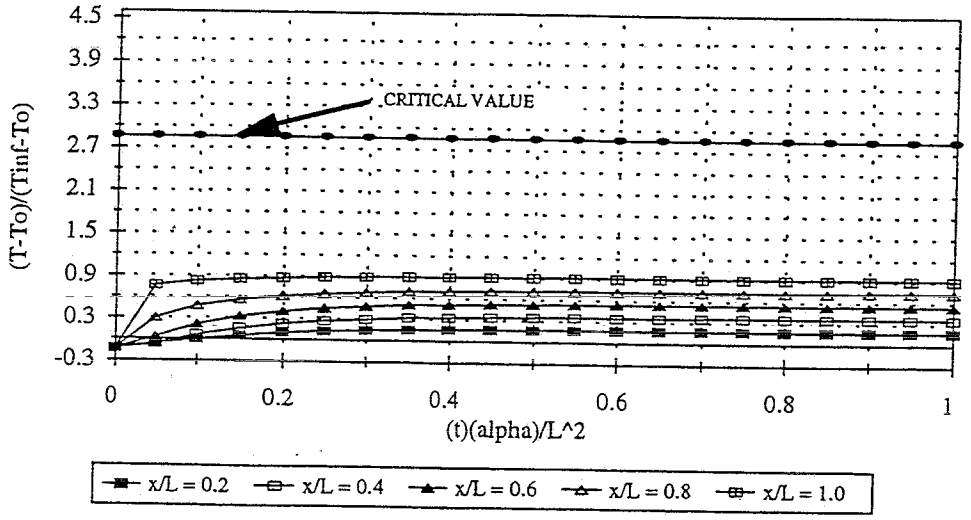

Fig. E12. Normalized Temperature Vs. Normalized Time at Several Depths for Neodymium Boride with a Boiling Water Backface and $T_\infty = 1800°R$

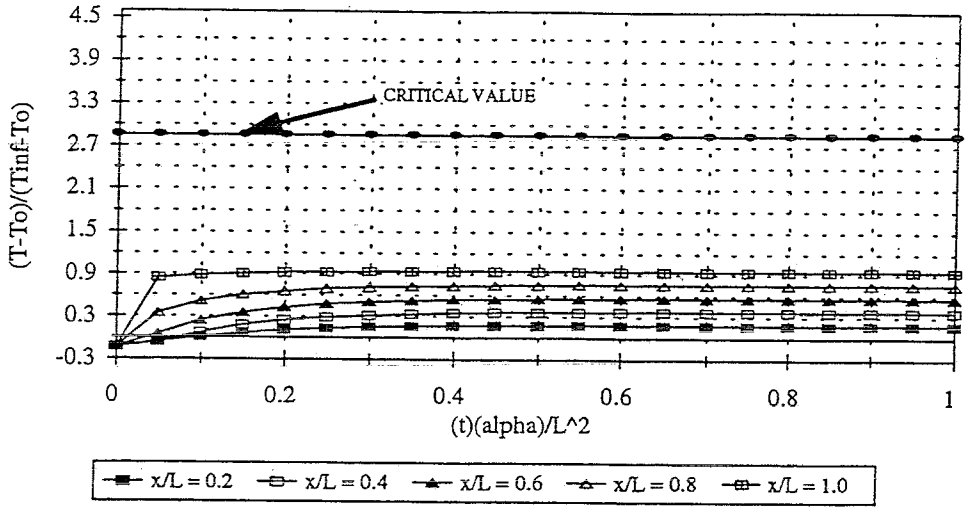

Fig. E13. Normalized Temperature Vs. Normalized Time at Several Depths for Calcium Oxide with a Boiling Water Backface and $T_\infty = 1800°R$

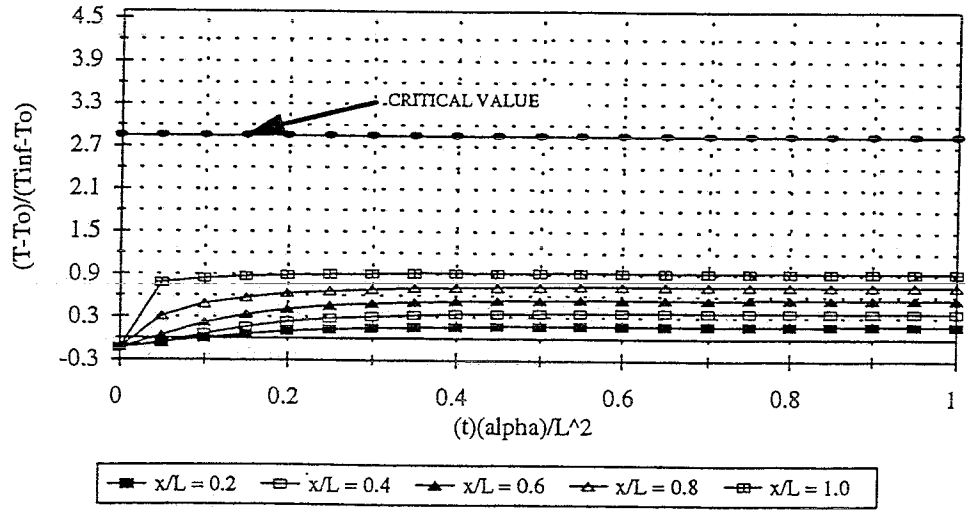

Fig. E14. Normalized Temperature Vs. Normalized Time at Several Depths for Praesodymium Boride with a Boiling Water Backface and $T_\infty = 1800°R$

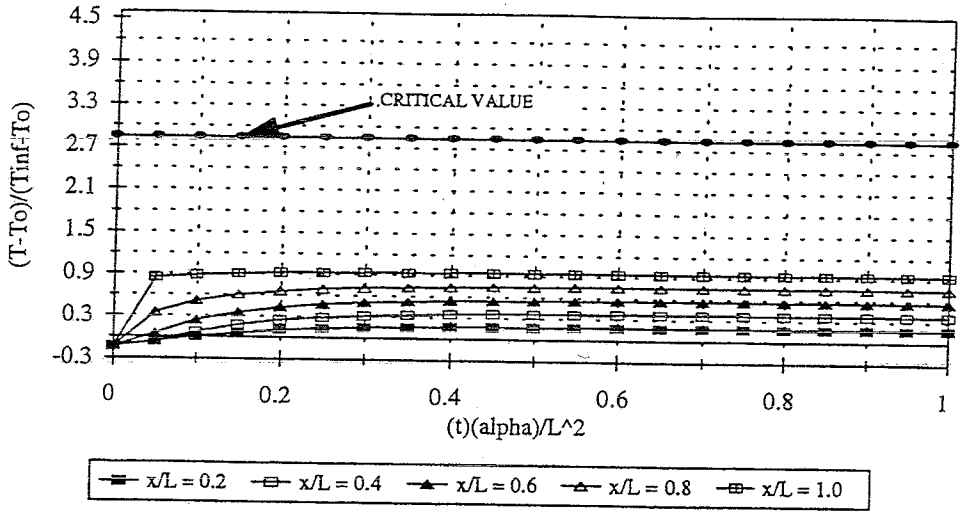

Fig. E15. Normalized Temperature Vs. Normalized Time at Several Depths for Yttrium Boride with a Boiling Water Backface and $T_\infty = 1800°R$

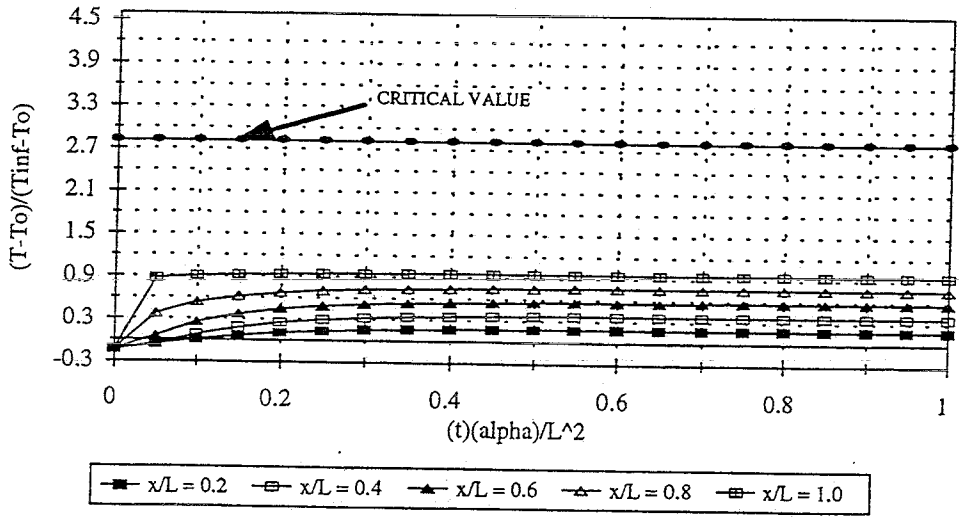

Fig. E16. Normalized Temperature Vs. Normalized Time at Several Depths for Europium Boride with a Boiling Water Backface and $T_\infty = 1800°R$

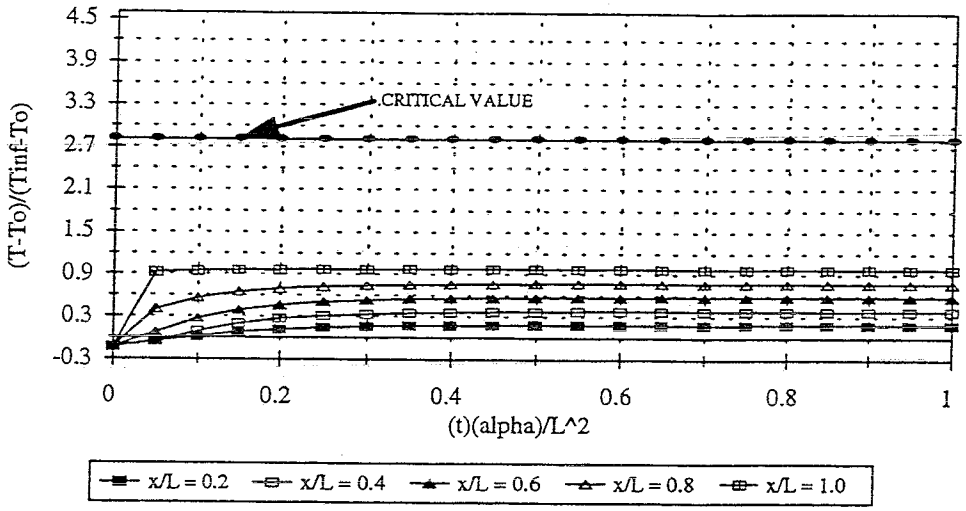

Fig. E17. Normalized Temperature Vs. Normalized Time at Several Depths for Samarium Boride with a Boiling Water Backface and $T_\infty = 1800°R$

APPENDIX F

STEADY STATE SOLUTION FOR A SINGLE LAYER TILE PROTECTION SYSTEM

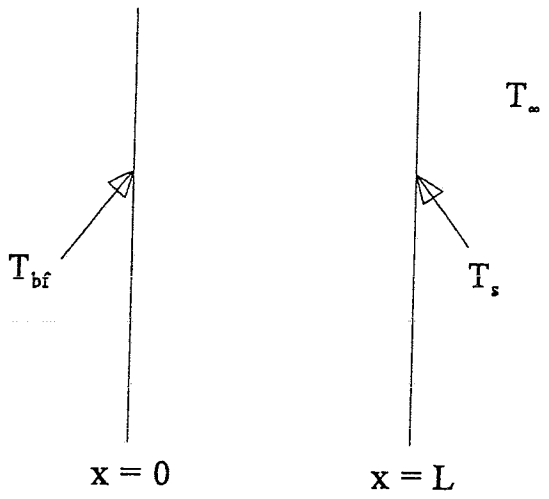

Fig. F1. Single Layer Plane Wall at Steady State with a Convective Boundary Condition at x = L

The boundary conditions for the steady state solution are

$$T(0)=T_{bf} \qquad \frac{\partial T}{\partial x}(L)=-\frac{h}{k}(T_s-T_\infty)$$

The temperature through the material is linear and is in the form of

$$T=c_1x+c_2 \qquad \textbf{(F1)}$$

Substitute the boundary conditions into the Equation F1 to determine the coefficients

$$T(0)=c_1(0)+c_2=T_{bf}$$

$$\therefore \quad c_2=T_{bf}$$

$$\frac{\partial T}{\partial x}=c_1=-\frac{h}{k}(T_s-T_\infty)$$

$$T=-\frac{h}{k}(T_s-T_\infty)x+T_{bf}$$

At the surface of the material, x = L, so the solution for the surface is

$$T_s=-\frac{hL}{k}(T_s-T_\infty)+T_{bf}$$

Solve for T_s

$$T_s+\frac{hL}{k}T_s=T_{bf}+\frac{hL}{k}T_\infty$$

$$T_s = \frac{T_{bf} + \frac{hL}{k} T_\infty}{1 + \frac{hL}{k}} \qquad \textbf{(F2)}$$

With the use of Fourier's law of heat conduction, the steady state heat rate equation becomes

$$\frac{q}{A} = -k\frac{\Delta T}{\Delta x} = -k\frac{T_s - T_{bf}}{L}$$

Substitute Equation F2 into the above equation to obtain Equation F3.

$$\frac{q}{A} = -k\frac{\dfrac{T_{bf} + \frac{hL}{k} T_\infty}{1 + \frac{hL}{k}} - T_{bf}}{L}$$

$$\frac{q}{A} = -\frac{h}{1 + \frac{hL}{k}}(T_\infty - T_{bf}) \qquad \textbf{(F3)}$$

A nondimensional form of this equation is obtained by dividing both sides of Equation F3 by hT_∞.

$$\frac{q}{hAT_\infty} = -\frac{1}{1+\frac{hL}{k}} \frac{T_\infty - T_{bf}}{T_\infty}$$

This equation reduces to

$$\frac{q}{hAT_\infty} = -\frac{1}{1+Bi} \left(1 - \frac{T_{bf}}{T_\infty}\right) \qquad \textbf{(F4)}$$

where Bi = hL/k.

Considering heat flow to be positive from the hot plume into the insulation material, the negative of this equation is obtained

$$\frac{q}{A} = \frac{h}{1+\frac{hL}{k}} (T_\infty - T_{bf}) \qquad \textbf{(F5)}$$

APPENDIX G

SOLUTION TO THE BOUNDARY VALUE PROBLEM WITH AN INSULATED BACKFACE CONDITION

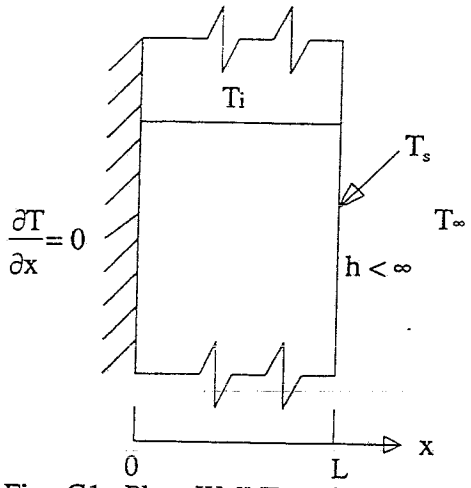

Fig. G1. Plane Wall Transient with a Convective Boundary Condition at x = L for the Insulated Backface Condition

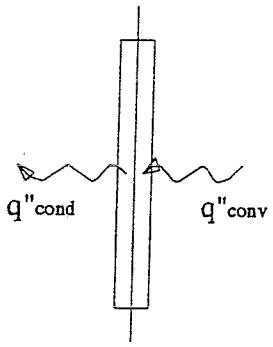

Fig. G2. System Boundary at Convective Surface for the Insulated Backface Condition

The governing equation for this problem is

$$\frac{\partial^2 T}{\partial x^2} = \frac{1}{\alpha}\frac{\partial T}{\partial t}$$

Energy balance across the system boundary

$$q''_{conducted} = q''_{convected}$$

Substitute the rate equations to obtain the boundary condition at x = L

$$-k\frac{\partial T}{\partial x} = h(T_s - T_\infty)$$

or

$$\frac{\partial T}{\partial x}(L,t)=-\frac{h}{k}(T_s-T_\infty)$$

The second boundary condition is that $\partial T/\partial x = 0$ at $x = 0$ or

$$\frac{\partial T}{\partial x}(0,t)=0$$

The initial condition for this problem is that $T = T_i$ at $t = 0$ or

$T(x,0) = T_i$

In the form shown above, the boundary condition is nonhomogeneous, but it can be made homogeneous by substituting $T = T - T_\infty$ in place of T. In addition, the problem is normalized by defining

$$u=\frac{T-T_\infty}{T_i-T_\infty} \qquad \bar{x}=\frac{x}{L} \qquad \theta=\frac{\alpha t}{L^2}$$

so that the normalized problem is given by the partial differential equation:

$$u_{xx} = u_\theta \tag{G1}$$

where the bars have been dropped from x and θ

The boundary conditions are

$$u_x(0,\theta) = 0 \tag{G2}$$

and

$$u_x(1,\theta) = -Hu(1,\theta) \tag{G3}$$

The initial condition is given by

$u(x,0) = 1$ (G4)

Since the problem is homogeneous, the solution for $u(x, \theta)$ is found using separation of variables.

$u(x, \theta) = X\theta$

Equation G1 now becomes

$X''\theta = X\theta'$

$$\frac{X''}{X} = \frac{\theta'}{\theta} = -\lambda^2$$

This results in two ordinary differential equations. First,

$X'' + \lambda^2 X = 0$

whose solution is

$X = A\sin\lambda x + B\cos\lambda x$

And second,

$\theta' + \lambda^2\theta = 0$

whose solution is

$\theta = Ce^{-\lambda^2\theta}$

$X = A\sin\lambda x + B\cos\lambda x$

$X' = A\lambda\cos\lambda x - B\lambda\sin\lambda x$

$X'(0) = A\lambda\cos(0) - B\lambda\sin(0) = 0$

$\therefore A = 0$

$X = B\cos\lambda x$

$X'(1) = -B\lambda sin\lambda = -Hbcos\lambda$

$\therefore Hcot\lambda = \lambda$

$u_n = X\theta = A_n \cos\lambda_n x[e^{-\lambda_n^2\theta}]$ where $Hcot\lambda_n = \lambda_n$

$$u(x,\theta) = \sum_{n=1}^{\infty} A_n \cos\lambda_n x[e^{-\lambda_n^2\theta}]$$

From the initial condition

$u(x,0)=1$

$$u(x,0)=1 = \sum_{n=1}^{\infty} A_n \cos\lambda_n x$$

Multiply through by $cos\ \lambda_m x\ dx$ and integrate between 0 and 1

$$\int_0^1 1\cos\lambda_m x dx = \sum_{n=1}^{\infty} A_n \int_0^1 \cos\lambda_n x \cos\lambda_m x dx$$

When n = m, this equation becomes

$$\int_0^1 1\cos\lambda_m x dx = A_m \int_0^1 \cos^2\lambda_m x dx$$

$$A_m = \frac{\int_0^1 \cos\lambda_m x dx}{\int_0^1 \cos^2\lambda_m x dx} = \frac{\frac{1}{\lambda_m}[\sin\lambda_m x]_0^1}{\frac{1}{\lambda_m}[\frac{\lambda_m x}{2} + \frac{\sin 2\lambda_m x}{4}]_0^1}$$

$$A_m = \frac{4\sin\lambda_m}{2\lambda_m + sin2\lambda_m}$$

Substitute A_m into the equation for $u(x,\theta)$ to get

$$u(x,\theta) = \sum_{n=1}^{\infty} \frac{4\sin\lambda_n}{2\lambda_n + \sin 2\lambda_n} \cos\lambda_n x e^{-\lambda_n^2 \theta} = \sum_{n=1}^{\infty} \frac{4\sin\lambda_n}{2\lambda_n + 2\sin\lambda_n \cos\lambda_n} \cos\lambda_n x e^{-\lambda_n^2 \theta} \qquad \textbf{(G5)}$$

The eigencondition can be written as

$$\cos\lambda_n = \frac{\lambda_n \sin\lambda_n}{H}$$

Substitute this form of the eigencondition into Equation G5 to get

$$u(x,\theta) = \sum_{n=1}^{\infty} \frac{2H\sin\lambda_n}{H\lambda_n + \lambda_n \sin^2\lambda_n} \cos\lambda_n x e^{-\lambda_n^2 \theta} \qquad \textbf{(G6)}$$

APPENDIX H

STEADY STATE SOLUTION FOR A COMPOSITE LAYER TILE PROTECTION SYSTEM

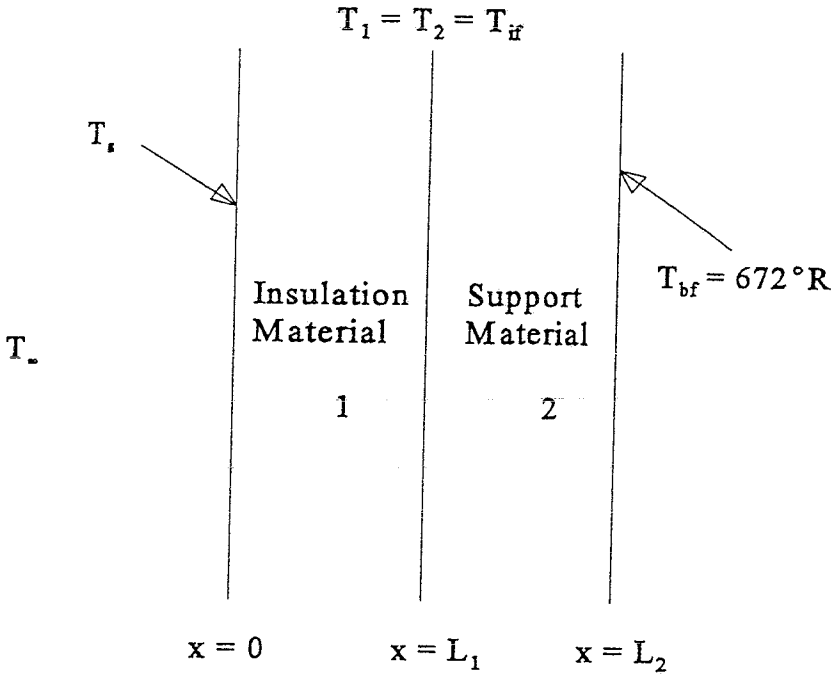

Fig. H1. Composite Layer Plane Wall at Steady State with a Convective Boundary Condition at x = L

The two energy balance equations across the system are

$$h(T_\infty - T_s) = \frac{k_1(T_s - T_{if})}{L_1} \qquad \textbf{(H1)}$$

$$h(T_\infty - T_s) = \frac{k_2(T_{if} - T_{bf})}{L_2 - L_1} \qquad \textbf{(H2)}$$

Solve Equation H1 for the surface temperature to obtain

$$T_s = \frac{hT_\infty L_1 + k_1 T_{if}}{hL_1 + k_1} \qquad \textbf{(H3)}$$

Substitute Equation H3 into Equation H2

$$h\left(T_\infty - \frac{hT_\infty L_1 + k_1 T_{if}}{hL_1 + k_1}\right) = k_2 \frac{T_{if} - T_{bf}}{L_2 - L_1} \qquad \textbf{(H4)}$$

Solve Equation H4 for the interface temperature, T_{if}

$$T_{if} = \frac{hT_\infty k_1 L_2 - hT_\infty k_1 L_1 + k_2 T_{bf} hL_1 + k_2 T_{bf} k_1}{hk_1 L_2 - hk_1 L_1 + k_2 hL_1 + k_2 k_1} \qquad \textbf{(H5)}$$

Substitute Equation H5 into Equation H3 and solve for the surface temperature, T_s

$$T_s = \frac{hT_\infty k_1 L_2 - hT_\infty k_1 L_1 + k_2 T_{bf} k_1 + hT_\infty L_1 k_2}{hk_1 L_2 - hk_1 L_1 + k_2 hL_1 + k_2 k_1} \qquad \textbf{(H6)}$$

APPENDIX I

STEADY STATE SURFACE AND INTERFACE TEMPERATURES IN AN EXHAUST TEMPERATURE REGION OF 6538°R FOR A COMPOSITE WALL DESIGN WITH VARIOUS SUPPORT MATERIALS

Table I1. Steady State Surface and Interface Temperatures in an Exhaust Temperature Region of 6538°R for a Composite Wall Design with Titanium as the Support Material with a Boiling Water Backface

Material	k (Btu/hr•ft•°R)	T_{crit} (°R)	T_s (°R)	T_{if} (°R)
Tantalum Carbide	12.71	5751	6419	3612
Hafnium Carbide	12.71	5697	6419	3612
Niobium Carbide	17.34	5252	6402	4042
Zirconium Boride (ZrB_2)	23.11	4752	6386	4419
Magnesium Oxide	36.40	4185	6365	4942
Titanium Carbide	28.89	4509	6376	4689
Zirconium Carbide	11.56	4982	6425	3478
Titanium Nitride	19.07	4347	6397	4170
Silicon Carbide	23.11	4401	6386	4419
Lanthanum Boride	27.73	4037	6377	4641
Beryllium Carbide	28.89	3605	6376	4689
Vanadium Carbide	22.54	3942	6388	4387
Neodymium Boride	26.58	3902	6380	4591
Niobium Boride	9.82	4469	6434	3249
Zirconium Nitride	12.13	4347	6422	3547
Praesodymium Boride	23.69	3888	6385	4450
Calcium Oxide	16.76	3898	6404	3996
Aluminum Nitride	19.07	3780	6397	4170
Scandium Nitride	15.60	3807	6408	3898
Yttrium Boride	16.76	3875	6404	3996

Table I2. Steady State Surface and Interface Temperatures in an Exhaust Temperature Region of 6538°R for a Composite Wall Design with Steel as the Support Material with a Boiling Water Backface

Material	k (Btu/hr•ft•°R)	T_{crit} (°R)	$\bar{T}_s$ (°R)	$\bar{T}_{if}$ (°R)
Tantalum Carbide	12.71	5751	6396	3048
Hafnium Carbide	12.71	5697	6396	3048
Niobium Carbide	17.34	5252	6371	3475
Zirconium Boride (ZrB_2)	23.11	4752	6347	3869
Magnesium Oxide	36.40	4185	6312	4452
Titanium Carbide	28.89	4509	6329	4164
Zirconium Carbide	11.56	4982	6404	2920
Titanium Nitride	19.07	4347	6363	3606
Silicon Carbide	23.11	4401	6347	3869
Lanthanum Boride	27.73	4037	6333	4111
Berylilium Carbide	28.89	3605	6329	4164
Vanadium Carbide	22.54	3942	6349	3835
Neodymium Boride	26.58	3902	6336	4056
Niobium Boride	9.82	4469	6417	2706
Zirconium Nitride	12.13	4347	6400	2985
Praesodymium Boride	23.69	3888	6345	3902
Calcium Oxide	16.76	3898	6373	3428
Aluminum Nitride	19.07	3780	6363	3606
Scandium Nitride	15.60	3807	6379	3329
Yttrium Boride	16.76	3875	6373	3428

Table I3. Steady State Surface and Interface Temperatures in an Exhaust Temperature Region of 6538°R for a Composite Wall Design with Copper as the Support Material with a Boiling Water Backface

Material	k (Btu/hr•ft•°R)	T_{crit} (°R)	T_s (°R)	T_{if} (°R)
Tantalum Carbide	12.71	5751	6312	966
Hafnium Carbide	12.71	5697	6312	966
Niobium Carbide	17.34	5252	6239	1060
Zirconium Boride (ZrB_2)	23.11	4752	6154	1170
Magnesium Oxide	36.40	4185	5981	1394
Titanium Carbide	28.89	4509	6075	1272
Zirconium Carbide	11.56	4982	6330	941
Titanium Nitride	19.07	4347	6213	1094
Silicon Carbide	23.11	4401	6154	1170
Lanthanum Boride	27.73	4037	6091	1252
Beryllium Carbide	28.89	3605	6075	1272
Vanadium Carbide	22.54	3942	6162	1159
Neodymium Boride	26.58	3902	6106	1232
Niobium Boride	9.82	4469	6359	904
Zirconium Nitride	12.13	4347	6321	953
Praesodymium Boride	23.69	3888	6146	1181
Calcium Oxide	16.76	3898	6248	1049
Aluminum Nitride	19.07	3780	6213	1094
Scandium Nitride	15.60	3807	6266	1025
Yttrium Boride	16.76	3875	6248	1049

APPENDIX J

STEADY STATE SURFACE AND INTERFACE TEMPERATURES IN AN EXHAUST TEMPERATURE REGION OF 5400°R FOR A COMPOSITE WALL DESIGN WITH VARIOUS SUPPORT MATERIALS

Table J1. Steady State Surface and Interface Temperatures in an Exhaust Temperature Region of 5400°R for a Composite Wall Design with Titanium as the Support Material with a Boiling Water Backface

Material	k (Btu/hr•ft•°R)	T_{crit} (°R)	T_s (°R)	T_{if} (°R)
Tantalum Carbide	12.71	5751	5304	3042
Hafnium Carbide	12.71	5697	5304	3042
Niobium Carbide	17.34	5252	5290	3388
Zirconium Carbide	11.56	4982	5309	2934
Zirconium Boride (ZrB_2)	23.11	4752	5278	3692
Titanium Carbide	28.89	4509	5269	3909
Magnesium Oxide	36.40	4185	5261	4114
Titanium Nitride	19.07	4347	5286	3492
Silicon Carbide	23.11	4401	5278	3692
Lanthanum Boride	27.73	4037	5271	3871
Niobium Boride	9.82	4469	5316	2749
Zirconium Nitride	12.13	4347	5306	2989
Vanadium Carbide	22.54	3942	5279	3666
Beryllium Carbide	28.89	3605	5269	3909
Neodymium Boride	26.58	3902	5272	3830
Praesodymium Boride	23.69	3888	5277	3717
Calcium Oxide	16.76	3898	5292	3351
Yttrium Boride	16.76	3875	5292	3351
Scandium Nitride	15.60	3807	5295	3272
Aluminum Nitride	19.07	3780	5286	3492

Table J2. Steady State Surface and Interface Temperatures in an Exhaust Temperature Region of 5400°R for a Composite Wall Design with Steel as the Support Material with a Boiling Water Backface

Material	k (Btu/hr•ft•°R)	T_{crit} (°R)	$\bar{T}_s$ (°R)	$\bar{T}_{if}$ (°R)
Tantalum Carbide	12.71	5751	5286	2587
Hafnium Carbide	12.71	5697	5286	2587
Niobium Carbide	17.34	5252	5265	2931
Zirconium Carbide	11.56	4982	5292	2483
Zirconium Boride (ZrB_2)	23.11	4752	5246	3249
Titanium Carbide	28.89	4509	5232	3487
Magnesium Oxide	36.40	4185	5218	3719
Titanium Nitride	19.07	4347	5259	3037
Silicon Carbide	23.11	4401	5246	3249
Lanthanum Boride	27.73	4037	5234	3444
Niobium Boride	9.82	4469	5302	2312
Zirconium Nitride	12.13	4347	5289	2536
Vanadium Carbide	22.54	3942	5248	3221
Beryllium Carbide	28.89	3605	5232	3487
Neodymium Boride	26.58	3902	5237	3399
Praesodymium Boride	23.69	3888	5245	3276
Calcium Oxide	16.76	3898	5267	2893
Yttrium Boride	16.76	3875	5267	2893
Scandium Nitride	15.60	3807	5272	2813
Aluminum Nitride	19.07	3780	5259	3037

Table J3. Steady State Surface and Interface Temperatures in an Exhaust Temperature Region of 5400°R for a Composite Wall Design with Copper as the Support Material with a Boiling Water Backface

Material	k (Btu/hr•ft•°R)	T_{crit} (°R)	T_s (°R)	T_{if} (°R)
Tantalum Carbide	12.71	5751	5217	909
Hafnium Carbide	12.71	5697	5217	909
Niobium Carbide	17.34	5252	5159	985
Zirconium Carbide	11.56	4982	5233	889
Zirconium Boride (ZrB_2)	23.11	4752	5091	1073
Titanium Carbide	28.89	4509	5027	1156
Magnesium Oxide	36.40	4185	4951	1254
Titanium Nitride	19.07	4347	5138	1012
Silicon Carbide	23.11	4401	5091	1073
Lanthanum Boride	27.73	4037	5039	1140
Niobium Boride	9.82	4469	5256	859
Zirconium Nitride	12.13	4347	5225	899
Vanadium Carbide	22.54	3942	5097	1065
Beryllium Carbide	28.89	3605	5027	1156
Neodymium Boride	26.58	3902	5052	1123
Praesodymium Boride	23.69	3888	5084	1082
Calcium Oxide	16.76	3898	5166	975
Yttrium Boride	16.76	3875	5166	975
Scandium Nitride	15.60	3807	5180	957
Aluminum Nitride	19.07	3780	5138	1012

APPENDIX K

STEADY STATE SURFACE AND INTERFACE TEMPERATURES IN AN EXHAUST TEMPERATURE REGION OF 3600°R FOR A COMPOSITE WALL DESIGN WITH VARIOUS SUPPORT MATERIALS

Table K1. Steady State Surface and Interface Temperatures in an Exhaust Temperature Region of 3600°R for a Composite Wall Design with Titanium as the Support Material with a Boiling Water Backface

Material	k (Btu/hr•ft•°R)	T_{crit} (°R)	T_s (°R)	T_{if} (°R)
Aluminum Nitride	19.07	3780	3529	2418
Beryllium Carbide	28.89	3605	3519	2677
Boron Carbide	17.34	3537	3532	2354
Boron Nitride	9.82	3510	3548	1958
Calcium Oxide	16.76	3898	3533	2331
Cerium Oxide	6.93	3605	3558	1721
Europium Boride	13.29	2848	3535	2171
Gadolinium Boride	12.13	3753	3542	2107
Hafnium Carbide	23.60	5697	3541	2139
Lanthanum Boride	27.73	4037	3520	2653
Magnesium Oxide	36.40	4185	3514	2803
Molybdenum Carbide	4.62	3773	3568	1471
Neodymium Boride	26.58	3902	3521	2628
Niobium Boride	9.82	4469	3548	1958
Niobium Carbide	17.34	5252	3532	2354
Praesodymium Boride	23.69	3888	3524	2558
Samarium Boride	8.09	3848	3553	1824
Scandium Nitride	15.60	3807	3535	2282
Scandium Oxide	4.62	3605	3568	1471
Silicon Carbide	23.11	4401	3524	2542
Tantalum Carbide	23.60	5751	3541	2139
Terbium Boride	11.56	3524	3543	2072
Titanium Carbide	28.89	4509	3519	2677

Table K1. (Continued)

Material	k (Btu/hr•ft•°R)	T_{crit} (°R)	T_s (°R)	T_{if} (°R)
Titanium Nitride	19.07	4347	3529	2418
Vanadium Carbide	22.54	3942	3525	2526
Vanadium Nitride	7.51	3551	3555	1774
Ytterbium Boride	14.45	3564	3537	2229
Ytterbium Silicate	3.47	3645	3574	1317
Yttrium Boride	16.76	3875	3533	2331
Yttrium Oxide	9.82	3686	3548	1958
Zirconium Boride (ZrB_2)	23.11	4752	3524	2542
Zirconium Carbide	11.56	4982	3543	2072
Zirconium Nitride	12.13	4347	3542	2107
Zirconium Oxide	9.82	3983	3548	1958
Zirconium Silicate	3.47	3645	3574	1317
Molybdenum Silicide	28.31	3132	3519	2665
Barium Boride	20.80	3375	3527	2475

Table K2. Steady State Surface and Interface Temperatures in an Exhaust Temperature Region of 3600°R for a Composite Wall Design with Steel as the Support Material with a Boiling Water Backface

Material	k (Btu/hr•ft•°R)	T_{crit} (°R)	T_s (°R)	T_{if} (°R)
Aluminum Nitride	19.07	3780	3513	2137
Beryllium Carbide	28.89	3605	3496	2415
Boron Carbide	17.34	3537	3516	2071
Boron Nitride	9.82	3510	3539	1687
Calcium Oxide	16.76	3898	3518	2047
Cerium Oxide	6.93	3605	3552	1476
Europium Boride	13.29	2848	3527	1888
Gadolinium Boride	12.13	3753	3531	1826
Hafnium Carbide	12.71	5697	3529	1858
Lanthanum Boride	27.73	4037	3497	2389
Magnesium Oxide	36.40	4185	3487	2559
Molybdenum Carbide	4.62	3773	3565	1265
Neodymium Boride	26.58	3902	3499	2361
Niobium Boride	9.82	4469	3539	1687
Niobium Carbide	17.34	5252	3516	2071
Praesodymium Boride	23.69	3888	3504	2284
Samarium Boride	8.09	3848	3547	1566
Scandium Nitride	15.60	3807	3521	1998
Scandium Oxide	4.62	3605	3565	1265
Silicon Carbide	23.11	4401	3505	2268
Tantalum Carbide	23.60	5751	3529	1858
Terbium Boride	11.56	3524	3533	1794
Titanium Carbide	28.89	4509	3496	2415

Table K2. (Continued)

Material	k (Btu/hr•ft•°R)	T_{crit} (°R)	T_s (°R)	T_{if} (°R)
Titanium Nitride	19.07	4347	3513	2137
Vanadium Carbide	22.54	3942	3506	2251
Vanadium Nitride	7.51	3551	3549	1522
Ytterbium Boride	14.45	3564	3524	1945
Ytterbium Silicate	3.47	3645	3572	1142
Yttrium Boride	16.76	3875	3518	2047
Yttrium Oxide	9.82	3686	3539	1687
Zirconium Boride (ZrB_2)	23.11	4752	3505	2268
Zirconium Carbide	11.56	4982	3533	1794
Zirconium Nitride	12.13	4347	3531	1826
Zirconium Oxide	9.82	3983	3539	1687
Zirconium Silicate	3.47	3645	3572	1142
Molybdenum Silicide	28.31	3132	3497	2402
Barium Boride	20.80	3375	3509	2196

Table K3. Steady State Surface and Interface Temperatures in an Exhaust Temperature Region of 3600°R for a Composite Wall Design with Copper as the Support Material with a Boiling Water Backface

Material	k (Btu/hr•ft•°R)	T_{crit} (°R)	T_s (°R)	T_{if} (°R)
Aluminum Nitride	19.07	3780	3438	882
Beryllium Carbide	28.89	3605	3369	971
Boron Carbide	17.34	3537	3451	866
Boron Nitride	9.82	3510	3511	787
Calcium Oxide	16.76	3898	3455	860
Cerium Oxide	6.93	3605	3536	755
Europium Boride	13.29	2848	3482	824
Gadolinium Boride	12.13	3753	3492	812
Hafnium Carbide	12.71	5697	3487	818
Lanthanum Boride	27.73	4037	3377	961
Magnesium Oxide	36.40	4185	3322	1032
Molybdenum Carbide	4.62	3773	3556	728
Neodymium Boride	26.58	3902	3384	951
Niobium Boride	9.82	4469	3511	787
Niobium Carbide	17.34	5252	3451	866
Praesodymium Boride	23.69	3888	3404	926
Samarium Boride	8.09	3848	3526	768
Scandium Nitride	15.60	3807	3464	848
Scandium Oxide	4.62	3605	3556	728
Silicon Carbide	23.11	4401	3408	920
Tantalum Carbide	23.60	5751	3487	818
Terbium Boride	11.56	3524	3496	806
Titanium Carbide	28.89	4509	3369	971

Table K3. (Continued)

Material	k (Btu/hr•ft•°R)	T_{crit} (°R)	T_s (°R)	T_{if} (°R)
Titanium Nitride	19.07	4347	3438	882
Vanadium Carbide	22.54	3942	3412	915
Vanadium Nitride	7.51	3551	3531	762
Ytterbium Boride	14.45	3564	3473	836
Ytterbium Silicate	3.47	3645	3567	714
Yttrium Boride	16.76	3875	3455	860
Yttrium Oxide	9.82	3686	3511	787
Zirconium Boride (ZrB_2)	23.11	4752	3408	920
Zirconium Carbide	11.56	4982	3496	806
Zirconium Nitride	12.13	4347	3492	812
Zirconium Oxide	9.82	3983	3511	787
Zirconium Silicate	3.47	3645	3567	714
Molybdenum Silicide	28.31	3132	3373	966
Barium Boride	20.80	3375	3425	899

APPENDIX L

STEADY STATE SURFACE AND INTERFACE TEMPERATURES IN AN EXHAUST TEMPERATURE REGION OF 1800°R FOR A COMPOSITE WALL DESIGN WITH VARIOUS SUPPORT MATERIALS

Table L1. Steady State Surface and Interface Temperatures in an Exhaust Temperature Region of 1800°R for a Composite Wall Design with Titanium as the Support Material with a Boiling Water Backface

Material	k (Btu/hr•ft•°R)	T_{crit} (°R)	T_s (°R)	T_{if} (°R)
Aluminum Nitride	19.07	3780	1773	1345
Aluminum Oxide	21.96	3135	1771	1380
Aluminum Silicate	3.47	2866	1790	920
Barium Boride	20.80	3375	1772	1367
Beryllium Carbide	28.89	3605	1769	1444
Boron Carbide	17.34	3537	1774	1320
Boron Nitride	9.82	3510	1780	1167
Calcium Boride	13.29	3375	1777	1249
Calcium Oxide	16.76	3898	1774	1311
Calcium Zirconate	2.02	3524	1794	832
Cerium Boride	19.65	3321	1772	1352
Cerium Oxide	6.93	3605	1784	1076
Chromium Boride (CrB)	11.56	3208	1778	1211
Chromium Boride (CrB_2)	12.71	3267	1772	1237
Chromium Carbide ($Cr_{23}C_6$)	10.40	2498	1779	1183
Chromium Carbide (Cr_3C_2)	10.98	2808	1779	1198
Chromium Nitride	12.71	2592	1772	1237
Chromium Silicide	6.36	2695	1785	1054
Europium Boride	13.29	3848	1777	1249
Gadolinium Boride	12.13	3753	1778	1225
Gadolinium Oxide	1.16	3497	1796	769
Hafnium Carbide	12.71	5697	1777	1237

Table L1. (Continued)

Material	k (Btu/hr•ft•°R)	T_{crit} (°R)	T_s (°R)	T_{if} (°R)
Lanthanum Boride	27.74	4037	1769	1435
Lanthanum Sulfide	7.51	3335	1783	1097
Magnesium Aluminate	6.93	3251	1784	1076
Magnesium Oxide	36.40	4185	1767	1493
Magnesium Silicate	2.89	2930	1791	888
Molybdenum Beryllide	28.89	2592	1769	1444
Molybdenum Carbide	4.62	3773	1788	980
Molybdenum Silicide	28.31	3132	1769	1440
Neodymium Boride	26.58	3902	1770	1425
Neodymium Sulfide	0.58	3254	1798	723
Niobium Boride	9.82	4469	1780	1167
Niobium Carbide	17.34	5252	1774	1320
Niobium Nitride	2.31	3510	1793	851
Praesodymium Boride	23.69	3888	1771	1398
Samarium Boride	8.09	3848	1782	1116
Scandium Nitride	15.60	3807	1775	1292
Scandium Oxide	4.62	3605	1788	980
Silicon Carbide	23.11	4401	1771	1392
Silicon Oxide	0.58	2695	1798	723
Silicon Nitride	26.00	2903	1770	1420
Strontium Boride	15.02	3386	1775	1282
Tantalum Carbide	12.71	5751	1777	1237
Terbium Boride	11.56	3524	1778	1211

Table L1. (Continued)

Material	k (Btu/hr•ft•°R)	T_{crit} (°R)	T_s (°R)	T_{if} (°R)
Thorium Boride	26.58	3267	1770	1425
Titanium Carbide	28.89	4509	1769	1444
Titanium Nitride	19.07	4347	1773	1345
Titanium Oxide	6.36	2889	1785	1054
Titanium Silicide	8.67	3227	1781	1134
Vanadium Carbide	22.54	3942	1771	1386
Vanadium Nitride	7.51	3551	1783	1097
Ytterbium Boride	14.45	3564	1776	1272
Ytterbium Silicate	3.47	3645	1790	920
Yttrium Boride	16.76	3875	1774	1311
Yttrium Oxide	9.82	3686	1780	1167
Zirconium Beryllide	23.11	2970	1771	1392
Zirconium Boride (ZrB_2)	23.11	4752	1771	1392
Zirconium Boride (ZrB_{12})	7.51	3402	1783	1097
Zirconium Carbide	11.56	4982	1778	1211
Zirconium Nitride	12.13	4347	1778	1225
Zirconium Oxide	9.82	3983	1780	1167
Zirconium Silicate	3.47	3645	1790	920

Table L2. Steady State Surface and Interface Temperatures in an Exhaust Temperature Region of 1800°R for a Composite Wall Design with Steel as the Support Material with a Boiling Water Backface

Material	k (Btu/hr•ft•°R)	T_{crit} (°R)	T_s (°R)	T_{if} (°R)
Aluminum Nitride	19.07	3780	1766	1236
Aluminum Oxide	21.96	3135	1764	1273
Aluminum Silicate	3.47	2866	1789	853
Barium Boride	20.80	3375	1765	1259
Beryllium Carbide	28.89	3605	1760	1343
Boron Carbide	17.34	3537	1768	1211
Boron Nitride	9.82	3510	1777	1063
Calcium Boride	13.29	3375	1772	1140
Calcium Oxide	16.76	3898	1769	1202
Calcium Zirconate	2.02	3524	1793	787
Cerium Boride	19.65	3321	1766	1244
Cerium Oxide	6.93	3605	1782	981
Chromium Boride (CrB)	11.56	3208	1774	1104
Chromium Boride (CrB_2)	12.71	3267	1773	1129
Chromium Carbide ($Cr_{23}C_6$)	10.40	2498	1776	1077
Chromium Carbide (Cr_3C_2)	10.98	2808	1775	1091
Chromium Nitride	12.71	2592	1773	1129
Chromium Silicide	6.36	2695	1783	963
Europium Boride	13.29	3848	1772	1140
Gadolinium Boride	12.13	3753	1773	1117
Gadolinium Oxide	1.16	3497	1796	740
Hafnium Carbide	12.71	5697	1773	1129

Table L2. (Continued)

Material	k (Btu/hr•ft•°R)	T_{crit} (°R)	T_s (°R)	T_{if} (°R)
Lanthanum Boride	27.74	4037	1761	1333
Lanthanum Sulfide	7.51	3335	1780	999
Magnesium Aluminate	6.93	3251	1782	981
Magnesium Oxide	36.40	4185	1757	1399
Magnesium Silicate	2.89	2930	1791	828
Molybdenum Beryllide	28.89	2592	1760	1343
Molybdenum Carbide	4.62	3773	1786	900
Molybdenum Silicide	28.31	3132	1760	1338
Neodymium Boride	26.58	3902	1761	1323
Neodymium Sulfide	0.58	3254	1798	707
Niobium Boride	9.82	4469	1777	1063
Niobium Carbide	17.34	5252	1768	1211
Niobium Nitride	2.31	3510	1792	800
Praesodymium Boride	23.69	3888	1763	1293
Samarium Boride	8.09	3848	1779	1016
Scandium Nitride	15.60	3807	1769	1183
Scandium Oxide	4.62	3605	1786	900
Silicon Carbide	23.11	4401	1763	1287
Silicon Oxide	0.58	2695	1798	707
Silicon Nitride	26.00	2903	1761	1317
Strontium Boride	15.02	3386	1770	1173
Tantalum Carbide	12.71	5751	1773	1129
Terbium Boride	11.56	3524	1774	1104

Table L2. (Continued)

Material	k (Btu/hr•ft•°R)	T_{crit} (°R)	T_s (°R)	T_{if} (°R)
Thorium Boride	26.58	3267	1761	1323
Titanium Carbide	28.89	4509	1760	1343
Titanium Nitride	19.07	4347	1766	1236
Titanium Oxide	6.36	2889	1783	963
Titanium Silicide	8.67	3227	1778	1033
Vanadium Carbide	22.54	3942	1764	1280
Vanadium Nitride	7.51	3551	1780	999
Ytterbium Boride	14.45	3564	1771	1162
Ytterbium Silicate	3.47	3645	1789	853
Yttrium Boride	16.76	3875	1768	1202
Yttrium Oxide	9.82	3686	1777	1063
Zirconium Beryllide	23.11	2970	1763	1287
Zirconium Boride (ZrB_2)	23.11	4752	1763	1287
Zirconium Boride (ZrB_{12})	7.51	3402	1780	999
Zirconium Carbide	11.56	4982	1774	1104
Zirconium Nitride	12.13	4347	1773	1117
Zirconium Oxide	9.82	3983	1777	1063
Zirconium Silicate	3.47	3645	1789	853

Table L3. Steady State Surface and Interface Temperatures in an Exhaust Temperature Region of 1800°R for a Composite Wall Design with Copper as the Support Material with a Boiling Water Backface

Material	k (Btu/hr•ft•°R)	T_{crit} (°R)	T_s (°R)	T_{if} (°R)
Aluminum Nitride	19.07	3780	1737	753
Aluminum Oxide	21.96	3135	1729	763
Aluminum Silicate	3.47	2866	1787	688
Barium Boride	20.80	3375	1733	759
Beryllium Carbide	28.89	3605	1711	787
Boron Carbide	17.34	3537	1742	746
Boron Nitride	9.82	3510	1766	716
Calcium Boride	13.29	3375	1755	731
Calcium Oxide	16.76	3898	1744	744
Calcium Zirconate	2.02	3524	1793	681
Cerium Boride	19.65	3321	1736	755
Cerium Oxide	6.93	3605	1775	704
Chromium Boride (CrB)	11.56	3208	1760	724
Chromium Boride (CrB_2)	12.71	3267	1756	728
Chromium Carbide ($Cr_{23}C_6$)	10.40	2498	1764	719
Chromium Carbide (Cr_3C_2)	10.98	2808	1762	721
Chromium Nitride	12.71	2592	1756	728
Chromium Silicide	6.36	2695	1777	701
Europium Boride	13.29	3848	1755	731
Gadolinium Boride	12.13	3753	1758	726
Gadolinium Oxide	1.16	3497	1796	677
Hafnium Carbide	12.71	5697	1756	728

Table L3. (Continued)

Material	k (Btu/hr•ft•°R)	T_{crit} (°R)	T_s (°R)	T_{if} (°R)
Lanthanum Boride	27.74	4037	1714	783
Lanthanum Sulfide	7.51	3335	1773	706
Magnesium Aluminate	6.93	3251	1775	704
Magnesium Oxide	36.40	4185	1693	811
Magnesium Silicate	2.89	2930	1789	686
Molybdenum Beryllide	28.89	2592	1711	787
Molybdenum Carbide	4.62	3773	1783	693
Molybdenum Silicide	28.31	3132	1712	785
Neodymium Boride	26.58	3902	1717	779
Neodymium Sulfide	0.58	3254	1798	674
Niobium Boride	9.82	4469	1766	716
Niobium Carbide	17.34	5252	1742	746
Niobium Nitride	2.31	3510	1791	683
Praesodymium Boride	23.69	3888	1725	770
Samarium Boride	8.09	3848	1771	709
Scandium Nitride	15.60	3807	1748	740
Scandium Oxide	4.62	3605	1783	693
Silicon Carbide	23.11	4401	1726	768
Silicon Oxide	0.58	2695	1798	674
Silicon Nitride	26.00	2903	1718	778
Strontium Boride	15.02	3386	1749	737
Tantalum Carbide	12.71	5751	1756	728
Terbium Boride	11.56	3524	1760	724

Table L3. (Continued)

Material	k (Btu/hr•ft•°R)	T_{crit} (°R)	T_s (°R)	T_{if} (°R)
Thorium Boride	26.58	3267	1717	779
Titanium Carbide	28.89	4509	1711	787
Titanium Nitride	19.07	4347	1737	753
Titanium Oxide	6.36	2889	1777	701
Titanium Silicide	8.67	3227	1769	711
Vanadium Carbide	22.54	3942	1728	765
Vanadium Nitride	7.51	3551	1773	706
Ytterbium Boride	14.45	3564	1751	735
Ytterbium Silicate	3.47	3645	1787	688
Yttrium Boride	16.76	3875	1744	744
Yttrium Oxide	9.82	3686	1766	716
Zirconium Beryllide	23.11	2970	1726	768
Zirconium Boride (ZrB_2)	23.11	4752	1726	768
Zirconium Boride (ZrB_{12})	7.51	3402	1773	706
Zirconium Carbide	11.56	4982	1760	724
Zirconium Nitride	12.13	4347	1758	726
Zirconium Oxide	9.82	3983	1766	716
Zirconium Silicate	3.47	3645	1787	688

APPENDIX M

HEAT RATES AND VOLUMETRIC FLOWRATES IN AN EXHAUST TEMPERATURE REGION OF 6538°R FOR A COMPOSITE WALL DESIGN WITH VARIOUS SUPPORT MATERIALS

Table M1. Heat Rates and Volumetric Flowrates in an Exhaust Temperature Region of 6538°R for a Composite Wall Design with Titanium as the Support Material with a Boiling Water Backface

Material	H	T_{if} (°R)	q/A (Btu/hr•ft^2)	$(m/A)_{bf}$ (gal/min•ft^2)	m_{total} (gal/min)	% decrease in water flowrate
Tantalum Carbide	23.60	3612	2.14e+05	0.44	8984	97
Hafnium Carbide	23.60	3612	2.14e+05	0.44	8984	97
Niobium Carbide	17.31	4042	2.45e+05	0.51	10299	97
Zirconium Boride (ZrB_2)	12.98	4419	2.73e+05	0.56	11449	96
Magnesium Oxide	8.24	4942	3.11e+05	0.64	13047	96
Titanium Carbide	10.38	4689	2.92e+05	0.60	12273	96
Zirconium Carbide	25.96	3478	2.04e+05	0.42	8574	97
Titanium Nitride	15.73	4170	2.55e+05	0.52	10689	96
Silicon Carbide	12.98	4419	2.73e+05	0.56	11449	96
Lanthanum Boride	10.82	4641	2.89e+05	0.59	12127	96
Beryllium Carbide	10.38	4689	2.92e+05	0.60	12273	96
Vanadium Carbide	13.31	4387	2.70e+05	0.56	11352	96
Neodymium Boride	11.29	4591	2.85e+05	0.59	11973	96
Niobium Boride	30.54	3249	1.88e+05	0.39	7876	97
Zirconium Nitride	24.72	3547	2.09e+05	0.43	8784	97
Praesodymium Boride	12.66	4450	2.75e+05	0.57	11544	96
Calcium Oxide	17.90	3996	2.42e+05	0.50	10158	97
Aluminum Nitride	15.73	4170	2.55e+05	0.52	10689	96
Scandium Nitride	19.23	3898	2.35e+05	0.48	9858	97
Yttrium Boride	17.90	3996	2.42e+05	0.50	10158	97

Table M2. Heat Rates and Volumetric Flowrates in an Exhaust Temperature Region of 6538°R for a Composite Wall Design with Steel as the Support Material with a Boiling Water Backface

Material	H	T_{if} (°R)	q/A (Btu/hr•ft^2)	$(m/A)_{bf}$ (gal/min•ft^2)	m_{total} (gal/min)	% decrease in water flowrate
Tantalum Carbide	23.60	3048	2.55e+05	0.53	10717	96
Hafnium Carbide	23.60	3048	2.55e+05	0.53	10717	96
Niobium Carbide	17.31	3475	3.01e+05	0.62	12642	96
Zirconium Boride (ZrB_2)	12.98	3869	3.44e+05	0.71	14421	95
Magnesium Oxide	8.24	4452	4.06e+05	0.84	17051	94
Titanium Carbide	10.38	4164	3.75e+05	0.77	15752	95
Zirconium Carbide	25.96	2920	2.42e+05	0.50	10138	97
Titanium Nitride	15.73	3606	3.15e+05	0.65	13236	96
Silicon Carbide	12.98	3869	3.44e+05	0.71	14421	95
Lanthanum Boride	10.82	4111	3.70e+05	0.76	15513	95
Beryllium Carbide	10.38	4164	3.75e+05	0.77	15752	95
Vanadium Carbide	13.31	3835	3.40e+05	0.70	14267	95
Neodymium Boride	11.29	4056	3.64e+05	0.75	15262	95
Niobium Boride	30.54	2706	2.19e+05	0.45	9177	97
Zirconium Nitride	24.72	2985	2.49e+05	0.51	10434	97
Praesodymium Boride	12.66	3902	3.47e+05	0.71	14572	95
Calcium Oxide	17.90	3428	2.96e+05	0.61	12430	96
Aluminum Nitride	15.73	3606	3.15e+05	0.65	13236	96
Scandium Nitride	19.23	3329	2.86e+05	0.59	11984	96
Yttrium Boride	17.90	3428	2.96e+05	0.61	12430	96

Table M3. Heat Rates and Volumetric Flowrates in an Exhaust Temperature Region of 6538°R for a Composite Wall Design with Copper as the Support Material with a Boiling Water Backface

Material	H	T_{if} (°R)	q/A (Btu/hr•ft^2)	$(m/A)_{bf}$ (gal/min•ft^2)	m_{total} (gal/min)	% decrease in water flowrate
Tantalum Carbide	23.60	966	4.08e+05	0.84	17109	94
Hafnium Carbide	23.60	966	4.08e+05	0.84	17109	94
Niobium Carbide	17.31	1060	5.39e+05	1.11	22605	92
Zirconium Boride (ZrB_2)	12.98	1170	6.91e+05	1.42	29005	90
Magnesium Oxide	8.24	1394	1.00e+06	2.06	42048	86
Titanium Carbide	10.38	1272	8.33e+05	1.71	34943	88
Zirconium Carbide	25.96	941	3.74e+05	0.77	15682	95
Titanium Nitride	15.73	1094	5.86e+05	1.21	24577	92
Silicon Carbide	12.98	1170	6.91e+05	1.42	29005	90
Lanthanum Boride	10.82	1252	8.05e+05	1.66	33789	89
Beryllium Carbide	10.38	1272	8.33e+05	1.71	34943	88
Vanadium Carbide	13.31	1159	6.76e+05	1.39	28387	91
Neodymium Boride	11.29	1232	7.77e+05	1.60	32620	89
Niobium Boride	30.54	904	3.22e+05	0.66	13495	96
Zirconium Nitride	24.72	953	3.91e+05	0.80	16399	95
Praesodymium Boride	12.66	1181	7.06e+05	1.45	29620	90
Calcium Oxide	17.90	1049	5.23e+05	1.08	21937	93
Aluminum Nitride	15.73	1094	5.86e+05	1.21	24577	92
Scandium Nitride	19.23	1025	4.90e+05	1.01	20585	93
Yttrium Boride	17.90	1049	5.23e+05	1.08	21937	93

APPENDIX N

HEAT RATES AND VOLUMETRIC FLOWRATES IN AN EXHAUST TEMPERATURE REGION OF 5400°R FOR A COMPOSITE WALL DESIGN WITH VARIOUS SUPPORT MATERIALS

Table N1. Heat Rates and Volumetric Flowrates in an Exhaust Temperature Region of 5400°R for a Composite Wall Design with Titanium as the Support Material with a Boiling Water Backface

Material	H	T_{if} (°R)	q/A (Btu/hr•ft^2)	$(m/A)_{bf}$ (gal/min•ft^2)	m_{total} (gal/min)	% decrease in water flowrate
Tantalum Carbide	23.60	3042	1.73e+05	0.36	32299	89
Hafnium Carbide	23.60	3042	1.73e+05	0.36	32299	89
Niobium Carbide	17.31	3388	1.98e+05	0.41	33230	89
Zirconium Carbide	25.96	2934	1.65e+05	0.52	35242	88
Zirconium Boride (ZrB_2)	12.98	3692	2.20e+05	0.69	38364	87
Titanium Carbide	10.38	3909	2.36e+05	0.74	39257	87
Magnesium Oxide	8.24	4114	2.51e+05	0.79	40098	87
Titanium Nitride	15.73	3492	2.05e+05	0.65	37539	87
Silicon Carbide	12.98	3692	2.20e+05	0.69	38364	87
Lanthanum Boride	10.82	3871	2.33e+05	0.73	39099	87
Niobium Boride	30.54	2749	1.51e+05	0.48	34485	89
Zirconium Nitride	24.72	2989	1.69e+05	0.53	35470	88
Vanadium Carbide	13.31	3666	2.18e+05	0.69	38258	87
Beryllium Carbide	10.38	3909	2.36e+05	0.74	39257	87
Neodymium Boride	11.29	3830	2.30e+05	0.73	38932	87
Praesodymium Boride	12.66	3717	2.22e+05	0.70	38467	87
Calcium Oxide	17.90	3351	1.95e+05	0.62	36961	88
Yttrium Boride	17.90	3351	1.95e+05	0.62	36961	88
Scandium Nitride	19.23	3272	1.89e+05	0.60	36636	88
Aluminum Nitride	15.73	3492	2.05e+05	0.65	37539	87

Table N2. Heat Rates and Volumetric Flowrates in an Exhaust Temperature Region of 5400°R for a Composite Wall Design with Steel as the Support Material with a Boiling Water Backface

Material	H	T_{if} (°R)	q/A (Btu/hr•ft^2)	$(m/A)_{bf}$ (gal/min•ft^2)	m_{total} (gal/min)	% decrease in water flowrate
Tantalum Carbide	23.60	2587	2.06e+05	0.42	33526	89
Hafnium Carbide	23.60	2587	2.06e+05	0.42	33526	89
Niobium Carbide	17.31	2931	2.43e+05	0.50	34890	88
Zirconium Carbide	25.96	2483	1.95e+05	0.40	33117	89
Zirconium Boride (ZrB_2)	12.98	3249	2.77e+05	0.57	36150	88
Titanium Carbide	10.38	3487	3.03e+05	0.62	37093	88
Magnesium Oxide	8.24	3719	3.27e+05	0.67	38013	87
Titanium Nitride	15.73	3037	2.54e+05	0.52	35311	88
Silicon Carbide	12.98	3249	2.77e+05	0.57	36150	88
Lanthanum Boride	10.82	3444	2.98e+05	0.61	36924	88
Niobium Boride	30.54	2312	1.76e+05	0.36	32435	89
Zirconium Nitride	24.72	2536	2.00e+05	0.41	33326	89
Vanadium Carbide	13.31	3221	2.74e+05	0.56	36041	88
Beryllium Carbide	10.38	3487	3.03e+05	0.62	37093	88
Neodymium Boride	11.29	3399	2.93e+05	0.60	36746	88
Praesodymium Boride	12.66	3276	2.80e+05	0.58	36257	88
Calcium Oxide	17.90	2893	2.39e+05	0.49	34740	88
Yttrium Boride	17.90	2893	2.39e+05	0.49	34740	88
Scandium Nitride	19.23	2813	2.30e+05	0.47	34424	89
Aluminum Nitride	15.73	3037	2.54e+05	0.52	35311	88

Table N3. Heat Rates and Volumetric Flowrates in an Exhaust Temperature Region of 5400°R for a Composite Wall Design with Copper as the Support Material with a Boiling Water Backface

Material	H	T_{if} (°R)	q/A (Btu/hr•ft^2)	$(m/A)_{bf}$ (gal/min•ft^2)	m_{total} (gal/min)	% decrease in water flowrate
Tantalum Carbide	23.60	909	3.29e+05	0.68	38054	87
Hafnium Carbide	23.60	909	3.29e+05	0.68	38054	87
Niobium Carbide	17.31	985	4.34e+05	0.89	41947	86
Zirconium Carbide	25.96	889	3.01e+05	0.62	37043	88
Zirconium Boride (ZrB_2)	12.98	1073	5.57e+05	1.15	46481	85
Titanium Carbide	10.38	1156	6.71e+05	1.38	50687	83
Magnesium Oxide	8.24	1254	8.08e+05	1.66	55720	81
Titanium Nitride	15.73	1012	4.72e+05	0.97	43344	86
Silicon Carbide	12.98	1073	5.57e+05	1.15	46481	85
Lanthanum Boride	10.82	1140	6.49e+05	1.34	49870	83
Niobium Boride	30.54	859	2.59e+05	0.53	35494	88
Zirconium Nitride	24.72	899	3.15e+05	0.65	37552	87
Vanadium Carbide	13.31	1065	5.45e+05	1.12	46043	85
Beryllium Carbide	10.38	1156	6.71e+05	1.38	50687	83
Neodymium Boride	11.29	1123	6.26e+05	1.29	49042	84
Praesodymium Boride	12.66	1082	5.69e+05	1.17	46917	84
Calcium Oxide	17.90	975	4.21e+05	0.87	41474	86
Yttrium Boride	17.90	975	4.21e+05	0.87	41474	86
Scandium Nitride	19.23	957	3.95e+05	0.81	40516	86
Aluminum Nitride	15.73	1012	4.72e+05	0.97	43344	86

APPENDIX O

HEAT RATES AND VOLUMETRIC FLOWRATES IN AN EXHAUST TEMPERATURE REGION OF 3600°R FOR A COMPOSITE WALL DESIGN WITH VARIOUS SUPPORT MATERIALS

Table O1. Heat Rates and Volumetric Flowrates in an Exhaust Temperature Region of 3600°R for a Composite Wall Design with Titanium as the Support Material with a Boiling Water Backface

Material	H	T_{if} (°R)	q/A (Btu/hr•ft^2)	$(m/A)_{bf}$ (gal/min•ft^2)	m_{total} (gal/min)	% decrease in water flowrate
Aluminum Nitride	15.73	2418	1.27e+05	0.26	91768	69
Beryllium Carbide	10.38	2677	1.46e+05	0.30	92230	69
Boron Carbide	17.31	2354	1.22e+05	0.25	91653	69
Boron Nitride	30.54	1958	9.37e+04	0.19	90945	70
Calcium Oxide	17.90	2331	1.21e+05	0.25	91612	69
Cerium Oxide	43.27	1721	7.64e+04	0.16	90520	70
Europium Boride	22.57	2171	1.09e+05	0.22	91325	70
Gadolinium Boride	24.72	2107	1.04e+05	0.22	91210	70
Hafnium Carbide	23.60	2139	1.07e+05	0.22	91269	70
Lanthanum Boride	10.82	2653	1.44e+05	0.30	92188	69
Magnesium Oxide	8.24	2803	1.55e+05	0.32	92457	69
Molybdenum Carbide	64.89	1471	5.82e+04	0.12	90071	70
Neodymium Boride	11.29	2628	1.42e+05	0.29	92143	69
Niobium Boride	30.54	1958	9.37e+04	0.19	90945	70
Niobium Carbide	17.31	2354	1.22e+05	0.25	91653	69
Praesodymium Boride	12.66	2558	1.37e+05	0.28	92017	69
Samarium Boride	37.09	1824	8.39e+04	0.17	90704	70
Scandium Nitride	19.23	2282	1.17e+05	0.24	91524	69
Scandium Oxide	64.89	1471	5.82e+04	0.12	90071	70
Silicon Carbide	12.98	2542	1.36e+05	0.28	91990	69
Tantalum Carbide	23.60	2139	1.07e+05	0.22	91269	70

Table O1. (Continued)

Material	H	T_{if} (°R)	q/A (Btu/hr•ft^2)	$(m/A)_{bf}$ (gal/min•ft^2)	m_{total} (gal/min)	% decrease in water flowrate
Terbium Boride	25.96	2072	1.02e+05	0.21	91149	70
Titanium Carbide	10.38	2677	1.46e+05	0.30	92230	69
Titanium Nitride	15.73	2418	1.27e+05	0.26	91767	69
Vanadium Carbide	13.31	2526	1.35e+05	0.28	91961	69
Vanadium Nitride	39.94	1774	8.03e+04	0.17	90615	70
Ytterbium Boride	20.77	2229	1.13e+05	0.23	91429	70
Ytterbium Silicate	86.53	1317	4.70e+04	0.10	89796	70
Yttrium Boride	17.90	2331	1.21e+05	0.25	91612	69
Yttrium Oxide	30.54	1958	9.37e+04	0.19	90945	70
Zirconium Boride (ZrB_2)	12.98	2542	1.36e+05	0.28	91990	69
Zirconium Carbide	25.96	2072	1.02e+05	0.21	91149	70
Zirconium Nitride	24.72	2107	1.04e+05	0.22	91210	70
Zirconium Oxide	30.54	1958	9.37e+04	0.19	90945	70
Zirconium Silicate	86.53	1317	4.70e+04	0.10	89796	70
Molybdenum Silicide	10.60	2665	1.45e+05	0.30	92209	69
Barium Boride	14.42	2475	1.31e+05	0.27	91869	69

Table O2. Heat Rates and Volumetric Flowrates in an Exhaust Temperature Region of 3600°R for a Composite Wall Design with Steel as the Support Material with a Boiling Water Backface

Material	H	T_{if} (°R)	q/A (Btu/hr•ft^2)	$(m/A)_{bf}$ (gal/min•ft^2)	m_{total} (gal/min)	% decrease in water flowrate
Aluminum Nitride	15.73	2137	1.57e+05	0.32	92513	69
Beryllium Carbide	10.38	2415	1.87e+05	0.39	93248	69
Boron Carbide	17.31	2071	1.50e+05	0.31	92338	69
Boron Nitride	30.54	1687	1.09e+05	0.22	91325	70
Calcium Oxide	17.90	2047	1.48e+05	0.30	92276	69
Cerium Oxide	43.27	1476	8.64e+04	0.18	90765	70
Europium Boride	22.57	1888	1.31e+05	0.27	91855	69
Gadolinium Boride	24.72	1826	1.24e+05	0.26	91693	69
Hafnium Carbide	23.60	1858	1.27e+05	0.26	91775	69
Lanthanum Boride	10.82	2389	1.85e+05	0.38	93178	69
Magnesium Oxide	8.24	2559	2.03e+05	0.42	93628	69
Molybdenum Carbide	64.89	1265	6.38e+04	0.13	90209	70
Neodymium Boride	11.29	2361	1.82e+05	0.37	93105	69
Niobium Boride	30.54	1687	1.09e+05	0.22	91325	70
Niobium Carbide	17.31	2071	1.50e+05	0.31	92338	69
Praesodymium Boride	12.66	2284	1.73e+05	0.36	92903	69
Samarium Boride	37.09	1566	9.61e+04	0.20	91005	70
Scandium Nitride	19.23	1998	1.43e+05	0.29	92146	69
Scandium Oxide	64.89	1265	6.38e+04	0.13	90209	70
Silicon Carbide	12.98	2268	1.72e+05	0.35	92859	69
Tantalum Carbide	23.60	1858	1.27e+05	0.26	91775	69

Table O2. (Continued)

Material	H	T_{if} (°R)	q/A (Btu/hr•ft^2)	$(m/A)_{bf}$ (gal/min•ft^2)	m_{total} (gal/min)	% decrease in water flowrate
Terbium Boride	25.96	1794	1.21e+05	0.25	91606	69
Titanium Carbide	10.38	2415	1.87e+05	0.39	93248	69
Titanium Nitride	15.73	2137	1.57e+05	0.32	92512	69
Vanadium Carbide	13.31	2251	1.70e+05	0.35	92814	69
Vanadium Nitride	39.94	1522	9.14e+04	0.19	90888	70
Ytterbium Boride	20.77	1945	1.37e+05	0.28	92006	69
Ytterbium Silicate	86.53	1142	5.05e+04	0.10	89884	70
Yttrium Boride	17.90	2047	1.48e+05	0.30	92276	69
Yttrium Oxide	30.54	1687	1.09e+05	0.22	91325	70
Zirconium Boride (ZrB_2)	12.98	2268	1.72e+05	0.35	92859	69
Zirconium Carbide	25.96	1794	1.21e+05	0.25	91606	69
Zirconium Nitride	24.72	1826	1.24e+05	0.26	91693	69
Zirconium Oxide	30.54	1687	1.09e+05	0.22	91325	70
Zirconium Silicate	86.53	1142	5.05e+04	0.10	89884	70
Molybdenum Silicide	10.60	2402	1.86e+05	0.38	93214	69
Barium Boride	14.42	2196	1.64e+05	0.34	92670	69

Table O3. Heat Rates and Volumetric Flowrates in an Exhaust Temperature Region of 3600°R for a Composite Wall Design with Copper as the Support Material with a Boiling Water Backface

Material	H	T_{if} (°R)	q/A (Btu/hr•ft^2)	$(m/A)_{bf}$ (gal/min•ft^2)	m_{total} (gal/min)	% decrease in water flowrate
Aluminum Nitride	15.73	882	2.92e+05	0.60	95830	68
Beryllium Carbide	10.38	971	4.16e+05	0.86	98861	67
Boron Carbide	17.31	866	2.69e+05	0.55	95252	68
Boron Nitride	30.54	787	1.61e+05	0.33	92588	69
Calcium Oxide	17.90	860	2.61e+05	0.54	95057	68
Cerium Oxide	43.27	755	1.16e+05	0.24	91486	70
Europium Boride	22.57	824	2.12e+05	0.44	93852	69
Gadolinium Boride	24.72	812	1.95e+05	0.40	93437	69
Hafnium Carbide	23.60	818	2.04e+05	0.42	93645	69
Lanthanum Boride	10.82	961	4.02e+05	0.83	98523	67
Magnesium Oxide	8.24	1032	5.00e+05	1.03	100939	66
Molybdenum Carbide	64.89	728	7.84e+04	0.16	90570	70
Neodymium Boride	11.29	951	3.88e+05	0.80	98182	67
Niobium Boride	30.54	787	1.61e+05	0.33	92588	69
Niobium Carbide	17.31	866	2.69e+05	0.55	95252	68
Praesodymium Boride	12.66	926	3.52e+05	0.73	97304	68
Samarium Boride	37.09	768	1.34e+05	0.28	91932	69
Scandium Nitride	19.23	848	2.45e+05	0.50	94661	68
Scandium Oxide	64.89	728	7.84e+04	0.16	90570	70
Silicon Carbide	12.98	920	3.45e+05	0.71	97124	68
Tantalum Carbide	23.60	818	2.04e+05	0.42	93645	69

Table O3. (Continued)

Material	H	T_{if} (°R)	q/A (Btu/hr•ft^2)	$(m/A)_{bf}$ (gal/min•ft^2)	m_{total} (gal/min)	% decrease in water flowrate
Terbium Boride	25.96	806	1.87e+05	0.38	93227	69
Titanium Carbide	10.38	971	4.16e+05	0.86	98861	67
Titanium Nitride	15.73	882	2.92e+05	0.60	95829	68
Vanadium Carbide	13.31	915	3.38e+05	0.70	96943	68
Vanadium Nitride	39.94	762	1.25e+05	0.26	91710	69
Ytterbium Boride	20.77	836	2.29e+05	0.47	94260	69
Ytterbium Silicate	86.53	714	5.93e+04	0.12	90100	70
Yttrium Boride	17.90	860	2.61e+05	0.54	95057	68
Yttrium Oxide	30.54	787	1.61e+05	0.33	92588	69
Zirconium Boride (ZrB_2)	12.98	920	3.45e+05	0.71	97124	68
Zirconium Carbide	25.96	806	1.87e+05	0.38	93227	69
Zirconium Nitride	24.72	812	1.95e+05	0.40	93437	69
Zirconium Oxide	30.54	787	1.61e+05	0.33	92588	69
Zirconium Silicate	86.53	714	5.93e+04	0.12	90100	70
Molybdenum Silicide	10.60	966	4.09e+05	0.84	98693	67
Barium Boride	14.42	899	3.15e+05	0.65	96393	68

APPENDIX P

HEAT RATES AND VOLUMETRIC FLOWRATES IN AN EXHAUST TEMPERATURE REGION OF 1800°R FOR A COMPOSITE WALL DESIGN WITH VARIOUS SUPPORT MATERIALS

Table P1. Heat Rates and Volumetric Flowrates in an Exhaust Temperature Region of 1800°R for a Composite Wall Design with Titanium as the Support Material with a Boiling Water Backface

Material	H	T_{if} (°R)	q/A (Btu/hr•ft^2)	$(m/A)_{bf}$ (gal/min•ft^2)	m_{total} (gal/min)	% decrease in water flowrate
Aluminum Nitride	15.73	1345	4.90e+04	0.10	151960	49
Aluminum Oxide	13.66	1380	5.16e+04	0.11	151992	49
Aluminum Silicate	86.53	920	1.81e+04	0.04	151580	49
Barium Boride	14.42	1367	5.06e+04	0.10	151980	49
Beryllium Carbide	10.38	1444	5.62e+04	0.12	152049	49
Boron Carbide	17.31	1320	4.72e+04	0.10	151938	49
Boron Nitride	30.54	1167	3.61e+04	0.07	151802	49
Calcium Boride	22.57	1249	4.21e+04	0.09	151875	49
Calcium Oxide	17.90	1311	4.66e+04	0.10	151930	49
Calcium Zirconate	148.37	832	1.17e+04	0.02	151501	49
Cerium Boride	15.27	1352	4.95e+04	0.10	151967	49
Cerium Oxide	43.27	1076	2.94e+04	0.06	151720	49
Chromium Boride (CrB)	25.96	1211	3.93e+04	0.08	151841	49
Chromium Boride (CrB_2)	23.60	1237	4.12e+04	0.08	151864	49
Chromium Carbide ($Cr_{23}C_6$)	28.84	1183	3.72e+04	0.08	151816	49
Chromium Carbide (Cr_3C_2)	27.33	1198	3.83e+04	0.08	151829	49
Chromium Nitride	23.60	1237	4.12e+04	0.08	151864	49
Chromium Silicide	47.20	1054	2.79e+04	0.06	151700	49
Europium Boride	22.57	1249	4.21e+04	0.09	151875	49

Table P1. (Continued)

Material	H	T_{if} (°R)	q/A (Btu/hr•ft^2)	$(m/A)_{bf}$ (gal/min•ft^2)	m_{total} (gal/min)	% decrease in water flowrate
Gadolinium Boride	24.72	1225	4.03e+04	0.08	151853	49
Gadolinium Oxide	259.52	769	7.12e+03	0.01	151446	50
Hafnium Carbide	23.60	1237	4.12e+04	0.08	151864	49
Lanthanum Boride	10.82	1435	5.56e+04	0.11	152041	49
Lanthanum Sulfide	39.94	1097	3.09e+04	0.06	151738	49
Magnesium Aluminate	43.27	1076	2.94e+04	0.06	151720	49
Magnesium Oxide	8.24	1493	5.98e+04	0.12	152093	49
Magnesium Silicate	103.84	888	1.57e+04	0.03	151551	49
Molybdenum Beryllide	10.38	1444	5.62e+04	0.12	152049	49
Molybdenum Carbide	64.89	980	2.24e+04	0.05	151634	49
Molybdenum Silicide	10.60	1440	5.59e+04	0.12	152045	49
Neodymium Boride	11.29	1425	5.49e+04	0.11	152033	49
Neodymium Sulfide	519.03	723	3.73e+03	0.01	151404	50
Niobium Boride	30.54	1167	3.61e+04	0.07	151802	49
Niobium Carbide	17.31	1320	4.72e+04	0.10	151938	49
Niobium Nitride	129.81	851	1.31e+04	0.03	151519	49
Praesodymium Boride	12.66	1398	5.29e+04	0.11	152008	49
Samarium Boride	37.09	1116	3.23e+04	0.07	151756	49

Table P1. (Continued)

Material	H	T_{if} (°R)	q/A (Btu/hr•ft^2)	$(m/A)_{bf}$ (gal/min•ft^2)	m_{total} (gal/min)	% decrease in water flowrate
Scandium Nitride	19.23	1292	4.52e+04	0.09	151913	49
Scandium Oxide	64.89	980	2.24e+04	0.05	151634	49
Silicon Carbide	12.98	1392	5.25e+04	0.11	152003	49
Silicon Oxide	519.03	723	3.73e+03	0.01	151404	50
Silicon Nitride	11.54	1420	5.45e+04	0.11	152028	49
Strontium Boride	19.97	1282	4.44e+04	0.09	151904	49
Tantalum Carbide	23.60	1237	4.12e+04	0.08	151864	49
Terbium Boride	25.96	1211	3.93e+04	0.08	151841	49
Thorium Boride	11.29	1425	5.49e+04	0.11	152033	49
Titanium Carbide	10.38	1444	5.62e+04	0.12	152049	49
Titanium Nitride	15.73	1345	4.90e+04	0.10	151960	49
Titanium Oxide	47.20	1054	2.79e+04	0.06	151700	49
Titanium Silicide	34.61	1134	3.37e+04	0.07	151772	49
Vanadium Carbide	13.31	1386	5.20e+04	0.11	151998	49
Vanadium Nitride	39.94	1097	3.09e+04	0.06	151738	49
Ytterbium Boride	20.77	1272	4.37e+04	0.09	151895	49
Ytterbium Silicate	86.53	920	1.81e+04	0.04	151580	49
Yttrium Boride	17.90	1311	4.66e+04	0.10	151930	49
Yttrium Oxide	30.54	1167	3.61e+04	0.07	151802	49
Zirconium Beryllide	12.98	1392	5.25e+04	0.11	152003	49
Zirconium Boride (ZrB_2)	12.98	1392	5.25e+04	0.11	152003	49
Zirconium Boride (ZrB_{12})	39.94	1097	3.09e+04	0.06	151738	49

Table P1. (Continued)

Material	H	T_{if} (°R)	q/A (Btu/hr•ft^2)	$(m/A)_{bf}$ (gal/min•ft^2)	m_{total} (gal/min)	% decrease in water flowrate
Zirconium Carbide	25.96	1211	3.93e+04	0.08	151841	49
Zirconium Nitride	24.72	1225	4.03e+04	0.08	151853	49
Zirconium Oxide	30.54	1167	3.61e+04	0.07	151802	49
Zirconium Silicate	86.53	920	1.81e+04	0.04	151580	49

Table P2. Heat Rates and Volumetric Flowrates in an Exhaust Temperature Region of 1800°R for a Composite Wall Design with Steel as the Support Material with a Boiling Water Backface

Material	H	T_{if} (°R)	q/A (Btu/hr•ft^2)	$(m/A)_{bf}$ (gal/min•ft^2)	m_{total} (gal/min)	% decrease in water flowrate
Aluminum Nitride	15.73	1236	6.07e+04	0.12	152104	49
Aluminum Oxide	13.66	1273	6.47e+04	0.13	152153	49
Aluminum Silicate	86.53	853	1.95e+04	0.04	151597	49
Barium Boride	14.42	1259	6.31e+04	0.13	152134	49
Beryllium Carbide	10.38	1343	7.22e+04	0.15	152246	49
Boron Carbide	17.31	1211	5.79e+04	0.12	152070	49
Boron Nitride	30.54	1063	4.21e+04	0.09	151875	49
Calcium Boride	22.57	1140	5.04e+04	0.10	151977	49
Calcium Oxide	17.90	1202	5.70e+04	0.12	152058	49
Calcium Zirconate	148.37	787	1.22e+04	0.03	151508	49
Cerium Boride	15.27	1244	6.15e+04	0.13	152114	49
Cerium Oxide	43.27	981	3.33e+04	0.07	151767	49
Chromium Boride (CrB)	25.96	1104	4.65e+04	0.10	151929	49
Chromium Boride (CrB_2)	23.60	1129	4.91e+04	0.10	151962	49
Chromium Carbide ($Cr_{23}C_6$)	28.84	1077	4.36e+04	0.09	151894	49
Chromium Carbide (Cr_3C_2)	27.33	1091	4.51e+04	0.09	151912	49
Chromium Nitride	23.60	1129	4.91e+04	0.10	151962	49
Chromium Silicide	47.20	963	3.13e+04	0.06	151742	49
Europium Boride	22.57	1140	5.04e+04	0.10	151977	49

Table P2. (Continued)

Material	H	T_{if} (°R)	q/A (Btu/hr•ft^2)	$(m/A)_{bf}$ (gal/min•ft^2)	m_{total} (gal/min)	% decrease in water flowrate
Gadolinium Boride	24.72	1117	4.78e+04	0.10	151946	49
Gadolinium Oxide	259.52	740	7.33e+03	0.02	151448	50
Hafnium Carbide	23.60	1129	4.91e+04	0.10	151962	49
Lanthanum Boride	10.82	1333	7.11e+04	0.15	152232	49
Lanthanum Sulfide	39.94	999	3.52e+04	0.07	151791	49
Magnesium Aluminate	43.27	981	3.33e+04	0.07	151767	49
Magnesium Oxide	8.24	1399	7.81e+04	0.16	152319	49
Magnesium Silicate	103.84	828	1.67e+04	0.03	151563	49
Molybdenum Beryllide	10.38	1343	7.22e+04	0.15	152246	49
Molybdenum Carbide	64.89	900	2.46e+04	0.05	151660	49
Molybdenum Silicide	10.60	1338	7.17e+04	0.15	152239	49
Neodymium Boride	11.29	1323	6.99e+04	0.14	152218	49
Neodymium Sulfide	519.03	707	3.78e+03	0.01	151405	50
Niobium Boride	30.54	1063	4.21e+04	0.09	151875	49
Niobium Carbide	17.31	1211	5.79e+04	0.12	152070	49
Niobium Nitride	129.81	800	1.38e+04	0.03	151527	49
Praesodymium Boride	12.66	1293	6.68e+04	0.14	152179	49
Samarium Boride	37.09	1016	3.70e+04	0.08	151813	49

Table P2. (Continued)

Material	H	T_{if} (°R)	q/A (Btu/hr•ft^2)	$(m/A)_{bf}$ (gal/min•ft^2)	m_{total} (gal/min)	% decrease in water flowrate
Scandium Nitride	19.23	1183	5.49e+04	0.11	152033	49
Scandium Oxide	64.89	900	2.46e+04	0.05	151660	49
Silicon Carbide	12.98	1287	6.61e+04	0.14	152171	49
Silicon Oxide	519.03	707	3.78e+03	0.01	151405	50
Silicon Nitride	11.54	1317	6.93e+04	0.14	152211	49
Strontium Boride	19.97	1173	5.38e+04	0.11	152020	49
Tantalum Carbide	23.60	1129	4.91e+04	0.10	151962	49
Terbium Boride	25.96	1104	4.65e+04	0.10	151929	49
Thorium Boride	11.29	1323	6.99e+04	0.14	152218	49
Titanium Carbide	10.38	1343	7.22e+04	0.15	152246	49
Titanium Nitride	15.73	1236	6.07e+04	0.12	152104	49
Titanium Oxide	47.20	963	3.13e+04	0.06	151742	49
Titanium Silicide	34.61	1033	3.88e+04	0.08	151835	49
Vanadium Carbide	13.31	1280	6.54e+04	0.13	152162	49
Vanadium Nitride	39.94	999	3.52e+04	0.07	151791	49
Ytterbium Boride	20.77	1162	5.27e+04	0.11	152006	49
Ytterbium Silicate	86.53	853	1.95e+04	0.04	151597	49
Yttrium Boride	17.90	1202	5.70e+04	0.12	152058	49
Yttrium Oxide	30.54	1063	4.21e+04	0.09	151875	49
Zirconium Beryllide	12.98	1287	6.61e+04	0.14	152171	49
Zirconium Boride (ZrB_2)	12.98	1287	6.61e+04	0.14	152171	49
Zirconium Boride (ZrB_{12})	39.94	999	3.52e+04	0.07	151791	49

Table P2. (Continued)

Material	H	T_{if} (°R)	q/A (Btu/hr•ft^2)	$(m/A)_{bf}$ (gal/min•ft^2)	m_{total} (gal/min)	% decrease in water flowrate
Zirconium Carbide	25.96	1104	4.65e+04	0.10	151929	49
Zirconium Nitride	24.72	1117	4.78e+04	0.10	151946	49
Zirconium Oxide	30.54	1063	4.21e+04	0.09	151875	49
Zirconium Silicate	86.53	853	1.95e+04	0.04	151597	49

Table P3. Heat Rates and Volumetric Flowrates in an Exhaust Temperature Region of 1800°R for a Composite Wall Design with Copper as the Support Material with a Boiling Water Backface

Material	H	T_{if} (°R)	q/A (Btu/hr•ft^2)	$(m/A)_{bf}$ (gal/min•ft^2)	m_{total} (gal/min)	% decrease in water flowrate
Aluminum Nitride	15.73	753	1.13e+05	0.23	152743	49
Aluminum Oxide	13.66	763	1.27e+05	0.26	152922	49
Aluminum Silicate	86.53	688	2.29e+04	0.05	151639	49
Barium Boride	14.42	759	1.21e+05	0.25	152851	49
Beryllium Carbide	10.38	787	1.60e+05	0.33	153327	49
Boron Carbide	17.31	746	1.04e+05	0.21	152632	49
Boron Nitride	30.54	716	6.18e+04	0.13	152118	49
Calcium Boride	22.57	731	8.17e+04	0.17	152362	49
Calcium Oxide	17.90	744	1.01e+05	0.21	152594	49
Calcium Zirconate	148.37	681	1.35e+04	0.03	151524	49
Cerium Boride	15.27	755	1.16e+05	0.24	152779	49
Cerium Oxide	43.27	704	4.46e+04	0.09	151906	49
Chromium Boride (CrB)	25.96	724	7.19e+04	0.15	152242	49
Chromium Boride (CrB_2)	23.60	728	7.84e+04	0.16	152322	49
Chromium Carbide ($Cr_{23}C_6$)	28.84	719	6.52e+04	0.13	152160	49
Chromium Carbide (Cr_3C_2)	27.33	721	6.86e+04	0.14	152201	49
Chromium Nitride	23.60	728	7.84e+04	0.16	152322	49
Chromium Silicide	47.20	701	4.10e+04	0.08	151862	49
Europium Boride	22.57	731	8.17e+04	0.17	152362	49

Table P3. (Continued)

Material	H	T_{if} (°R)	q/A (Btu/hr•ft^2)	$(m/A)_{bf}$ (gal/min•ft^2)	m_{total} (gal/min)	% decrease in water flowrate
Gadolinium Boride	24.72	726	7.52e+04	0.15	152282	49
Gadolinium Oxide	259.52	677	7.76e+03	0.02	151453	50
Hafnium Carbide	23.60	728	7.84e+04	0.16	152322	49
Lanthanum Boride	10.82	783	1.55e+05	0.32	153262	49
Lanthanum Sulfide	39.94	706	4.81e+04	0.10	151949	49
Magnesium Aluminate	43.27	704	4.46e+04	0.09	151906	49
Magnesium Oxide	8.24	811	1.93e+05	0.40	153727	49
Magnesium Silicate	103.84	686	1.91e+04	0.04	151593	49
Molybdenum Beryllide	10.38	787	1.60e+05	0.33	153327	49
Molybdenum Carbide	64.89	693	3.02e+04	0.06	151730	49
Molybdenum Silicide	10.60	785	1.58e+05	0.32	153294	49
Neodymium Boride	11.29	779	1.50e+05	0.31	153196	49
Neodymium Sulfide	519.03	674	3.90e+03	0.01	151406	50
Niobium Boride	30.54	716	6.18e+04	0.13	152118	49
Niobium Carbide	17.31	746	1.04e+05	0.21	152632	49
Niobium Nitride	129.81	683	1.54e+04	0.03	151547	49
Praesodymium Boride	12.66	770	1.36e+05	0.28	153027	49
Samarium Boride	37.09	709	5.16e+04	0.11	151992	49

REPORT DOCUMENTION PAGE

Form Approved
OMB No. 0704-0188

1. AGENCY USE ONLY *(Leave blank)*	2. REPORT DATE	3. REPORT TYPE AND DATES COVERED
	October 1996	Final Contractor Report

4. TITLE AND SUBTITLE

THERMAL INSULATION SYSTEM FOR LARGE FLAME BUCKETS

5. FUNDING NUMBERS

Contract No. 31-4136-59060
and NASA (1995)-Stennis-06
and NAS13-580

6. AUTHOR(S)

E. Eugene Callens, Jr.
Tonya Pleshette Gamblin

7. PERFORMING ORGANIZATION NAME(S) AND ADDRESS(ES)

Department of Mechanical and Industrial Engineering
Louisiana Tech University
P.O. Box 10348
Ruston, LA 71272-0046

8. PERFORMING ORGANIZATION REPORT NUMBER

9. SPONSORING/MONITORING AGENCY NAME(S) AND ADDRESS(ES)

National Aeronautics and Space Administration
Washington, DC 20546-0001

10. SPONSORING/MONITORING AGENCY REPORT NUMBER

SE-1998-01-00003-SSC

11. SUPPLEMENTARY NOTES

12a. DISTRIBUTION/AVAILABILITY STATEMENT

Subject Category: Distribution: Unlimited
Availability: NASA CASI (301) 621-0390

12b. DISTRIBUTION CODE

13. ABSTRACT *(Maximum 200 words)*

The objective of this study is to investigate the use of thermal protection coatings, single tiles, and layered insulation systems to protect the walls of the flame buckets used in the testing of the Space Shuttle Main Engine, while reducing the cost and maintenance of the system. The physical behavior of the system is modeled by a plane wall boundary value problem with a convective frontface condition and a backface condition designed to provide higher heat rates through the material. The research includes a study of various ceramics and metals that may be suitable for use in a thermal protection system depending on their theoretical performance under simulated plume conditions. The equations developed here were used to calculate important thermal parameters including temperature distributions through the material, maximum times the materials can withstand plume conditions before failure, steady state surface temperatures in single layer designs, steady state surface and interface temperatures in composite layer designs, and expected heat loads that the system must be able to handle. The designs with the best thermal performance involved partial replacement of the flame bucket material with either tantalum, hafnium, or niobium carbide as the insulation material and aluminum as the support material.

14. SUBJECT TERMS	15. NUMBER OF PAGES
THERMAL INSULATION, ROCKET EXHAUST, FLAME BUCKET	259
	16. PRICE CODE

17. SECURITY CLASSIFICATION OF REPORT	18. SECURITY CLASSIFICATION OF THIS PAGE	19. SECURITY CLASSIFICATION OF ABSTRACT	20. LIMITATION OF ABSTRACT
UNCLASSIFIED	UNCLASSIFIED	UNCLASSIFIED	UL